Low Temperature Waste Heat Recovery in Internal Combustion Engines

Singh, Vikram

2020

Document Version:
Publisher's PDF, also known as Version of record

Low Temperature Waste Heat Recovery in Internal Combustion Engines

Low Temperature Waste Heat Recovery in Internal Combustion Engines

Vikram Singh

LUND
UNIVERSITY

DOCTORAL DISSERTATION

by due permission from the Faculty of Engineering, Lund University, Sweden.
To be defended at the E-Building in the E:B room on the Thursday, 30th of April 2020 at 10:15

Faculty opponent
Vincent Lemort

Organization **LUND UNIVERSITY** Department of Energy Sciences P.O. Box 118 SE-221 00 Lund	**Document name: DOCTORAL THESIS**
	Date of issue 2020-04-30
Author(s): Vikram Singh	**Sponsoring organization** Swedish Energy Agency

Title and subtitle
Low Temperature Waste Heat Recovery in Internal Combustion Engines

Abstract

Over the past few decades, the automotive industry has increasingly looked towards increasing the efficiency of the internal combustion engine to meet more stringent emission norms and as a measure to meet demands for improved air quality in cities. One method to improve the internal combustion engine efficiency is to recover some of the energy lost to the coolant and the exhaust using a secondary thermodynamic cycle such as an Organic Rankine Cycle. Organic Rankine Cycle systems have been shown to be some of the most efficient systems for waste heat recovery in automotive applications.

While most research into Organic Rankine Cycle waste heat recovery systems studies the recovery of heat rejected to the exhaust gases, the coolant represents a large source of waste heat which is largely overlooked. This is because of the lower temperature of the coolant in comparison to the exhaust gases, which means a lower quality of energy and hence, lower recoverable power from the system.

This thesis aims to investigate methods to increase the energy quality for low temperature waste heat in the engine and optimise the waste heat recovery system to improve the recoverable power and powertrain efficiency. The work done was a combination of experiments and simulations. The engines studied were primarily the Scania D13 heavy duty engine, both in single cylinder and multi cylinder configurations, and the Volvo D4 light duty engine.

The thesis first numerically investigates the use of elevated coolant temperatures for a single cylinder Scania D13 engine to increase the recoverable power from the engine waste heat. The system simulated used two separate recovery loops for the recovery of waste heat from the exhaust gases and the coolant with ethanol as the working fluid. It was seen that there exists an optimum coolant temperature, depending on engine operating conditions, to maximise recoverable power from the coolant. On the other hand, the recoverable power from the exhaust increased consistently with increasing coolant temperatures due to higher exhaust gas temperatures. The gross indicated efficiency and the combustion were seen to be largely unaffected by the coolant temperature in the study.

The thesis then studies the use of an integrated waste heat recovery cooling circuit using simulations for the multi-cylinder Scania D13 engine. This is where the coolant is also used as the working fluid in the Organic Rankine Cycle and the engine cooling channels act as a part of the evaporator. Here, a significant increase in system gross indicated efficiency was seen with the use of evaporative cooling. On comparison, while the integrated waste heat recovery system was seen to perform better than using a dual loop Rankine cycle system with elevated coolant temperatures, there is also increased mechanical complexity in implementing such a system, which lowers its viability for application.

The next study uses experimental data from the Volvo D4 light duty engine to optimise the waste heat recovery process for different operating points. An expansive study of working fluids was done to see the fluids that could recover the maximum power from the different waste heat sources. It was seen that for the low temperature heat, cyclopentane performed the best, whereas for high temperature heat, methanol and acetone were the best performing working fluids. An analysis of the working fluids showed that this was due to a combination of thermodynamic properties of these fluids and the constraints imposed for the simulations. The system brake efficiency was increased by 5.2 percentage points when using heat from both the exhaust gases and the coolant. From this, the increase in brake efficiency solely as the effect of increasing the coolant temperature was 1.7 percentage points.

Finally, the thesis evaluates the use of an optimised coolant temperature strategy to see the reduction in fuel consumption over a standard World Harmonized Transient Cycle for the multi-cylinder Scania D13 engine. It was seen that cyclopentane and methanol, again, performed the best, showing a total potential reduction of 9% in fuel consumption over the cycle.

This thesis thus gives insights on the optimisation process of implementing low temperature waste heat recovery systems for internal combustion engines and improving the powertrain efficiency.

Key words: Low Temperature Waste Heat Recovery, Rankine Cycle, Coolant Temperature, Working Fluids

Classification system and/or index terms (if any)

Supplementary bibliographical information		**Language** English
ISSN and key title 0282-1990		**ISBN** 978-91-7895-460-5 (print) 978-91-7895-461-2 (pdf)
Recipient's notes	**Number of pages:** 191	Price
	Security classification	

Signature Date 2020-03-20

Low Temperature Waste Heat Recovery in Internal Combustion Engines

Vikram Singh

LUND
UNIVERSITY

Faculty of Engineering
Department of Energy Sciences

ISBN : 978-91-7895-460-5 (print)
ISBN : 978-91-7895-461-2 (pdf)
ISRN : LUTMDN/TMHP-19/1157-SE
ISSN : 0282-1990

Printed in Sweden by Media-Tryck, Lund University
Lund 2020

Fearlessly the idiot faced the crowd, smiling

Table of Contents

Acknowledgements

At the end of these four years of my life, as I look back, I realise I have a lot to be grateful for. I consider myself lucky to have gotten to know some very knowledgeable and kind people during my studies in Lund. While it is a daunting task to do a PhD half way across the world from your home country and your family, the people I've met here have made my life richer and have made me feel at home here in Sweden.

Firstly, I would like to thank my first supervisor Martin Tunér. You were the one who hired me and gave me the opportunity to work here. As your student, I learned a lot about engines, academia and how to do good research. You pushed me to be a better researcher, but also allowed me a lot of freedom for trying out new things. You also did not hesitate in coming to my defense in meetings when I struggled for answers to tough questions. I appreciated that so much and it made me feel as if I always had you in my corner.

Next, I would like to thank Sebastian Verhelst. Working with you for the past few years has been a very valuable learning experience for me. At the beginning, some of your suggestions or comments on my work didn't make much sense. But in hindsight, I see how heeding those suggestions made me into a much better researcher with a keener eye for detail. It has also always amazed me how much of an effort both you and Martin put into your work, which inspires me to do likewise.

I would like to thank all my colleagues, the people I met at the department over the course of these past four years. You've been exceptionally kind to me and are some of the best people I've had the pleasure of working with. Especially Sam, Niko, Changle, Erik, Kenan, Nhut and Pablo. You've all taught me something new over these four years and I cannot imagine my stay here at Lund without you.

I'm grateful to the professors at our division, Öivind and Per. I'm thankful for the help and guidance you've given me over the past few years. I've always felt that I could come to either of you with the silliest of questions and you would take the time to answer it. I've greatly enjoyed the conversations that I've had with you over fika whether it be about engines or books or anything else. Likewise, I'd like to thank Marcus Thern for his help and support with my research and his constant good humour, of which he has an ample supply.

To the technicians and our lab managers, Marcus and Patrick, I would like to say that this department would not work without you. Thank you for working tirelessly on the engines in our lab. Anders, I feel like I've asked you too many times now to do some needlessly complicated engine modification and thankfully you've managed to pull it off every single time. Similarly Tommy, Patrick, Tomas and Martin - most of the work in the following pages would have not been possible without your efforts.

For the opportunity to work with them, I consider myself indebted to the members of the waste heat recovery working group. I was fortunate enough to work amongst and present my research to some of the smartest people I've met. Especially Johan, Jonas and Fredrik, you've been extremely supportive of my work and have constantly given me advice or sent us components when something in the engine broke down. This work would not have been possible without your support. I'd like to thank the other members of the working group as well, for their extremely valuable feedback on all of my presentations. Some of the questions you asked were tough and challenged my way of thinking about the problem, but ultimately it helped me look at the research from a new perspective. Jelmer and Sandhya, thank you for all the help with your simulations and with the work. I've learned a lot from the work you've done and look forward reading your publications in the future. I'd also like to thank the Swedish Energy Agency for the funding and support for the project itself.

To Sam, Sayle, Stefan, Stina, Charlie, Max, Rasmus and Per, I am extremely grateful for being able to consider you all my friends. I could probably write a few pages each on how you have all affected my life, but for the sake of sparing some trees, I shall just say - Tack så mycket. I hope you all already know how much you mean to me.

I have met so many people along the way, too many to name in a single sheet of paper for my time in Lund. To the people I've lived with and met through the years, thank you for being in my life and adding a bit more colour to it with each day that I was fortunate enough to spend with you. Especially Riccardo, Jeff, Ana, Olga and Paula, I consider myself lucky to have gotten to know you all in these past four years.

And finally, my family. Mama and Papa, thank you for the 28 years of constant and selfless love, care and attention you've poured into defining me as a person. Bhaiya, thank you for constantly being a reminder of the person I strive to be and also being the most awesome brother you could wish for. Words will never be enough for you. I love you all.

Abstract

Over the past few decades, the automotive industry has increasingly looked towards increasing the efficiency of the internal combustion engine to meet more stringent emission norms and as a measure to meet demands for improved air quality in cities. One method to improve the internal combustion engine efficiency is to recover some of the energy lost to the coolant and the exhaust using a secondary thermodynamic cycle such as an Organic Rankine Cycle. Organic Rankine Cycle systems have been shown to be some of the most efficient systems for waste heat recovery in automotive applications.

While most research into Organic Rankine Cycle waste heat recovery systems studies the recovery of heat rejected to the exhaust gases, the coolant represents a large source of waste heat which is largely overlooked. This is because of the lower temperature of the coolant in comparison to the exhaust gases, which means a lower quality of energy and hence, lower recoverable power from the system.

This thesis aims to investigate methods to increase the energy quality for low temperature waste heat in the engine and optimise the waste heat recovery system to improve the recoverable power and powertrain efficiency. The work done was a combination of experiments and simulations. The engines studied were primarily the Scania D13 heavy duty engine, both in single cylinder and multi cylinder configurations, and the Volvo D4 light duty engine.

The thesis first numerically investigates the use of elevated coolant temperatures for a single cylinder Scania D13 engine to increase the recoverable power from the engine waste heat. The system simulated used two separate recovery loops for the recovery of waste heat from the exhaust gases and the coolant with ethanol as the working fluid. It was seen that there exists an optimum coolant temperature, depending on engine operating conditions, to maximise recoverable power from the coolant. On the other hand, the recoverable power from the exhaust increased consistently with increasing coolant temperatures due to higher exhaust gas temperatures. The gross indicated efficiency and the combustion were seen to be largely unaffected by the coolant temperature in the study.

The thesis then studies the use of an integrated waste heat recovery cooling circuit using simulations for the multi-cylinder Scania D13 engine. This is where the coolant is also used as the working fluid in the Organic Rankine Cycle and the engine cooling channels act as a part of the evaporator. Here, a significant increase

in system gross indicated efficiency was seen with the use of evaporative cooling. On comparison, while the integrated waste heat recovery system was seen to perform better than using a dual loop Rankine cycle system with elevated coolant temperatures, there is also increased mechanical complexity in implementing such a system, which lowers its viability for application.

The next study uses experimental data from the Volvo D4 light duty engine to optimise the waste heat recovery process for different operating points. An expansive study of working fluids was done to see the fluids that could recover the maximum power from the different waste heat sources. It was seen that for the low temperature heat, cyclopentane performed the best, whereas for high temperature heat, methanol and acetone were the best performing working fluids. An analysis of the working fluids showed that this was due to a combination of thermodynamic properties of these fluids and the constraints imposed for the simulations. The system brake efficiency was increased by 5.2 percentage points when using heat from both the exhaust gases and the coolant. From this, the increase in brake efficiency solely as the effect of increasing the coolant temperature was 1.7 percentage points.

Finally, the thesis evaluates the use of an optimised coolant temperature strategy to see the reduction in fuel consumption over a standard World Harmonized Transient Cycle for the multi-cylinder Scania D13 engine. It was seen that cyclopentane and methanol, again, performed the best, showing a total potential reduction of 9% in fuel consumption over the cycle.

This thesis thus gives insights on the optimisation process of implementing low temperature waste heat recovery systems for internal combustion engines and improving the powertrain efficiency.

Popular Science Summary

The predominant form of propulsion in today's world whether it be cars, trucks, ships or planes is through the use of internal combustion engines. They offer a simple and cost effective method to convert the chemical energy found in fuels to mechanical energy to be used for transportation. The diesel engine specifically, powers a large part of the commercial goods traffic and transportation for the world. Created in the late 19th century, the modern internal combustion engine has now spanned more than a century of continued use.

However, with the increased use of internal combustion engines, problems have emerged. The increase in levels of greenhouse gases in the atmosphere such as CO_2 as well as the worsening air quality in cities due to noxious emissions have prompted governments worldwide to put limits on the emissions from an engine. Hence, engine manufacturers are continuously researching methods to reduce these harmful emissions. One method for the reduction of harmful gas emissions is increasing the efficiency of the engine. Higher efficiency means less fuel is burned to achieve the same energy output, subsequently also reducing the carbon emissions and potentially other forms of noxious emissions as well.

The typical internal combustion engine has different kinds of losses which contribute to its inefficiency. Even the most efficient combustion engines in use nowadays have an efficiency of (only) approximately 50%. This means that at least half of the chemical energy available from burning the fuel is wasted in the form of heat losses. The most significant of these losses is that represented by the exhaust gases, where the hot combustion product gases are pushed out from the combustion chamber at higher pressures and temperatures than the ambient conditions. Similarly, the coolant, which is designed to keep the engine within proper operating temperatures, is another form of heat loss, where energy is rejected to the coolant from the combustion gases and is further wasted by transferring it to the ambient air.

One method of increasing the efficiency of the propulsion system as a whole is to try and recover some of this wasted heat. Systems that achieve this are aptly named Waste Heat Recovery systems. A form of waste heat recovery system implemented in automotive applications is the use of waste thermal energy to heat up a secondary working fluid to convert it to high pressure vapour, which can be expanded across an expander to get some mechanical work back. These systems are called Organic

Rankine Cycle (ORC) systems and have been shown to be some of the most efficient and well researched methods for the recovery of waste heat.

While the exhaust gases are the obvious choice as a source for waste heat recovery due to their high temperatures, which makes the recovery of energy easier; the coolant is also potentially a large source of energy for the waste heat recovery system, which is largely overlooked. The major drawback in using the coolant as a source of waste heat recovery is the relatively low temperature of the coolant for normal engine operation. This reduces the quality of energy, i.e. the energy that can be converted to mechanical work effectively.

This thesis studies the recovery of this low temperature waste heat from the coolant for internal combustion engines. It takes a holistic look at the engine and the waste heat recovery system by trying to maximise the powertrain efficiency as a whole.

The thesis first compares two different methods of increasing the viability of low temperature waste heat recovery. The first method is through the use of higher coolant temperatures in the engine and using separate ORC systems to recover the waste heat from the coolant and the exhaust. The second method is through the use of an evaporative cooling system which is also a part of the ORC. Here, the coolant also acts as the working fluid of the ORC. A comparative study shows that while the evaporative cooling system performs better than simply using higher coolant temperatures, the increased mechanical complexity and need to redesign major engine components makes the method not viable.

The thesis then looks to optimise the waste heat recovery system for an engine for different engine loads and speeds. An expansive study was done for multiple working fluids in the ORC to determine the ones that perform best. From these studies, using an optimised coolant temperature, a gain in brake efficiency of 5.2 percentage points was observed for the engine with the gain in brake efficiency of 1.7 percentage points purely from the increased coolant temperatures.

Finally, the thesis looks at determining the reduction in fuel consumption over a standardised test cycle for a full engine. For the full cycle, the fuel consumption can potentially be reduced by up to 9%, by implementing the elevated coolant temperature waste heat recovery system.

While there are still issues that need to be addressed for the use of a low temperature waste heat recovery system in actual application, this thesis provides an overview of the potential of such a system and its optimisation with respect to multiple parameters in order to improve the efficiency of the entire powertrain, and thus ultimately to reduce greenhouse gas emissions.

List of Publications

This thesis is based on the following publications, referred to by their Roman numerals. The papers are appended to the thesis.

I. **A Study on the Effect of Elevated Coolant Temperatures on HD Engines**
Singh, V., Tunestal, P., and Tuner, M.,
SAE Technical Paper 2017-01-2223, 2017, doi: 10.4271/2017-01-222

II. **Investigating the Potential of an Integrated Coolant Waste Heat Recovery System in an HD Engine Using PPC Operation**
Singh, V., Svensson, E., Verhelst, S. and Tuner, M.,
ASME 2018 Internal Combustion Engine Division Fall Technical Conference, 2019, doi: 10.1115/ICEF 2018-9708

III. **On the Effects of Increased Coolant Temperatures of Light Duty Engine on Waste Heat Recovery**
Singh V., Rijpkema J. J., Munch K., Andersson S. B., Verhelst S.
Applied Thermal Engineering, 2020,
doi:10.1016/j.applthermaleng.2020.115157

IV. **Optimization and Evaluation of a Low Temperature Waste Heat Recovery System for a Heavy Duty Engine over a Transient Cycle**
Singh V., Li X., Rijpkema J. J., Munch K., Andersson S. B., Verhelst S.
Submitted for the SAE Powertrains Fuels and Lubricants conference 2020

Nomenclature

BSFC	Brake Specific Fuel Consumption
CAC	Charge Air Cooler
CDC	Conventional Diesel Combustion
EGR	Exhaust Gas Recirculation
EGRC	Exhaust Gas Recirculation Cooler
EVO	Exhaust Valve Opening
GHG	Greenhouse Gas
HD	Heavy Duty
HLHS	High Load High Speed (operating point)
HLLS	High Load Low Speed (operating point)
ICE	Internal Combustion Engine
IMEP	Indicated Mean Effective Pressure
IVC	Intake Valve Closing
LD	Light Duty
LLHS	Low Load High Speed (operating point)
LLLS	Low Load Low Speed (operating point)
ORC	Organic Rankine Cycle
PMEP	Pumping Mean Effective Pressure
PPC	Partially Premixed Combustion
RPM	Revolutions Per Minute
SOI	Start of Injection
THC	Total Unburned Hydrocarbons
TRC	Transcritical Rankine Cycle

WHR	Waste Heat Recovery
WHTC	Worl Harmonized Transient Cycle

1. Introduction

1.1. The Transport Sector

In recent times, the transportation sector has moved increasingly towards higher fuel efficiency and low emission vehicles as a result of stricter emission regulations and as a reaction to trends in the market. Poor air quality in cities, increased greenhouse gas (GHG) emissions and an increased focus on implementing renewable energy sources has led to a higher emphasis on the reduction of the transportation sector's impact on the environment.

As per the 2014 Intergovernmental Panel on Climate Change (IPCC) report on the mitigation of climate change [1], the transportation industry accounts for 14% of GHG emissions worldwide. In 2010, the transport sector produced 7.0 $GtCO_2$ equivalent of direct GHG emissions which is approximately 23% of total energy-related CO_2 emissions. The primary reason for this is that 95% of the world's transportation energy comes from petroleum based fuels for use in internal combustion engines. While the market share of combustion engine-only vehicles is expected to decrease over the next few decades, studies by McKinsey & Company [2] show that internal combustion engines are still expected to be the dominant mode of propulsion for automotive applications till 2025 to 2035+ (depending on future regulations) and be used in hybrid electric vehicles(HEVs) till 2050.

In addition to this, the total fuel demand in transportation worldwide is expected to increase by 30% to 82% by 2050 over 2010 levels, depending again on future regulations and legislation [3]. The main contribution for this growth is fueled by trucks, airplanes, trains and ships. Over this period, the demand for diesel is also predicted to increase by 46% to 200% [3].

With the predicted increase in fossil fuel consumption as well as the continuing use of internal combustion engines in the transportation sector, regulations concerning emissions are progressively becoming more stringent. The European policy aims to reduce carbon dioxide emissions to 20% of 1990 levels by 2050 [4]. Limits are also imposed on the tailpipe pollutant emissions of vehicles such as nitrogen oxides (NOx) and particulate matter (PM) to improve air quality in cities. These limits take the form of governmental imposed regulations such as Euro norms or Bharat Stage norms [5] [6].

It is then important that with the predicted continued use of combustion engines in the future, the increasingly strict emission regulations and the need to reduce dependency on fossil fuels, the combustion engine and powertrain efficiency is improved.

Nowadays, research in combustion engines looks heavily at increasing combustion engine efficiencies. Some methods being investigated are optimising the gas exchange, using low temperature combustion modes, optimising the spray process inside the combustion chamber etc. [7] [8] [9] However, even then these studies aim for a brake efficiency of only 55%. This means that a large part of the fuel energy is not transmitted to the wheels. This energy loss is mainly in the form of heat from the exhaust gases and heat rejected to the coolant and oil. One method to improve on this is to recover some of the waste heat produced by the engine and deliver it back to the crankshaft. Hence, the following sections will review the different state of the art waste heat recovery systems and discuss their benefits and disadvantages.

1.2. Waste Heat Recovery Systems

1.2.1. Overview

There are multiple methods of recovering waste heat from an internal combustion engine that have been developed in the past few decades. Waste heat recovery has also been used for applications such as reducing the warm up time for the engine oil using heat from the exhaust gases [10] [11]. However in these cases, the steady state power output at the engine crankshaft is not affected.

The most prominent of the waste heat recovery technologies is turbocompounding. Turbocompound systems work by using the exhaust gases to drive a turbine which extracts mechanical power and delivers it to either the crankshaft (mechanical turbocompounding) or to a battery through a generator (electrical turbocompounding). Turbocompound systems are used downstream of the turbocharger in heavy duty applications. Here they've shown a reduction in fuel consumption of up to 10% [12]. However, turbocompound systems also negatively influence the pumping work in the engine by increasing the backpressure, which also increases the amount of internal exhaust gas recirculation (EGR). This adds the need to rematch the turbocharger for the engine as the operating conditions are changed for the system.

Another method to utilise waste thermal energy is to directly convert it to electric energy using the Seebeck effect. Such waste heat recovery devices are called thermoelectric generators. Thermoelectric generators have the advantage of being very compact compared to other WHR systems and having no moving components.

For current thermoelectric generators, however, the recovery efficiency is low (5%) in comparison to other systems [13] [14].

One way to recover the energy is to convert the thermal energy to high amplitude acoustic waves and then to electric energy. Such a system is called a thermoacoustic generator. While these systems have shown to obtain high efficiencies (up to 22%), they suffer from the drawback of having high spatial requirements [15]. Largely due to the packaging issues associated with thermoacoustic generators, there have been no applications shown in the automotive sector.

Stirling cycle and Joule cycle engines can also be used for waste heat recovery. These systems have high efficiencies showing up to 65% to 70% of the Carnot efficiency with current technology [16]. For waste heat recovery applications however, Stirling engines have shown only a 1% reduction in fuel consumption for truck engines in recent studies [17]. They also have higher spatial requirements in comparison to other waste heat recovery systems, which again raises issues with regards to packaging.

For use in automotive applications, turbocompound systems and Rankine cycle systems (introduced in the following Section) show the most promise. In an assessment by Legros et al. [18], the Rankine cycle system shows a higher efficiency in recovering the waste heat from the engine, while also having a lower cost than turbocompound systems (as shown in Figure 1). Rankine cycle systems have also been heavily researched for automotive applications, making them more mature than most other waste heat recovery technologies.

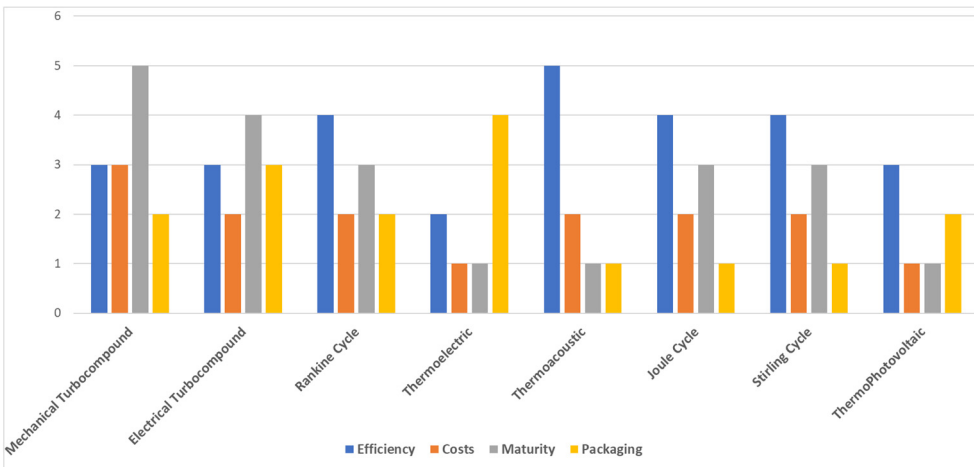

Figure 1:Performance indicators of each waste heat recovery technology for an automotive application (adapted from [18])

1.2.2. Rankine Cycle Recovery

A thermodynamic cycle waste heat recovery system uses a working fluid and circulates it through the system to generate power. For an ICE there are many thermodynamic cycles which can be used for the purpose of waste heat recovery from the engine's waste heat sources e.g. the trilateral flash cycle, Rankine cycle, transcritical cycle or the single flash cycle. In the study done by Rijpkema et al. [19] on a Heavy Duty (HD) engine, it was seen that when considering all the sources of waste heat from the engine, the Rankine Cycle performed better than the other thermodynamic cycles by a significant margin. This was largely due to the suitability of the temperature profiles of different sources of waste heat in the engine to the Rankine cycle implementation and the working fluids chosen for the simulations.

In a Rankine cycle, the working fluid is first pumped up to higher pressures and then vaporised using heat from a high temperature source (for example – the exhaust gases). The high pressure vapour is then passed through an expander, producing mechanical work. The working fluid, at a lower pressure and temperature, is then passed through a condenser and then again back to the pump. This process is shown in Figure 2.

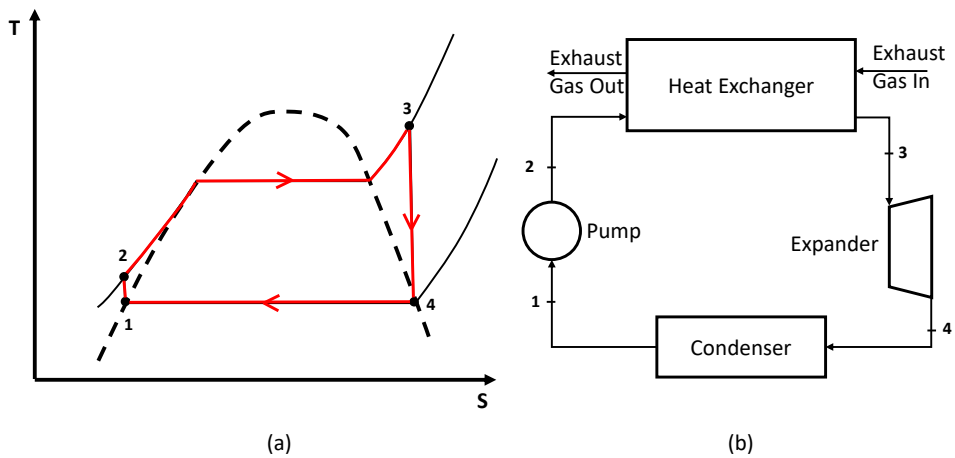

Figure 2: A Rankine cycle waste heat recovery system a) T-S Diagram for the cycle b) Schematic layout for the cycle

For a typical heavy duty engine, shown in Figure 3, the major sources of waste heat are the charge air cooler (CAC), the coolant, the exhaust gas recirculation cooler (EGRC) and the exhaust gases. From these the exhaust gases and the EGRC represent high temperature sources from which it is easier to extract heat, whereas the coolant and CAC represent low temperature heat sources. All these sources

represent energy inputs which can be used to power a separate thermodynamic cycle for additional power.

However, all sources are not equally viable for waste heat recovery. In the study done by Rijpkema et al. [19], out of all the sources evaluated, the exhaust gases, the EGRC and the coolant showed the most potential for recovering energy. The CAC was seen to not provide enough power to make energy recovery viable, due to lower enthalpy as well as lower temperatures.

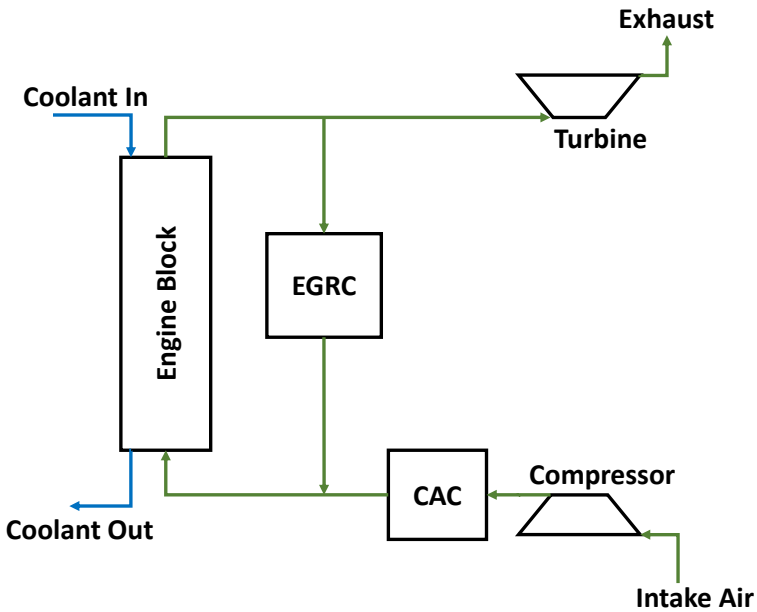

Figure 3: Schematic layout of a heavy duty diesel engine

Rankine cycle systems for waste heat recovery have mostly been implemented in stationary engines, largely due to the increased mass of the system and the requirements for space which is not readily available in vehicles. Additionally, stationary engines run at a steady operating point at high loads which allows the Rankine cycle to operate at more consistent conditions. However, there has been increasing research and implementation of Rankine cycle systems in HD engines in trucks [20] [21]. Here, generally the heat for the Rankine cycle is extracted from the exhaust gases as the exergy is higher. This has the disadvantage of being strongly variable, due to varying load and speed conditions for the engine. This further means that the Rankine cycle efficiency varies as the engine transitions between different operating points.

However, the coolant itself is a source of waste heat which is largely overlooked due to the lower quality of the available energy. The energy taken by the coolant

can be up to 35% of the fuel energy, depending on the type of engine being run, the mode of combustion as well as the operating point. This heat represents a large fraction of the total losses of the engine and is hence, a good potential source of energy for a waste heat recovery system.

1.2.3. Low Temperature Waste Heat Recovery

The coolant represents a large source of heat loss for an internal combustion engine. Additionally, the heat rejected to the coolant is further rejected to the ambient air through a radiator, which contributes to the aerodynamic drag. Hence, not only is the energy rejected to the coolant wasted but the propulsion of the vehicle is hindered by the increased drag as well. This makes the coolant a prime candidate for waste heat recovery. However, the primary disadvantage of using the coolant as a waste heat recovery source is the low temperature of the coolant itself and hence, the low energy quality. This reduces the amount of recoverable power that can be extracted from it.

The question then arises, is there a way to increase the recoverable power from the coolant? If so, how does it affect the engine and the waste heat recovery system? And what is the optimum system configuration in terms of working fluid selection and layout? There have been quite a few studies, shown below, that address these questions in parts. However, as described later, these studies do not present a complete picture of the waste heat recovery process from the engine coolant.

One method to increase the recoverable power from the coolant is to use higher coolant temperatures in the engine, thus also increasing the energy quality. Operating at higher coolant temperatures would also mean lower heat rejection to the coolant, which should translate to higher exhaust gas temperatures, which in turn increases the recoverable power for a Rankine cycle extracting heat from the exhaust gases as well. Another possible effect of reduced heat losses to the coolant could be a higher indicated efficiency for the engine.

Studies that investigate higher coolant temperatures, generally investigate only the effects on the engine efficiency itself. For spark ignition (SI) engines, some studies were done by Attar [22] and Mamum and Ehsan [23], where they show a decrease in indicated power with increasing temperatures due to a decrease in charge density as a result of a hotter engine. However, for a CI engine as the fuel injected is not a part of the charge inducted into the cylinder, these results do not seem applicable.

A study done by Slatar [24] on a Scania HD engine was done by increasing the coolant temperature for the cylinder head and the liner up to 110 °C and 130 °C respectively. It was seen that for medium and low engine speeds, higher coolant temperatures were favoured for the engine block whereas lower coolant temperatures were preferable in the cylinder head for increasing efficiency. The benefits in brake thermal efficiency were seen to be minimal (0.3%) with changing

coolant temperature and the study stated that fluctuations in measurement due to instabilities in injection could be a significant source of error.

Adler and Bandhauer [25] showed the effects of coolant temperature by sweeping upwards from 90 °C to 150 °C on a 3-cylinder light duty (LD) diesel engine. A relative decrease in brake efficiency was seen of up to 7.3% with increasing coolant temperatures. This is possibly due to longer combustion durations at higher temperatures, which also contributes to higher exhaust temperatures. The exhaust temperature also increased by up to 100 °C for the sweep, with the total exergy and coolant exergy increased by 20% to 40%. It should be noted that the oil temperature for the experiments was maintained at 80 °C, which would increase the heat transfer losses to the oil. The results also show unchanging engine NOx emissions with increasing coolant temperatures. However, contrary to this, a similar study was done by Abdelghaffar [26] who shows increasing NOx emissions with increasing coolant temperature.

Apart from the work done on elevated coolant temperatures, there are multiple studies that look at the recovery of low temperature waste heat from internal combustion engines.

Endo et al. [27] in their works have used higher coolant temperatures (189 °C) to see its effects on waste heat recovery systems for an LD engine. They showed a 13.2% relative increase in the engine's thermal efficiency from a waste heat recovery system installed in a car running at 100 km/h. However, the behaviour of the engine with changing coolant temperature is not characterised in this study, with only a single coolant temperature being tested.

A study by Fu et al. [28] evaluated four different working fluids for use in an Organic Rankine Cycle (ORC) to extract work from the coolant of an LD Gasoline Direct Injection (GDI) engine. Four working fluids were evaluated and R124 was selected for the simulations as having the largest working range of pressure ratios for the coolant temperatures used. The coolant temperature was kept fixed at 91.9 °C for the study. It was seen that at the maximum allowable pressure of 16 bar of the working fluid, the brake thermal efficiency was improved by 12.1%.

Similarly, Dolz et al. [29] [30] in their works looked at the waste heat recovery from a heavy duty diesel engine. They evaluated 8 working fluids for multiple sources of waste heat from the engine and also investigated different system architectures for the waste heat recovery system. They found that the maximum recoverable power is obtained from a binary/separated cycle for the low temperature and high temperature heat sources. They found water and R245fa to be the best working fluids for the low temperature and high temperature heat sources respectively, showing a power increment of up to 19% from the system.

Leduc et al. [31] in their work also look at low temperature waste heat recovery and its feasibility. Some of the advantages seen are lower pressure ratios compared to

waste heat recovery from exhaust gases, which also means the components for the system can be lighter. Another major advantage is the relatively stable behaviour of the coolant temperature with engine operation over a drive cycle, allowing better control of the ORC system. The systems in development aim at improvements in fuel economy of 2% to 3%.

There are also multiple studies on low temperature waste heat recovery systems for marine and heavy duty diesel engines [32] [33] [34] [35] [36]. These studies look at different working fluids, heat sources and system configurations for waste heat recovery systems. For example, the work by Song et al. [32] describes the study of low temperature waste heat recovery for a marine diesel engine looking at different recovery circuit configurations and 6 working fluids each for the low temperature and high temperature heat sources. The maximum recoverable power was obtained using a separate recovery circuit for the different heat sources, showing up to 10.2% improvement in brake efficiency for the engine using R245fa and benzene as the working fluids for the cooling water and exhaust gases respectively.

For most studies the best performing layout for the waste heat recovery system is the use of separate recovery loops for the low temperature and high temperature heat sources. The best performing working fluid differs between each study as the operating points and engines selected for the investigation are also different. However, another reason for this is that each study also takes into account a very small number of working fluids for its simulations and the list of working fluids compared is different between each study.

An alternative to directly raising the coolant temperature to increase the recoverable power from the coolant, is to use an integrated waste heat recovery system, where the coolant also acts as the working fluid for the Rankine cycle. In such a case, the engine behaves as the high temperature heat source in the cycle and it can be used to preheat and evaporate the coolant. Multiple studies on evaporative cooling systems have been done over the years, with most of them being concerned with making a more efficient cooling system with reduced mass. They also investigate the potential for increased durability of the engine due to faster warm up times and lower frictional losses. [37] [38] [39] [40]

An evaporative cooling system also has benefits from a waste heat recovery perspective. In a traditional thermodynamic cycle, the working fluid is at a lower temperature than the heat source for heat transfer to be effective. This means a lower efficiency for the thermodynamic cycle. However, if the coolant is the working fluid, it does not need to transfer heat to a lower temperature fluid, which increases the potential for energy recovery.

Another advantage of using evaporative cooling systems is the higher heat transfer coefficients which can be achieved. Figure 4 shows the change in heat transfer coefficient in an evaporator tube as the fluid is progressively vaporised and goes through different flow regimes. The overall heat transfer coefficient can be seen to

be higher in comparison to a normal convective heat transfer coefficient (αL0). Due to the higher heat transfer coefficient, it is possible to have higher coolant temperature while still maintaining and having more precise control of the metal temperatures in the engine.

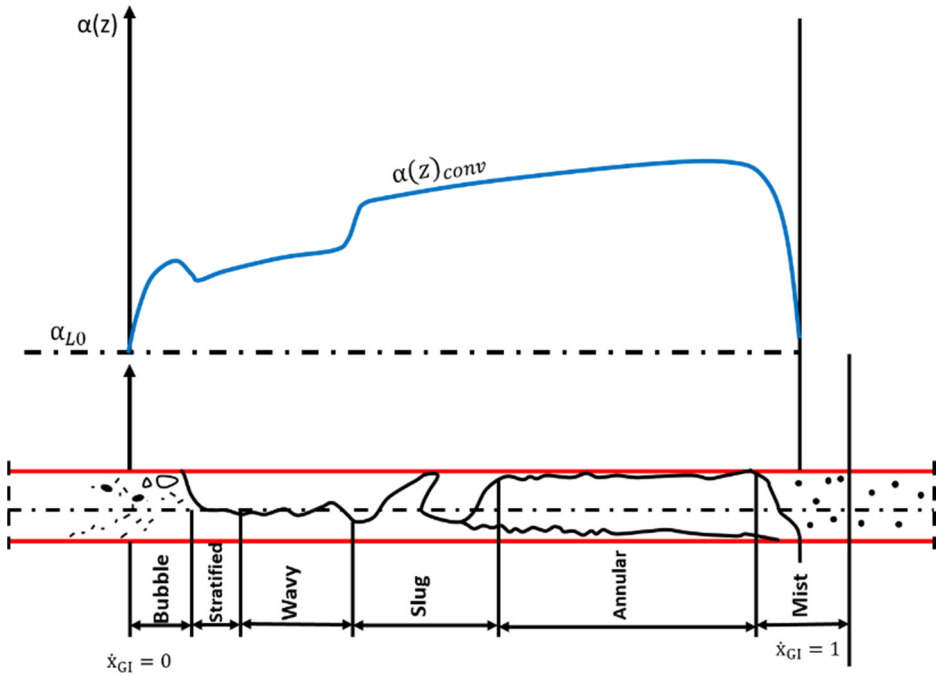

Figure 4: : Flow patterns in horizontal evaporator tubes (adapted from ref [41])

Dingel at al. [42] have shown the advantages of using an integrated waste heat recovery cooling circuit. In their work they found a reduction of brake specific fuel consumption (BSFC) of up to 9.3% when using an evaporative cooling system as part of the recovery cycle, as compared to 3.6% reduction in BSFC when only using traditional ORC cycles for waste heat recovery.

Using the engine in the recovery loop as an evaporator, however, raises mechanical design challenges. The cooling channels in the engine would have to withstand much higher pressures depending on the working fluid being used and the pressure ratio the cycle is being operated at. There is also the possibility of having flow regimes which have incomplete wall wetting, leading to uneven cooling in the channels. Flow regimes in complex channels in harsh and vibrating conditions are hard to predict and the heat transfer coefficient in practice varies significantly with changes in regimes.

Most studies that look at elevated coolant temperatures are concerned primarily with the effects on the brake efficiency of the engine itself. They are not as concerned

about the advantages in low temperature waste heat recovery. These studies also generally sweep the coolant temperature up to a limit of 120 °C.

On the other hand, the studies on low temperature waste heat recovery do not focus on optimising the engine along with the waste heat recovery system. Generally, a fixed operating point for the engine is taken and the waste heat recovery system is optimised for fixed engine parameters such as coolant temperature and coolant mass flow rates. These studies also generally compare 6 or fewer working fluids per heat source to find the optimum working fluid, without taking into account a larger group of test fluids in the simulations. As the different studies choose different fluids as candidates for potential working fluids, the best performing fluids tend to change from one study to the next.

Hence, keeping in mind the literature review presented above, there are still questions that need to be answered with regards to Rankine cycle waste heat recovery systems within the context of internal combustion engines. Is there a way to make low temperature waste heat recovery more viable? What is the best working fluid for low temperature heat sources? And how much fuel saving can be achieved by optimising the powertrain for waste heat recovery?

1.3. Thesis Objectives

The objective of the thesis is to develop an understanding of low temperature waste heat recovery from an internal combustion engine and to fill in the knowledge gaps described above.

The research works detailed in the previous sections show that there is potential in implementing low temperature waste heat recovery for engines. However, to fully understand this potential, a study is needed that looks at all the aspects of the system: the working fluids, the coolant temperatures, the different system architectures as well as the engine itself.

Therefore, the thesis first looks at increasing the quality of the heat rejected to the coolant through a simulation study of using elevated coolant temperatures in an HD engine and investigating the waste heat recovery potential from such a method. Most research works described in the previous sections on elevated coolant temperatures have been mainly restricted to lower temperatures (120 °C or lower) and have been more concerned with looking at changes in the engine performance and not the waste heat recovery aspects. This leaves room for a fundamental investigation into the energy balance of the engine with changing temperatures as well as the waste heat recovery system.

The thesis then looks at a comparison between an integrated waste heat recovery cooling system, using evaporative engine cooling in an HD engine as part of the Rankine cycle, and a dual loop Rankine cycle setup. Here, the aim is to evaluate the better method or system architecture for low temperature heat recovery while also taking into consideration the practical aspects of each system.

Then, a system study is done using detailed Rankine cycle simulations evaluating 48 working fluids using elevated coolant temperatures for a Light Duty (LD) engine. The study tries to determine the best working fluids for both low and high temperature sources within the engine and determine the behaviour of the engine with changing operating conditions and temperatures.

And lastly, the engine performance and Rankine cycle performance is mapped out for an HD engine as a function of different engine operating parameters. Using this, the thesis aims to implement this knowledge in the form of an optimised coolant temperature strategy over the World Harmonized Transient Cycle (WHTC) for the engine and see the potential benefits of the system in actual application.

This thesis provides a holistic view of low temperature waste heat recovery for internal combustion engines. Through different studies it optimises the waste heat recovery process from the coolant and evaluates the potential advantages from the implementation of such a system.

1.4. Thesis Structure

The remainder of this thesis consists of the following chapters with a corresponding brief explanation of the contents:

- The Methodology chapter explains in detail the different experimental setups used for the research work as well as the different setups for the simulations.
- The Results and Analysis chapter first describes the operating conditions chosen for each experimental or simulation campaign and then goes over the obtained results. The chapter analyses the data from the coolant temperature sweeps, the simulations for the integrated waste heat recovery cooling circuit and the optimisation of coolant temperature and waste heat recovery system.
- The Conclusions and Future Work chapter collectively describes the key contributions of the entire body of work presented here. It also briefly describes the limitations of the research work in this thesis and suggests topics for future research to help develop a better understanding of low temperature waste heat recovery.

2. Methodology

This chapter covers the methodology of the work discussed in this thesis. It details the experimental systems used as well as the models and the setup of the simulations. Largely, the methodology of the work presented here is first to do experimental runs for the engine part of the study and then use the experimental data in simulations of a Rankine cycle waste heat recovery system.

The chapter first goes over the three different types of engine setups used: a Scania D13 HD single-cylinder engine, a Volvo D4 LD four-cylinder engine and a full Scania D13 HD six-cylinder engine. It is also described here briefly for which experimental campaigns they are used. Then, the simulation models for each campaign are described along with the assumptions made in the model.

2.1. Experimental Setups

2.1.1. Scania D13 Single-Cylinder HD Engine

The first engine used in the thesis work was a Scania D13 HD engine which has been converted to operate on one cylinder (from six cylinder operation). The engine specifications are detailed in Table 1.

Table 1: Engine Specifications for the Scania D13 single cylinder engine

Parameter	Value
No. of Cylinders	1
Displaced Volume (cm^3)	2124
Bore x Stroke (mm)	130 x 160
Connecting Rod Length (mm)	255
Geometrical Compression Ratio	17.3:1
Number of valves	4
Swirl Ratio	2.1
Exhaust Valve Opening (EVO)	137° ATDC
Intake Valve Closing (IVC)	-141° ATDC

General System Layout

Figure 5 shows the engine, the gas exchange circuit and the dynamometer for the test setup. The engine is supplied with pressurised air on the intake and has a butterfly valve on the exhaust side to provide backpressure and simulate a turbocharger. A turbocharger is not used in this setup as the gas flow from a single cylinder is not adequate for driving the stock turbocharger for the engine at the speeds required. Additionally, the use of the back pressure valve and an intake valve allows greater control over the gas exchange process. The EGR valve in addition to the back pressure valve controls the amount of high-pressure EGR (HP-EGR) in the system. Additionally, the inlet air can be heated using a 7.5 kW heater in the intake system.

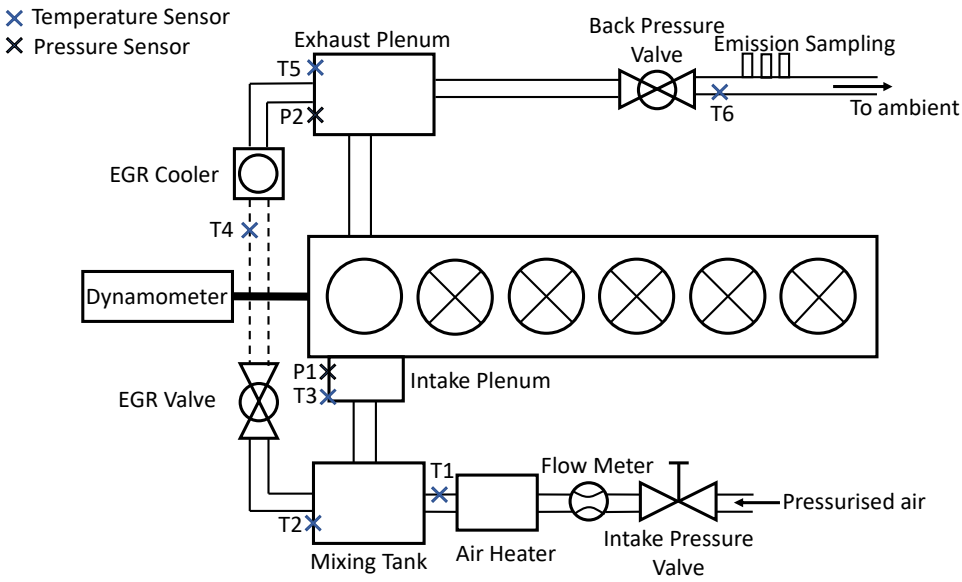

Figure 5: Scania D13 single cylinder HD engine setup

The mass flow rate of air in the intake is measured before the air heater using a Bronkhorst In-Flow thermal mass flow meter. The gas temperatures along the gas exchange circuit are measured using RS Pro Type K thermocouples (the locations of which are shown in Figure 5). The pressures in the gas exchange circuit are also measured, using Keller PAA-23S piezoresistive pressure transmitters, with the in-cylinder pressure being measured using a Kistler 7061b cylinder quartz pressure sensor. The crank angle is measured using a Leine and Linde incremental encoder which also provides a separate signal/pulse for Top Dead Centre (TDC) position.

The in-cylinder pressure is pegged by matching the cylinder pressure at the bottom dead centre (BDC) to the pressure measured in the intake plenum. The in-cylinder pressure is also offset relative to the crank angle to account for heat losses. This is done by offsetting the motored pressure trace for each measurement point to have the peak cylinder pressure (PCP) at 0.4 crank angle degree (CAD) before TDC [43]. The fired in-cylinder pressure for the same conditions as the motored pressure point is then offset by the same amount along the crank angle axis.

The exhaust gases are sampled downstream of the backpressure valve for measurement of emission concentrations. The emissions analyser used is an AVL AMA i60 system for measuring CO, CO_2, NO, NO_x, THC and CH_4. The analyser also uses a separate channel to detect the CO_2 in the intake plenum for the purpose

of EGR measurements. The detectors used in the emission analyser are shown in Table 2.

Table 2: AVL AMA i60 emission analyser detectors

Detector	Gases Detected
Chemiluminescense Detector (CLD)	NO, NO_x
Infrared Detector (IRD)	CO, CO_2
Flame Ionization Detector (FID)	Total Hydrocarbons (THC), CH_4
Paramagnetic Detector (PMD)	O_2

The fuel mass in the fuel supply tank for the engine is measured using a Radwag APP 10.R2 weighing scale. The fuel flow rate is measured by determining the rate of change of fuel weight in the engine supply tank during engine running.

Cooling System Layout

The cooling circuit for the Scania D13 single cylinder engine is shown in Figure 6. The engine coolant is circulated through a plate heat exchanger which is further cooled by circulating tap water. The coolant temperature is measured before and after the plate heat exchanger using RS Pro Type K thermocouples along with a Sandhurst Instruments LX-25 turbine flow rate meter for measuring the volume flow rate of coolant. In this test setup, the oil is cooled through the coolant, using the internal oil cooler in the engine. The coolant is pumped through the circuit using an externally driven pump, making the volumetric flow rate of the coolant independent of the engine speed.

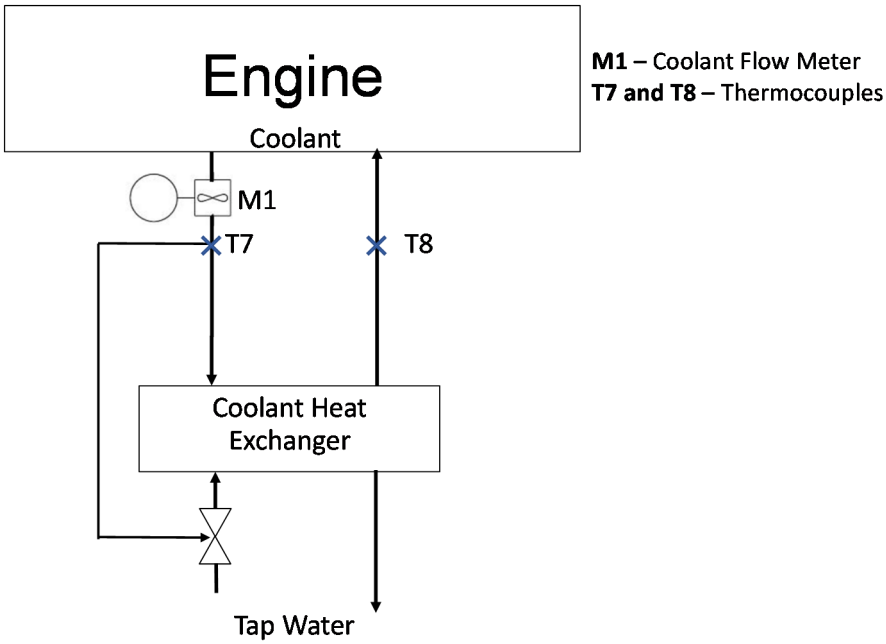

Figure 6: Cooling circuit configuration for Scania D13 single cylinder engine

A PID controlled valve is used to regulate the flow of tap water to provide a constant temperature of the coolant at the engine outlet (T7 in Figure 6). This means that the flow rate of coolant is unaffected when changing the cooling capacity of the heat exchanger.

The coolant used is a mixture of 50:50 ratio of ethylene glycol to water by volume.

Sensor Accuracy

The sensors used in the test setup and their accuracies are shown in Table 3.

Table 3: Sensor types and accuracies for Scania D13 single cylinder engine

Sensor	Type	Accuracy
Temperatures (Gas Exchange)	K – Type Thermocouple	± 1.5 °C
Pressures (Gas Exchange)	Piezoresistive sensor	± 0.02 bar
Air Mass Flow Rate	Thermal Mass Flow Sensor	± 0.16 L/min
Coolant Inlet and Outlet Temperature	K – Type Thermocouple	± 1.5 °C
Coolant Flow Rate Sensor	Turbine Flow Meter	± 0.5 %
Cylinder Pressure Sensor	Piezoelectric Pressure Sensor	± 1 bar
Fuel Weight	Weighing Scale	± 0.02 g
Crank Angle	Incremental Encoder	± 0.2 CAD

Experimental Campaigns

The Scania D13 single cylinder engine was used for the calibration of the GT-Power model of the test setup. The GT-Power model was then used to simulate the effect of elevated coolant temperatures to see the potential benefits. This study is discussed in more detail in Section 3.1.

2.1.2. Volvo D4 Multi-Cylinder LD Engine

The second engine used for the study was a 4 cylinder Volvo VED4 LD engine. The engine specifications are detailed in Table 4.

Table 4: Volvo D4 engine specifications

Engine Parameter	Value
No. Of Cylinders	4
Displacement (L)	2.0
Compression Ratio	13.7:1
Bore x Stroke (mm)	82 x 93.2
Connecting Rod Length (mm)	147
Number of Valves/ Cylinder	4
Inlet Temperature	50 °C
Fuel	Diesel MK1

General System Layout

The engine does not have a turbocharger, being replaced by a compressed air supply and a butterfly valve to give backpressure on the exhaust. This was done so as to have independent control of the intake pressure and backpressure for the engine. The inlet air temperature to the engine is controlled using an air heater. A schematic of the engine is shown in Figure 7.

Similar to the Scania D13 engine in Section 2.1.1 the temperature measurements in the gas exchange circuit are done using K Type thermocouples with the pressure measurements being done using piezoresistive pressure sensors. A Bronkhorst thermal mass flow sensor is used for measuring the mass flow rate of air.

For the fuel flow measurements, the supply fuel tank for the engine is mounted on a Sartorius weighing scale to measure the rate of change of fuel mass, obtained by linear fitting of the fuel mass measured.

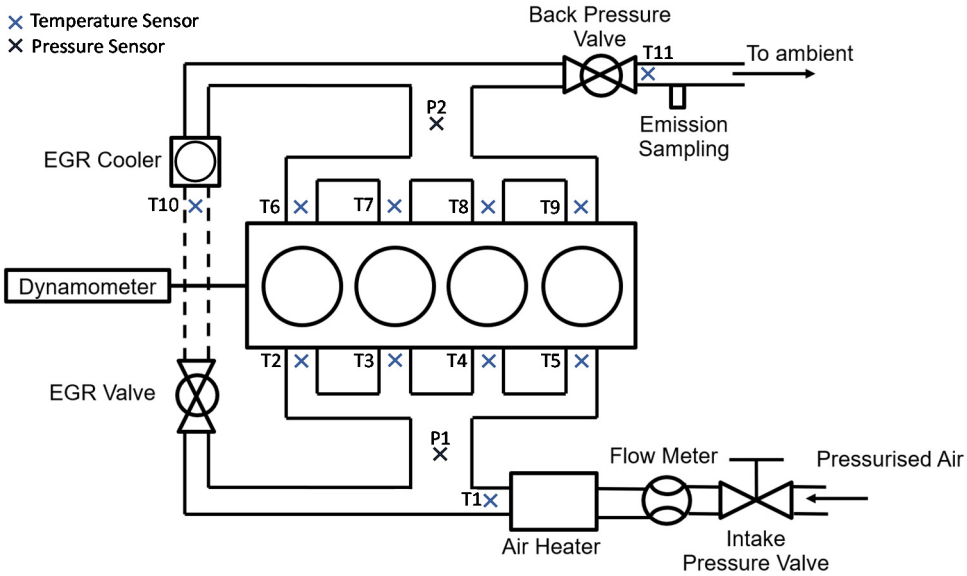

Figure 7: Volvo D4 Test Cell Layout

For this engine setup the torque is measured using an HBM T40B torque transducer mounted on the propeller shaft from the dynamometer. The in-cylinder pressure measurement is done using an AVL GH 14D pressure transducer. The in-cylinder pressure is pegged by matching the cylinder pressure to the intake pressure, similar to that described in Section 2.1.1 with the cylinder pressure being offset to account for heat losses to have the PCP for the motored pressure for each point at 0.4 CAD before TDC. The crank angle is measured using an incremental encoder with the TDC position measured as a separate signal from the encoder.

For emissions, an AVL AMA i60 emissions system is used to measure the components in the exhaust gas. This is the same emissions system described in Section 2.1.1 and Table 2.

Cooling System Layout

The oil and coolant cooling circuits for the Volvo D4 engine test setup are shown in Figure 8. The coolant in the engine is pumped by a belt driven water pump. Hence, the coolant flow rate is engine speed dependent. The coolant is circulated through a plate heat exchanger which is further cooled by circulating tap water. The tap water flow is regulated using a PID controlled valve to modify the cooling capacity of the heat exchanger. The circuit also has three-way valves installed to have some of the coolant or oil flow bypass the plate heat exchanger. This is done as at higher coolant or oil temperatures the tap water in the heat exchanger starts boiling which increases the heat transfer and restricts the coolant and oil temperature at a certain value. The three-way valve allows some of the coolant or oil to bypass the heat exchanger

making sure that the tap water does not start boiling. At increased coolant or oil temperatures, the three-way valve is opened more. The coolant used for the experiments was pure ethylene glycol. Two TE Connectivity Resistance Temperature Detectors (RTDs) were used to measure the temperature in and out of the heat exchanger (after the bypass, allowing sufficient mixing time) with a Sandhurst Instruments LX-25 turbine mass flow meter to measure the coolant flow rate.

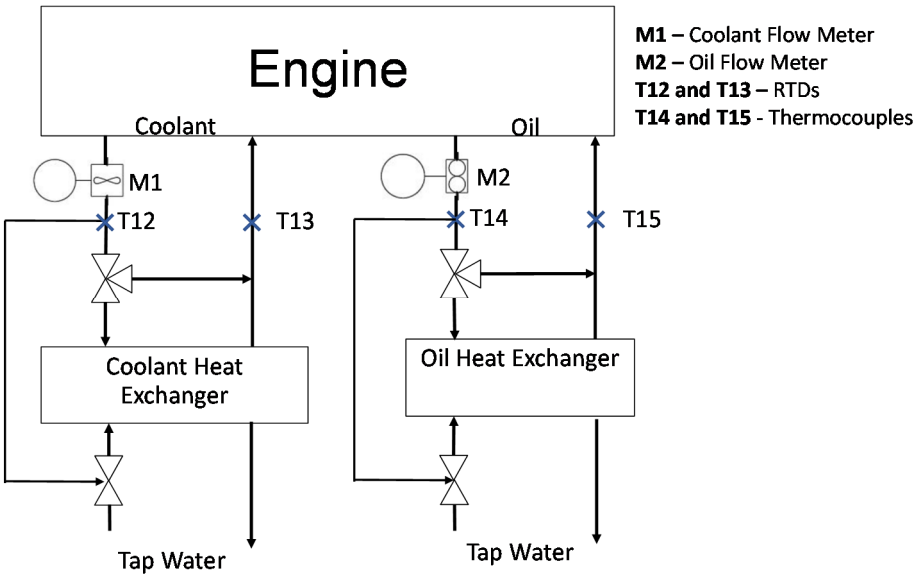

Figure 8: Cooling circuits for Volvo D4 engine

The oil cooling circuit for the engine was modified so as to cool it using tap water instead of using the coolant. This was done to maintain a lower engine oil temperature and prevent the engine from seizing due to possibly excessively low oil viscosities at higher coolant temperatures. The oil used for the experiments was SAE 10W-60. A Macnaught MX12 Oval gear flow meter was used to measure the volume flow rate of the oil with RS Pro Type K thermocouples to measure the inlet and outlet temperatures of the oil from the heat exchanger.

Sensor Accuracy

The list of sensors used for the engine and their accuracy are shown in Table 5.

Table 5: Sensor types and accuracies for Volvo D4 engine

Sensor	Type	Accuracy
Temperatures (Gas Exchange)	K – Type Thermocouple	± 1.5 °C
Pressures (Gas Exchange)	Piezoresistive sensor	± 0.02 bar
Air Mass Flow Rate	Thermal Mass Flow Sensor	± 0.16 L/min
Coolant Inlet and Outlet Temperature	Class AA RTD	± 0.24 °C at 80 °C ± 0.37 °C at 160 °C
Oil Inlet and Outlet Temperature	Thermocouple	± 1.5 °C
Oil Mass Flow Rate Sensor	Oval Gear Flowmeter	± 0.5 %
Coolant Mass Flow Rate Sensor	Turbine Mass Flow	± 0.5 %
Cylinder Pressure Sensor	Piezoelectric Pressure Sensor	± 1.25 bar
Fuel Weight	Weighing Scale	± 0.01 g
Crank Angle	Incremental Encoder	± 0.2 CAD

Experimental Campaigns

The Volvo D4 engine was used for a waste heat recovery analysis for LD engines. The engine was operated at different engine loads and speeds with the coolant temperature swept up from 80 °C to 160 °C. The results from the experimental study were then used for a dual Rankine cycle loop simulation evaluating multiple working fluids to determine the potential of waste heat recovery in LD engines and also to determine the best working fluids for both high temperature and low temperature waste heat recovery. This is further described in Section 3.4.

2.1.3. Scania D13 Multi-Cylinder HD Engine

The third engine used for the study is a full six cylinder Scania D13 HD engine. The engine specifications are given in Table 6.

Table 6: Engine Specifications for the Scania D13 six-cylinder engine

Parameter	Value
No.of Cylinders	6
Displaced Volume (cm^3)	12744
Bore x Stroke (mm)	130 x 160
Connecting Rod Length (mm)	255
Geometrical Compression Ratio	17.3:1
Number of valves/Cylinder	4
Swirl Ratio	2.1
Exhaust Valve Opening (EVO)	137° ATDC
Intake Valve Closing (IVC)	-141° ATDC

General System Layout

Figure 9 shows the gas exchange, the engine and the dynamometer for the full six cylinder Scania D13 engine setup. The turbocharger used in the setup is not the stock engine turbocharger, but is one used for partially premixed combustion operation. Temperature measurements along the intake and exhaust lines are done using RS Pro K Type thermocouples with pressure measurement being done using Keller piezoresistive sensors.

The engine setup has a low pressure EGR circuit as well as a high pressure EGR circuit. The gases for the EGR can be taken from before the turbine or after the turbine and introduced back in the circuit after the compressor or before the compressor respectively. Each EGR circuit can be independently controlled using a set of valves and the intake temperature can be controlled using EGR coolers. An intercooler is also used in the circuit to control the air temperature before the intake manifold.

The in-cylinder pressure in all the cylinders is measured using Kistler 7061B pressure transducers. For emissions, an AVL AMA i60 emissions system is used, the same as the one described in Section 2.1.1 and Table 2.

The in-cylinder pressure is again, pegged by matching the cylinder pressure to the intake pressure, similar to that described in the previous sections. Similar to previous test setups, the crank angle is measured using an incremental encoder.

The mass flow rate of fuel for the engine is measured using a Bronkhorst Mini Cori-Flow M15 coriolis flow meter.

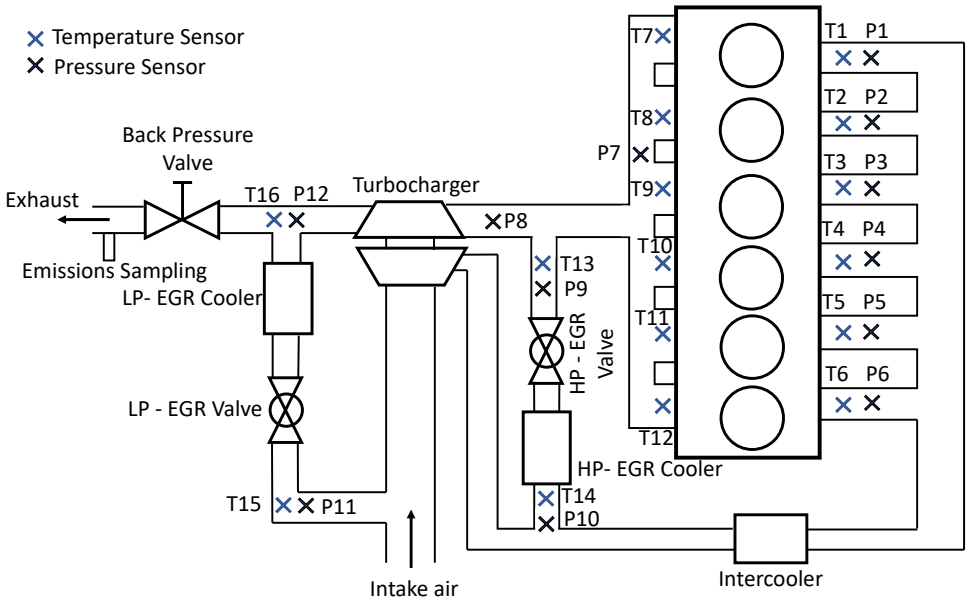

Figure 9: Scania D13 six-cylinder setup general layout

Cooling System Layout

The cooling layout for the six cylinder Scania D13 engine is shown in Figure 10. The coolant is cooled using tap water which is regulated by a PID controlled valve to vary the cooling capacity of the heat exchanger.

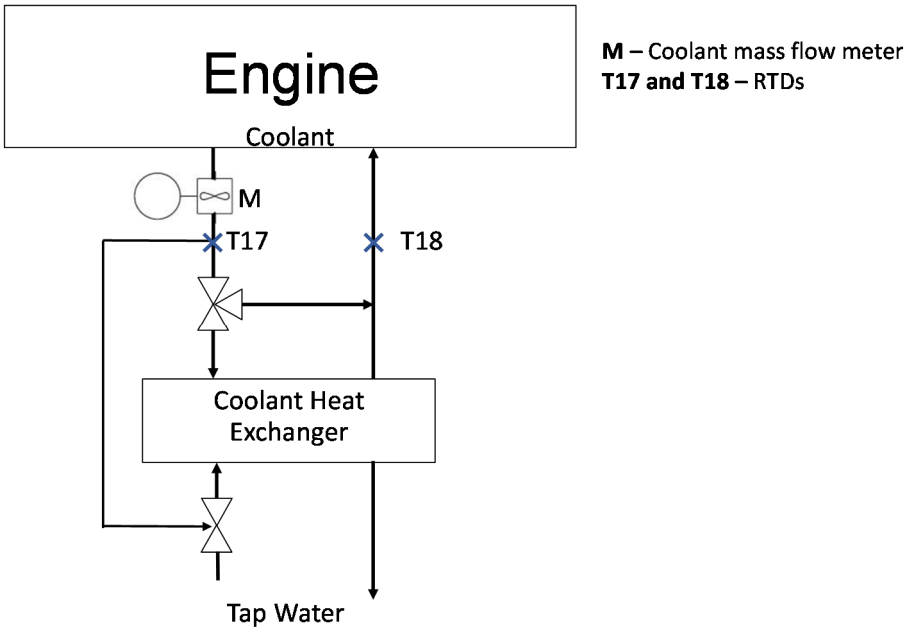

Figure 10: Cooling circuit configuration for the six cylinder Scania D13 engine

The oil in this setup is cooled by the coolant instead of tap water. This is to maintain a closer approximation to actual engine conditions where a separate cooling circuit is not used for the oil. The oil used in the setup is SAE 10W-60 to handle elevated coolant temperatures while maintaining sufficient viscosity to prevent engine seizure. The oil cooling circuit is also controlled by an internal thermostat which progressively opens up at higher temperatures to reject more heat to the coolant.

The measurement of the coolant temperature is done using Class AA RTDs. The volume flow rate for the coolant is measured using a Sandhurst LX-25 turbine flow meter.

Similar to the previous test setups, there are valves to regulate the flow of tap water to change the cooling capacity and there is a three way valve for the coolant to prevent the boiling of tap water in the heat exchanger.

Sensor Accuracy

The list of sensors used for the engine and their accuracy are shown in Table 7.

Table 7: Sensor types and accuracies for Scania D13 six-cylinder engine

Sensor	Type	Accuracy
Temperatures (Gas Exchange)	K – Type Thermocouple	± 1.5 °C
Pressures (Gas Exchange)	Piezoresistive sensor	± 0.02 bar
Air Mass Flow Rate	Thermal Mass Flow Sensor	± 0.16 L/min
Coolant Inlet and Outlet Temperature	Class AA RTD	± 0.24 °C at 80 °C ± 0.37 °C at 160 °C
Oil Inlet and Outlet Temperature	Thermocouple	± 1.5 °C
Oil Mass Flow Rate Sensor	Oval Gear Flowmeter	± 0.5 %
Coolant Mass Flow Rate Sensor	Turbine Mass Flow	± 0.5 %
Cylinder Pressure Sensor	Piezoelectric Pressure Sensor	± 1 bar
Fuel Flow Rate	Coriolis Flow Meter	± 0.2 %
Crank Angle	Incremental Encoder	± 0.2 CAD

Experimental Campaigns

The full Scania D13 engine setup was used in the campaign to determine the potential reduction in fuel consumption when using an adaptive coolant temperature strategy over the World Harmonized Transient Cycle (WHTC). The engine was first run with different loads, speeds and coolant temperatures to obtain data to generate models for the engine and waste heat recovery system. The models were then used to find an optimum coolant temperature strategy to minimise fuel consumption. Finally, an analysis was done using the optimised coolant temperature strategy to see the reduction in fuel consumption over the WHTC. The results and the setup for the campaign are discussed further in Section 3.5.

2.2. Engine Simulation Setups

2.2.1. Scania D13 Single Cylinder HD Engine

For the first study, on the effect of elevated coolant temperatures on an engine, a 1D GT Power model was used for the Scania D13 engine. The model is shown in Figure 11.

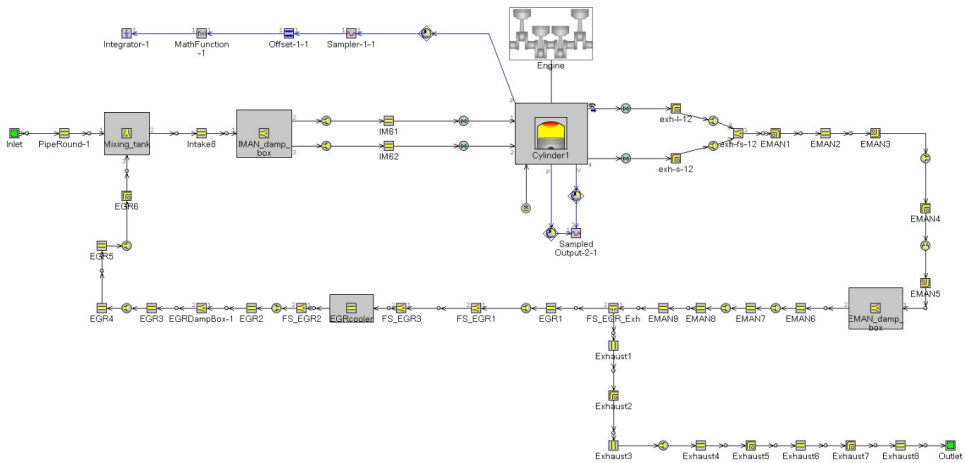

Figure 11: GT Power model for the Scania D13 single cylinder engine

The model describes the test setup shown in Figure 5 from the mixing tank on the intake side to the ambient atmosphere on the exhaust side. A high pressure EGR circuit is modelled and calibrated for the test setup including an EGR cooler. The amount of EGR is controlled by the backpressure and EGR valves which are modelled as orifice restrictors with variable diameters in the model.

A predictive DI-Pulse combustion model is used, calibrated for the engine operating range. A calibrated injector model provided by Scania was used with the DI-Pulse model, which describes the mass flow rate profiles of the injector as a function of injection pressure and injection duration. The calibration was done against a wide range of experimental conditions to determine the four calibration multipliers for the entrainment rate, the ignition delay, the premixed combustion rate and the diffusion combustion rate. The calibration of the predictive combustion model is described in the following section.

Calibration Method

As mentioned above, a predictive combustion model was used for the purpose of the simulation instead of using a predefined heat release rate. This was done to allow

studying the effect of coolant temperature on combustion characteristics such as the CA50 and the burn duration (CA10-CA90).

7 variables were taken and varied across the normal operating range of the engine. The variables and their different levels are described in Table 8.

Table 8: Combustion model calibration variables and levels

	Low	**Mid**	**High**
Load	5 bar	10 bar	18 bar
Speed	800 RPM	1100 RPM	1400 RPM
Air Inlet Temperature	30°C	50°C	70°C
EGR	0%	20%	40%
Lambda	1.3	1.8	2.4
Rail Pressure	800 bar	1200 bar	1400 bar
Coolant Temperature	60°C	80°C	100°C

From these values, 25 operating points were chosen to cover the engine operating range as well as extreme conditions such as: low lambda, high inlet temperature, high coolant temperature at high loads and high speeds (values taken as per Table 8).

The combustion model was first calibrated using data from 15 of these operating points at random and was then validated against the remaining 10 operating points. The entire engine model itself was validated against the 25 operating points. The THC and CO emission readings from the experiments were used in calibrating the combustion efficiencies in the model.

The maximum error observed in gross indicated mean effective pressure ($IMEP_g$) between experimental data and simulated results from the predictive model was observed to be below 3% with the maximum error in PMEP found to be less than 5%.

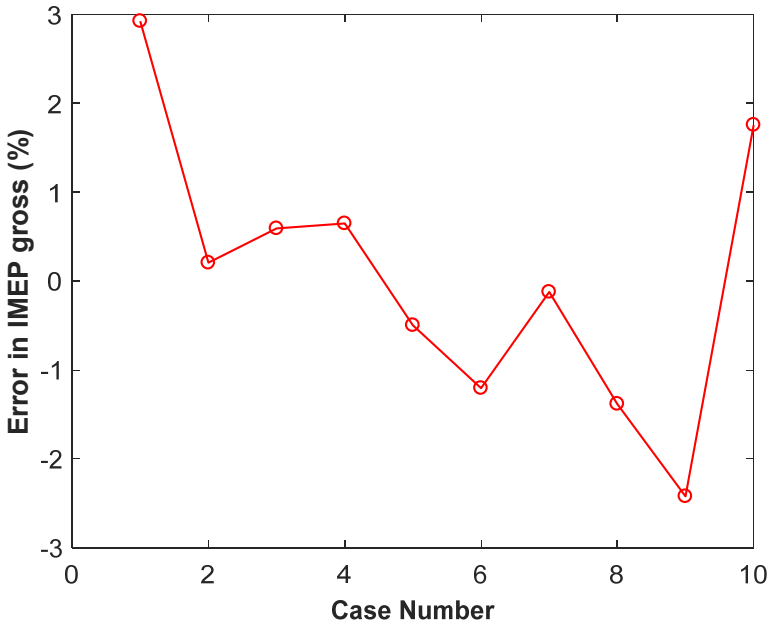

Figure 12: Error in IMEP gross between experimental and predicted values for validation cases

The heat transfer model was calibrated against data from the experiments under fired conditions. For modelling heat transfer, the Flow model [44] was used in GT-Power and the heat transfer coefficient multiplier was tuned to get a good match with the experimental data. The Flow model was taken as it shows good agreement between experimental crank angle resolved heat transfer and modelled values, taking into account the squish, swirl and tumble effects.

Implementing Coolant Heat Transfer Coefficients

With changing coolant temperatures, the properties of the coolant are changed, such as the viscosity and the density. This translates to varying heat transfer coefficients due to changes in the Reynolds and Prandtl number. To model the change in heat transfer coefficient, the Dittus Boelter equation can be used (developed from the Colburn relationship [45]), which can be seen in Equation (1). The Dittus Boelter correlation is valid for fully developed flows in smooth circular channels with Prandtl numbers from 0.6 to 160 and Reynolds numbers of above 10000.

$$Nu = (0.023 \,.\, Re^{0.8} . Pr^{0.4}) \quad (1)$$

The Nusselt number is defined as the ratio of the convective heat transfer to the conductive heat transfer across a boundary. The Nusselt number is defined in

Equation (2). Here, h is the heat transfer coefficient, L is the characteristic length and k is the thermal conductivity of the fluid.

$$Nu = \frac{hL}{k} \tag{2}$$

However, the empirical relation in eq. 1 does not take into account some physical phenomena. Firstly, as heat is being transferred to the coolant, the wall temperature of the cooling jackets is higher than the bulk coolant temperature. This means that the viscosity of the flow near the walls is lower than that in the bulk. This then modifies the Reynolds number of the coolant flow. Secondly, the equation does not take into account the effect of surface roughness on heat transfer as more surface roughness tends to increase the surface area as well as the heat transfer coefficient. To account for this, a modified form of the Dittus-Boelter relationship was implemented as shown in Equation (3).

$$Nu = (0.023 \,.\, Re^{0.8} . Pr^{0.4}) \left(0.091 \left(\frac{\varepsilon}{D_h} \right)^{-0.125} Re^{0.363 \left(\varepsilon / D_h \right)^{0.1}} \right) \left(\frac{\mu_{bulk}}{\mu_{wall}} \right)^{0.14} \tag{3}$$

Here, D_h is the hydraulic diameter of the channel, ε is the surface roughness and μ is the dynamic viscosity of the fluid. This method was developed by Robinson et al. [46] for predicting convective cooling in internal combustion engines.

In Equation (3), the right hand side shows three different terms. The first term shows the standard Dittus Boelter equation. The second term describes the effects of surface roughness on the heat transfer, such as increased turbulence and increased surface area. The third term accounts for the effect of wall temperature on the fluid flow. The modified equation by Robinson et al. [46] also accounts for boundary layer buildup on entry into the cooling channels. However, these terms are not included as the cooling system model in GT-Power is taken as zero dimensional and the flow is considered fully developed.

The coolant used for the simulation is a mixture of 50:50 by volume mixture of water and ethylene glycol. The pressure within the coolant channels is considered high enough at all times to suppress boiling and hence the coolant properties are always taken as for a binary liquid.

The variation in heat transfer coefficient computed from Equation (3) is shown in Figure 13. It can be seen that with increasing coolant as well as surface temperatures, the heat transfer coefficient increases. The map is then implemented in GT-Power in the form of a heat transfer coefficient multiplier.

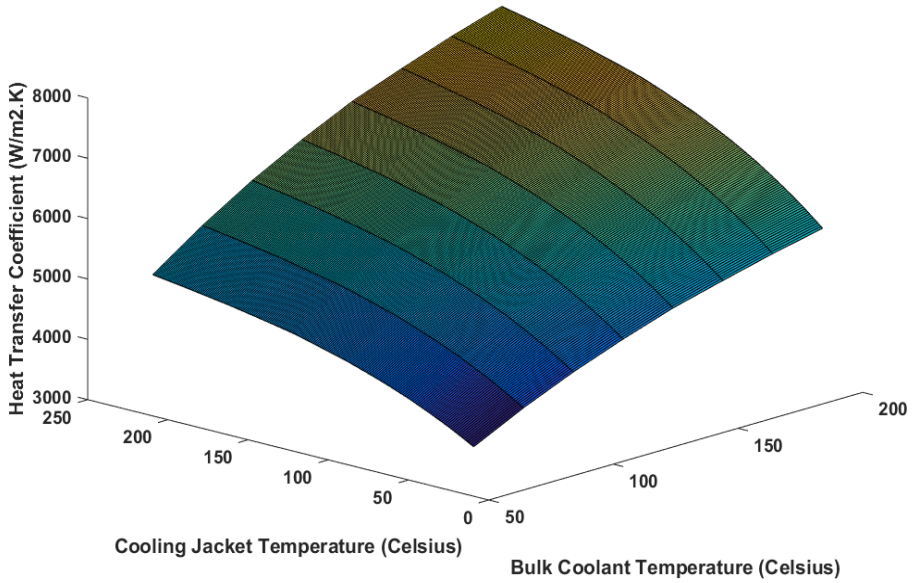

Figure 13: Variation of heat transfer coefficient of the coolant with cooling jacket surface temperature and bulk coolant temperature

2.2.2. Scania D13 Multi-Cylinder HD Engine

To study the potential of an integrated waste heat recovery cooling circuit, a model of a full Scania D13 engine was used. The GT-Power model used here is the one calibrated and implemented by Svensson et al. [47] for the same test setup. It describes the full engine for Partially Premixed Combustion (PPC) operation using Research Octane Number (RON) 89 gasoline as fuel. The model of the engine is shown in Figure 14.

The model describes the engine from the engine intake to the exhaust, both at ambient pressure and temperature. The model includes a turbocharger for the engine, developed specifically for use in partially premixed combustion (PPC) mode. The turbocharger has a variable turbine geometry which is represented in the model with adjustable actuators. The compressor and the turbine of the turbocharger have fully defined maps over the operating range of flow rates and the pressures for air and exhaust gases respectively.

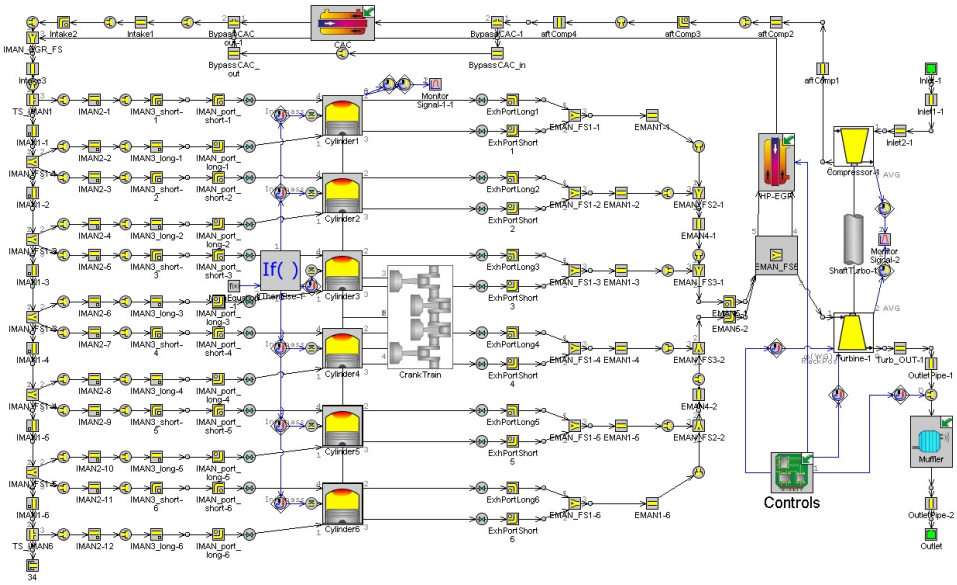

Figure 14: GT Power model for Scania D13 six-cylinder engine

The model includes a high pressure EGR circuit with the low pressure circuit being removed as it was not relevant for the study being performed. The model uses predefined burn rates for the combustion process which are measured experimentally, as detailed in the paper by Svensson et al. [47]

The Flow heat transfer model is used for the heat transfer from the combustion gases to the cylinder walls with a heat transfer coefficient multiplier tuned to get a good match with experimental data. For the heat transfer to the coolant from the cooling channels, no modifications were made from the original model.

2.3. Rankine Cycle Simulation Setups

2.3.1. Single Working Fluid

A Rankine cycle model was used for the early studies on the engine. For these simulations ethanol was chosen as the working fluid. As per Pascual [48], ethanol possesses good thermal characteristics for the range of temperatures seen in IC engine operations. Out of the 6 working fluids evaluated by him, it was seen that refrigerant fluids such as R-245fa have their vapor isobaric lines closer than fluids like ethanol and water. This means that for the same effective expansion ratio there is a lower enthalpy drop and hence lower power generated by the expander. He also

states that water has a narrower operating range due to its thermal characteristics, making ethanol the most suitable out of the working fluids studied. Hence, ethanol was taken as the first working fluid to evaluate the performance of the Rankine cycle.

The reference conditions and the constraints for the Rankine cycle simulation are shown in Table 9.

Table 9: Rankine cycle simulation reference conditions and constraints for single working fluid

Reference Conditions	
Working Fluid	Ethanol
Condensation Temperature (°C)	70
Subcooling (°C)	20
Evaporator Pinch Point (°C)	10
Pump/ Expander Isentropic Efficiency (%)	80
Constraints	
Pressure Ratio (-)	Maximum 40:1
Superheat (°C)	Minimum 20
Working Fluid Mass Flow Rate (g/s)	Unconstrained

The pump and expander efficiency were taken as 80% for this model, similar to values taken by Rijpkema et al. [19] in their study on waste heat recovery systems in HD engines. However, for subsequent models these values were reduced to 60% to reflect more realistic conditions in Rankine cycle systems. The subcooling and condensation temperature were defined so as to have the lowest temperature in the cycle as 50 °C while ensuring sufficient subcooling to maintain single phase inlet conditions to the pump. For this model, the condenser is taken as ideal, i.e. it provides the coolant to the pump at the specified subcooled temperatures at all times.

The evaporator itself is modelled using a pinch point analysis to determine fluid inlet and outlet temperatures. The model optimises for maximum expander power by sweeping the superheat, pressure ratio and working fluid mass flow rate (limited by the constraints) and finding the maximum power point.

2.3.2. Multiple Working Fluids

Rankine cycle models were used for the simulation of two separate waste heat recovery loops i.e. one for the exhaust gases and one for the coolant. The models used are the same as the ones developed by Rijpkema et al. [49]. The models for the Rankine cycles were developed in Modelica with the working fluid properties taken from CoolProp. Multiple working fluids were evaluated for both high temperature and low temperature waste heat recovery.

The boundary conditions and the constraints for the simulation are shown in Table 10.

Table 10: Boundary conditions and constraints for Rankine cycle simulations with multiple working fluids

Reference and Boundary Conditions	
Ambient Temperature (°C)	25
Ambient Pressure (bar)	1.013
Pump/ Expander Efficiency (%)	60
Pump Vapor Quality In	0
Constraints	
Max. Evaporation Pressure (bar)	$min\begin{Bmatrix} 125 \\ 0.9 \cdot pcrit \end{Bmatrix}$
Min. Condensation Temperature (°C)	50
Min. Condensation Pressure (bar)	1.013
Pinch Point (°C)	5
Max. Cycle Pressure (bar)	125
Max. Superheating (°C)	100

The pump and expander efficiency are set to 60% based on previous studies. Constraints are also placed on the evaporation pressure to limit the risk of failure on the system as well as to ensure that the critical pressure and temperature are not reached during operation.

2.4. Uncertainty Analysis

The error analysis for the experimental setups was done for the calculated energy balance terms: heat transfer to the oil, heat transfer to the coolant and exhaust enthalpy. The absolute values for each of the terms are defined as per Equation 4.

$$Heat\ Loss\ (HL) = \dot{m} C_p \Delta T \tag{4}$$

In Equation 4, $\dot{m}$, C_p and ΔT denote the mass flow rate, specific heat and the temperature change of each heat loss medium (the coolant, oil and exhaust gases). For the exhaust gases, the term ΔT denotes the temperature change from the measured temperature of the exhaust gases at the exhaust port to the inlet temperature. The error in the computation of these terms is done using Equation 5.

$$\delta HL = |HL| \cdot \sqrt{\left(\frac{\delta \dot{m}}{\dot{m}}\right)^2 + \left(\frac{\delta \Delta T}{\Delta T}\right)^2} \tag{5}$$

In Equation 5, the terms δHL, $\delta \dot{m}$ and $\delta \Delta T$ denote the error in calculation or measurement of the respective values of heat loss, mass flow rate and temperature difference for any media (coolant, oil and exhaust gas). C_p was assumed constant for the calculations as the specific heat at the mean temperature of the media inlet and outlet. Finally the term $\delta \Delta T$ is calculated using Equation 6.

$$\delta \Delta T = \sqrt{{\delta T_1}^2 + {\delta T_2}^2} \tag{6}$$

In the Equation above, δT_1 and δT_2 are the errors in the measurement of the two temperatures T_1 and T_2 used to calculate ΔT.

3. Results and Discussion

The aim of this thesis work is to develop an understanding of low temperature waste heat recovery from an internal combustion engine. It also looks at how to maximise the efficiency of the powertrain i.e. the engine and the waste heat recovery system combined. The literature review in Section 1.2 showed that the Rankine cycle is one of the most efficient and heavily researched methods for waste heat recovery and described the knowledge gaps in the field of low temperature waste heat recovery.

Most of the work, discussed in the literature review, optimised the waste heat recovery system while not trying to maximise the coolant exergy (keeping the engine operating conditions fixed). They also tended to propose the best working fluid for their application from a narrow range of potential candidates. This thesis, over multiple studies, looks at the combined engine and waste heat recovery system while later expanding the scope of the investigation to a large number of potential candidates for working fluids for the Rankine cycles.

This chapter discusses the results of the studies done in the thesis. It describes the operating points for the engines, the setup for the simulations and the discussions for the results shown.

3.1. Coolant Temperature Sweep Simulations for HD Engine

The first study was done to see the potential of increasing the coolant temperature for an HD engine. The study primarily looked at the effect on the engine itself and the changes in indicated efficiency and the changing energy balance with increasing coolant temperature. The waste heat recovery potential from the exhaust gases and coolant was also studied and how it is affected by the change in coolant temperatures.

For this, a simulation based analysis was done for the Scania D13 single cylinder engine using GT Power (described in Section 2.2.1). The GT Power model was calibrated against engine measurements as detailed in Section 2.2.1. The model was then run for two engine loads, two speeds and three lambda values with the coolant temperature swept from 60 °C to 200 °C for each load-speed-lambda point. The

parameters analysed from these simulations were the changes in heat transfer to the oil and coolant, the change in indicated efficiency and the exhaust gas temperatures. The results from the engine simulations were then used for Rankine cycle simulations in Matlab using a single working fluid (discussed in Section 2.3.1) to study the variation in recoverable power from the coolant and exhaust gases with changing coolant temperature.

3.1.1. Simulation Setup

The simulations for the coolant temperature sweeps were set up for a combination of engine load, speed and lambda values in GT-Power. Multiple operating points were taken for the study to see the trends in heat transfer to the coolant for different engine operating conditions. Varying the engine speed changes the time available for transferring heat from the burned gases to the coolant per cycle and changing engine load affects the heat transfer coefficients as well as the heat released within the combustion chamber thus also affecting the heat transfer. For each load-speed point, three lambda values were tested – λ = 2.4, 1.8 and 1.3. Changing values of lambda also mean changing burned gas temperatures within the combustion chamber which further affects heat transfer to the coolant. The load-speed points and the notations used for them are shown in Table 11. In the next section, these notations are used to explain the results.

Table 11: Notation for temperature sweep cases for Scania D13 single cylinder engine simulation study

	Notation	Conditions
High Load, High Speed	HLHS	18 bar (IMEP gross) 1400 RPM
High Load, Low Speed	HLLS	18 bar (IMEP gross) 800 RPM
Low Load, High Speed	LLHS	10 bar (IMEP gross) 1400 RPM
Low Load, Low Speed	LLLS	10 bar (IMEP gross) 800 RPM

For all load, speed and lambda points, the coolant temperature was swept up from 60 °C to 200 °C in steps of 20 °C. The temperature range was taken to cover a large range, from sub-normal temperatures (lower than 85 °C) to a maximum temperature limit of 200 °C. For each temperature sweep, the Fuel Mean Effective Pressure (Fuel MEP) was kept constant by keeping the amount of fuel injected per cycle constant.

The indicated efficiency (net and gross) and hence the IMEP were allowed to vary with changing coolant temperatures. The intake pressure and temperature for the engine were also kept constant. This means that with changing coolant temperature, the in-cylinder air temperature could be affected which further means varying in-cylinder air density, air mass and lambda value.

The constant parameters for all cases are stated in Table 12.

Table 12: Constant variables for all simulated cases

Rail Pressure	1200 bar
External EGR	0%
Inlet Temperature	50 °C

The inlet temperature specified is the air temperature measured at the intake manifold box before the intake port. The values specified in Table 12 are kept constant to reduce the variability in the analysis presented in this study. In reality the parameters in Table 12 change for different engine applications with different rail pressures, EGR rates and inlet temperatures being used depending on the engine and the operating conditions. An investigation of the impact of changes to these parameters is beyond the scope of this study.

After the coolant temperature sweep simulations, the results are used in the Rankine cycle simulations in Matlab. In the published paper by Singh et al. [50], a simple Carnot efficiency was used to determine recoverable power (described in Equation 7). Here $P_{coolant}$ is the energy transferred to the coolant by the engine per second. T_h and T_c represent the hot and cold source temperatures respectively.

$$Recoverable\ Power = P_{coolant} \cdot (1 - {}^{T_c}/_{T_h}) \tag{7}$$

However, for this thesis to give a more reasonable estimate, a more detailed Rankine cycle simulation was used, using ethanol as the working fluid (described in Section 2.3.1).

The layout of the recovery system is shown in Figure 15. There are two separate loops used for the recovery of waste heat from the coolant and the exhaust.

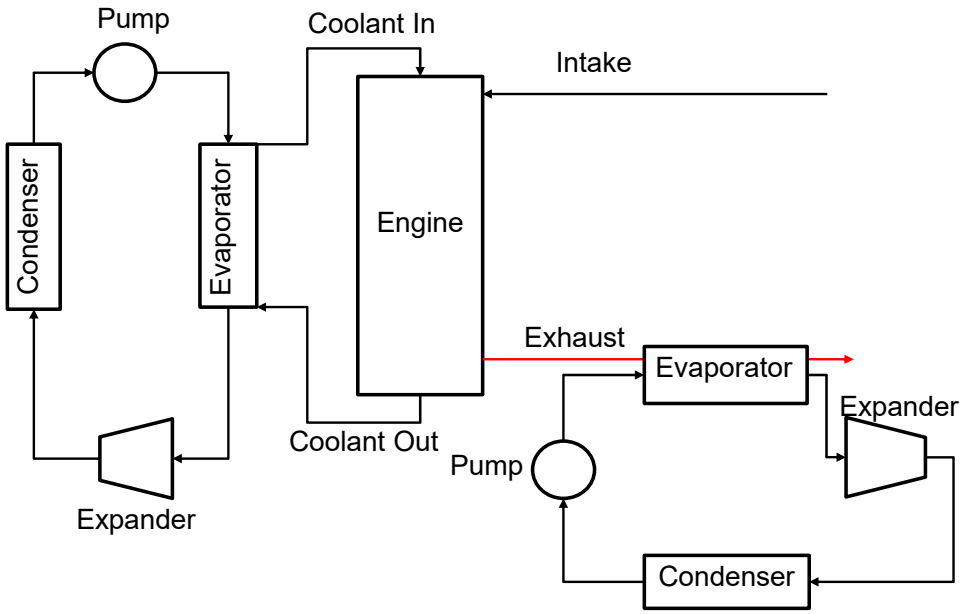

Figure 15: Dual loop waste heat recovery system layout for Rankine Cycle simulation

3.1.2. Results

Energy Balance and Heat Transfer

An energy balance for the engine was done using results from the engine simulations. For a lambda of 2.4, the energy balance is shown in Figure 16. The figure shows that with increasing coolant temperatures, an increase in exhaust gas enthalpy of approximately 2 percentage points is seen with the change in indicated work being insignificant. While the indicated work does show trends with increasing coolant temperature, these effects are small compared to changes in exhaust gas enthalpy. These trends in the energy balance were observed for all simulated lambda value cases.

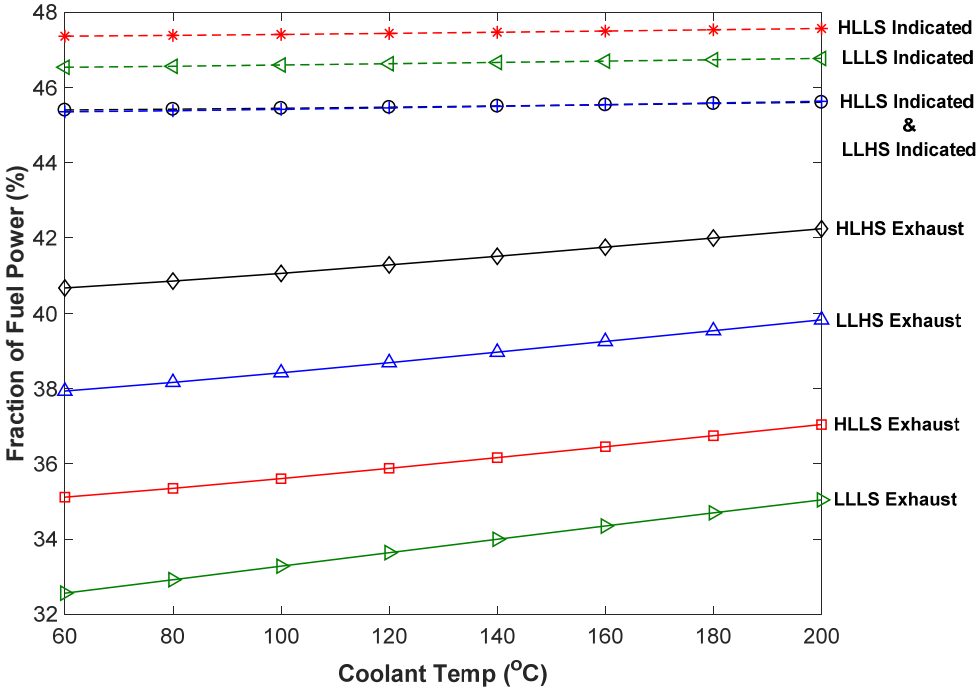

Figure 16: Energy balance (indicated power and exhaust power as fractions of fuel energy) for increasing coolant temperature at lambda 2.4. The indicated efficiency curves for LLHS and HLHS are overlapping

The changes in gross IMEP can be seen in Figure 17. At higher lambda values it was seen that an increase in coolant temperature leads to an increase in gross IMEP, whereas at lambda closer to stoichiometry the gross IMEP starts decreasing. It was also seen that the change in gross IMEP with changing coolant temperatures is higher at lower engine speeds. This is due to the reduced cycle time at higher engine speeds and hence reduced time for heat transfer to the coolant which makes the engine not as sensitive to heat transfer at the higher speed.

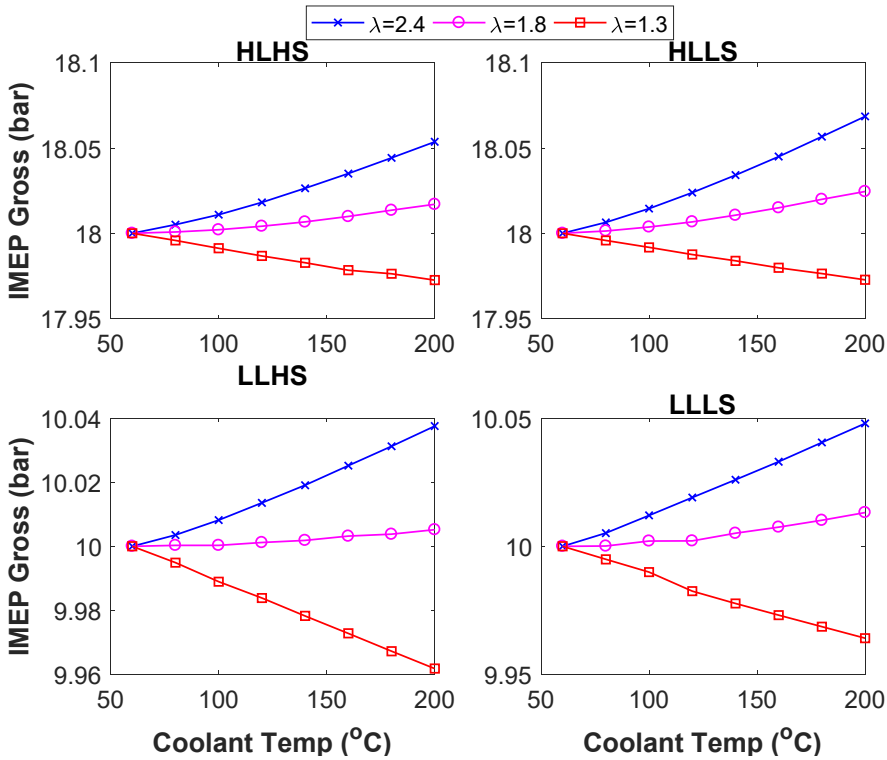

Figure 17: Gross IMEP variation for different load-speed-lambda operating points

From Figure 17 the indicated efficiency is seen to decrease at lower air-fuel ratios with increasing coolant temperatures. For the temperature sweep at each lambda point, the lambda value is fixed at the base coolant temperature of 60 °C and is allowed to vary with increasing coolant temperature. For example: for the coolant temperature sweep at a lambda 2.4 operating point, the lambda is fixed at a value of 2.4 at the coolant temperature of 60 °C and then varies with the temperature sweep.

As the coolant temperature is increased, the heat transfer to the coolant is reduced and the in-cylinder gas temperature increases, further reducing the air density within the combustion chamber. This means lower air mass trapped per cycle in the combustion chamber and a lower lambda value. This decrease in lambda value from its base value can be seen in Figure 18, with increasing coolant temperature.

Lower air mass inducted in the combustion chamber primarily shows two effects: increased combustion temperatures and lower specific heat ratio (γ) of the mixture in the combustion chamber. The increase in combustion gas temperatures means higher heat transfer to the coolant which partially counteracts the reduction in heat transfer to the coolant at higher coolant temperatures. The decrease in specific heat ratio translates to higher pressures and temperatures at exhaust valve opening (EVO). This means more of the energy is moved to the exhaust gases than being

used for producing work on the piston. This is further seen by the higher increase in exhaust gas temperatures at lower lambda values in Figure 20.

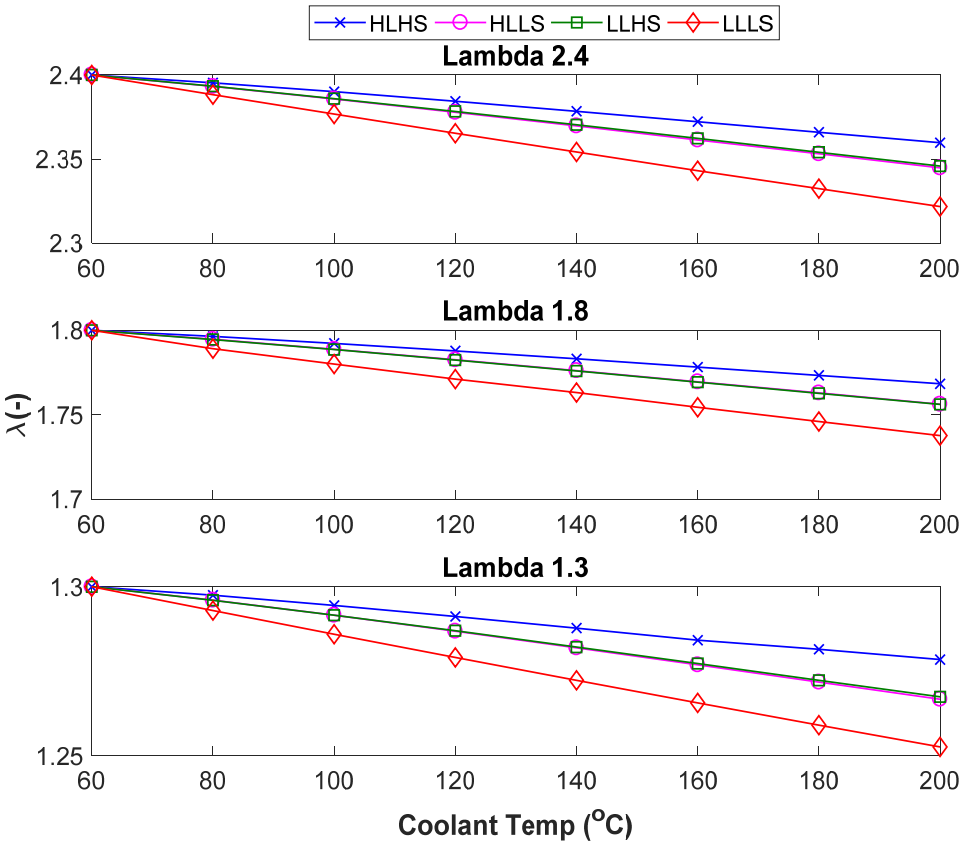

Figure 18: Change in lambda for increasing coolant temperatures

Figure 19 shows the changes in heat transfer from the engine to the oil and the coolant as the coolant temperature is changed. Here, the combined heat transfer to the oil and coolant is shown to decrease; with the heat transferred to the oil increasing. For the simulations, the oil is fixed at a constant temperature of 90 °C. However in actual application, the oil is cooled by the coolant and its temperature is hence dependent on the coolant temperature. For the oil to have a constant temperature, an independent oil cooling circuit is needed in the engine.

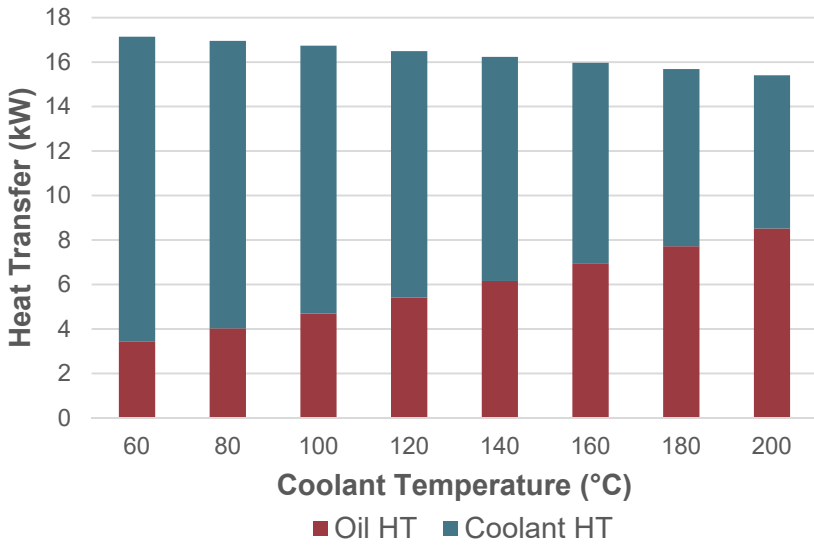

Figure 19: Heat transfer from engine for oil and coolant at lambda 1.8, and high load and high speed conditions

As shown before, the mass flow rate of air, and hence the mass flow rate of exhaust, is reduced through the engine with increasing coolant temperatures. However, Figure 16 showed an increase in exhaust gas enthalpy with higher temperatures. This is primarily because of the increase in exhaust gas temperature with increasing coolant temperatures, which compensates for the small reduction in exhaust gas mass flow rates. This is beneficial for any waste heat recovery cycle, as higher heat source temperatures translate to higher recovery cycle efficiencies. The exhaust gas temperatures are shown in Figure 20.

They are seen to increase by 30 °C to 40 °C for increasing the coolant temperature from 60 °C to 200 °C. It was also seen that for the same load-speed point, the increase in exhaust temperature was higher for lower lambda values, which means more energy is lost through the exhaust gases, leading to lower gross indicated efficiencies.

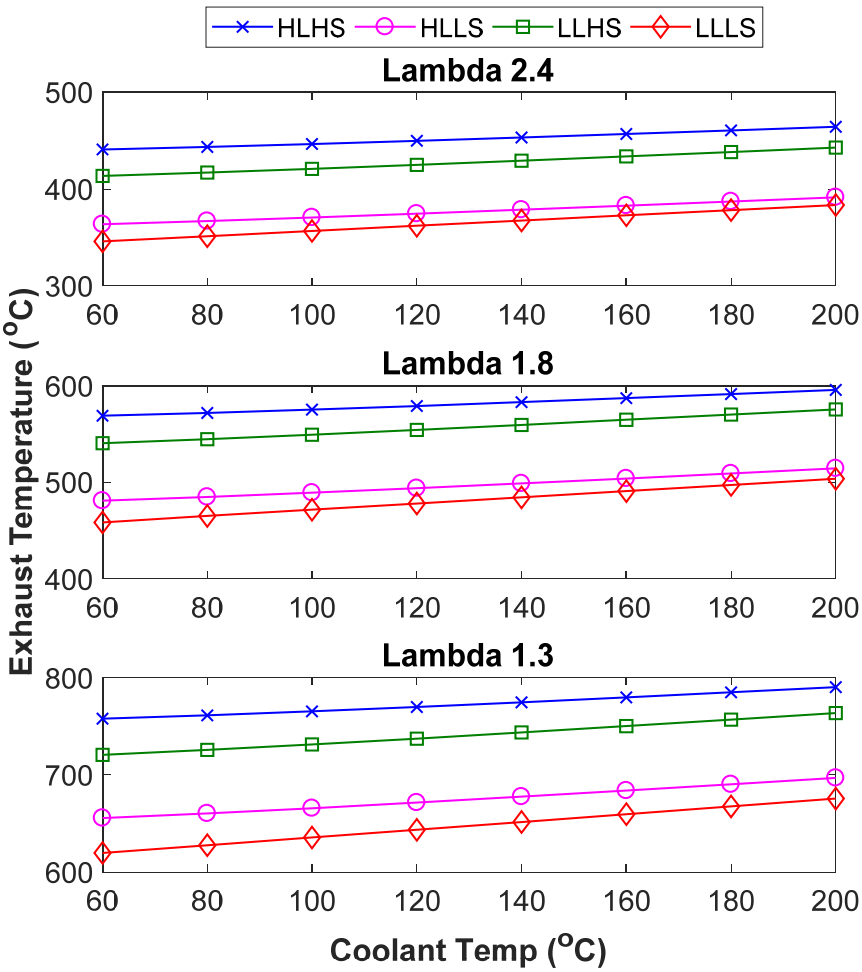

Figure 20: Exhaust temperatures for increasing coolant temperatures

While the total change in exhaust gas temperature is low as compared to the change in coolant temperature, a higher oil temperature might reduce the heat transfer to the oil and increase the exhaust gas temperatures even further.

Recoverable Power

The data from the simulations shown above were then used for Rankine cycle simulations. In the original work by Singh et al. [50], a simple Carnot efficiency was used to show the maximum recoverable power from the exhaust and coolant. However, for this thesis, the simulations are improved upon by simulating a full Rankine cycle with ethanol as the working fluid, to show a better estimate of the actual recoverable power from the engine. The simulation setup is described in Section 2.3.1.

Figure 21 shows the recoverable power from the coolant with changing coolant temperatures. For the lower temperatures of 60 °C and 80 °C the recoverable power is shown as 0 kW. This is because of the condensation temperature of 70 °C where at low temperatures there is no appreciable expansion of the working fluid and hence there is very little deliverable power from the expander. At coolant temperature of 100 °C and higher, the recoverable power increases initially and then decreases, showing an optimum value of temperature, dependent on the engine load and speed.

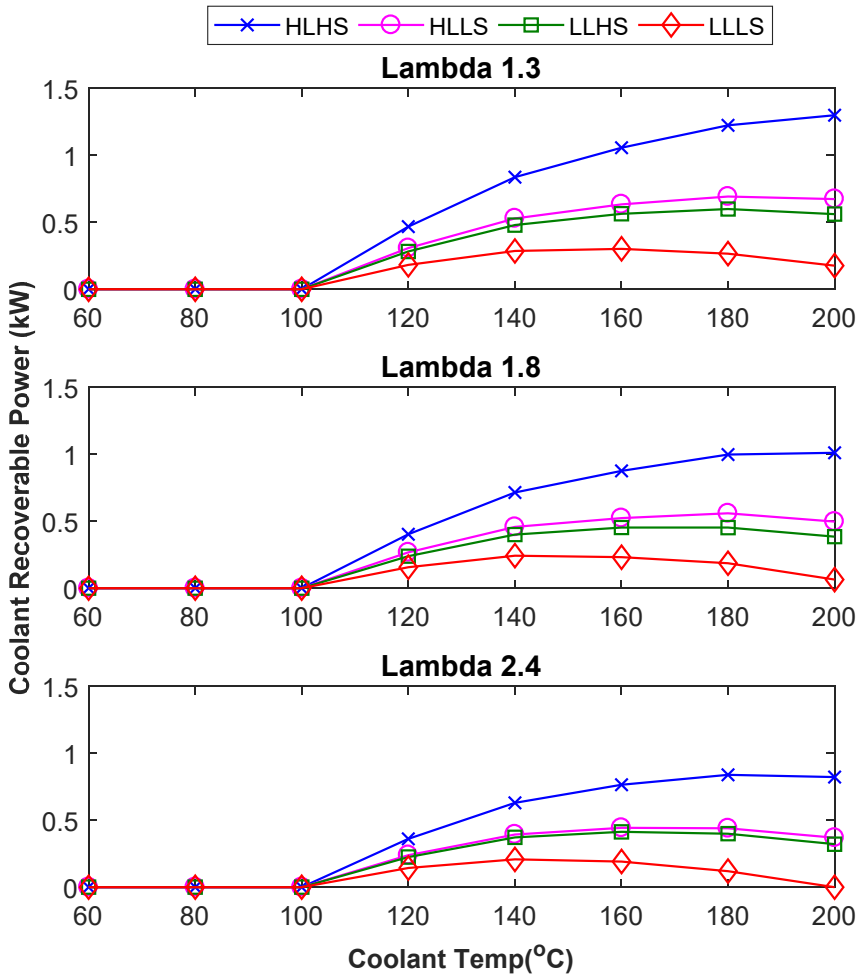

Figure 21: Recoverable power from the coolant with increasing coolant temperature

This is largely because, as the coolant temperature is increased, the recovery efficiency is also improved for the Rankine cycle. However, at higher coolant temperatures the engine also rejects lower amounts of energy to the coolant, thus having lower energy input to the Rankine cycle. Lower lambda values also increase

the heat transfer to the coolant due to higher in-cylinder gas temperatures, resulting in higher recoverable power from the Rankine cycle.

For the exhaust gases, the recoverable power consistently increases with increasing coolant temperature. This is because of higher exhaust gas temperatures and also higher exhaust gas enthalpy with increasing coolant temperatures. Figure 22 shows the recoverable power from the exhaust gases from the Rankine cycle simulations.

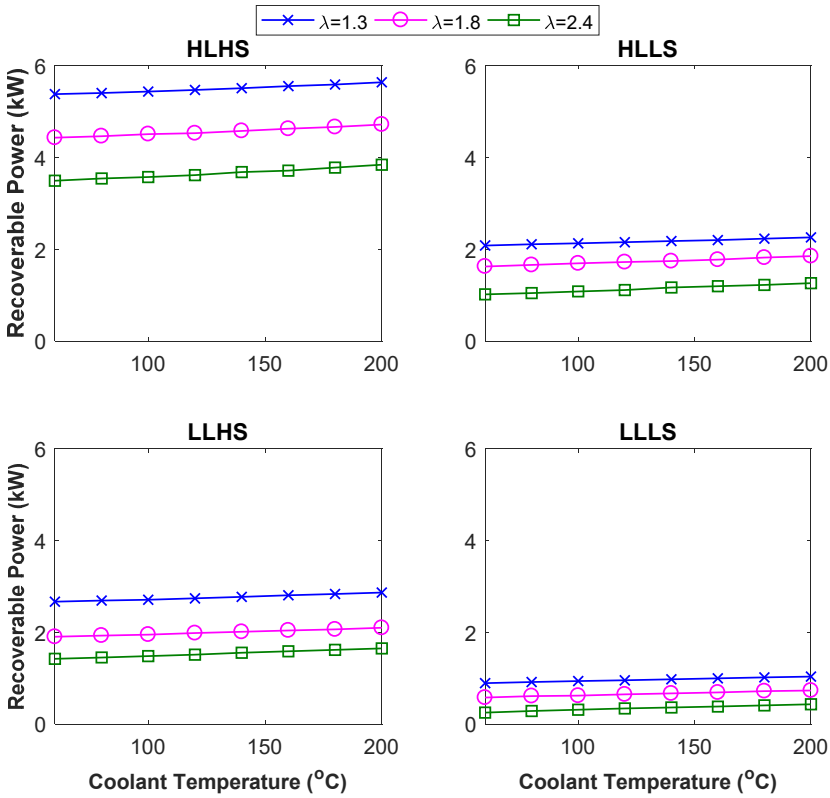

Figure 22: Recoverable energy from the exhaust gases with increasing coolant temperature

The recoverable power from the exhaust gases does not increase significantly with increasing coolant temperatures however. This is mainly because of restrictions placed on the pressure ratios in the simulations, of 40:1. For the coolant temperature sweeps in all cases, the advantage in recoverable power is seen from increasing superheat in the Rankine cycle at higher exhaust gas temperatures. Another reason for this is that a change in exhaust gas temperature of 40 °C is not significantly high enough to provide an appreciable change in Rankine cycle power output.

Figure 23 shows the change in indicated efficiency for the entire system of the engine and the waste heat recovery system by varying the coolant temperature from

60 °C to 200 °C for a lambda of 1.8. The change in indicated efficiency is calculated in reference to the indicated efficiency at 60 °C using Equation 8.

$$Indicated\ Efficiency\ Gain = \left[\frac{(P_{In} - P_{In,60}) + (P_R - P_{R,60})}{P_{fuel}}\right].100 \quad (8)$$

In Equation 2, P_{In}, P_R and P_{Fuel} represent the indicated power, the total recoverable power (exhaust and coolant) and the power from the fuel. $P_{In,60}$ and $P_{R,60}$ represent the indicated and recoverable power at 60°C. Here, both the increase in recoverable power as well as indicated power from the primary thermodynamic cycle are considered.

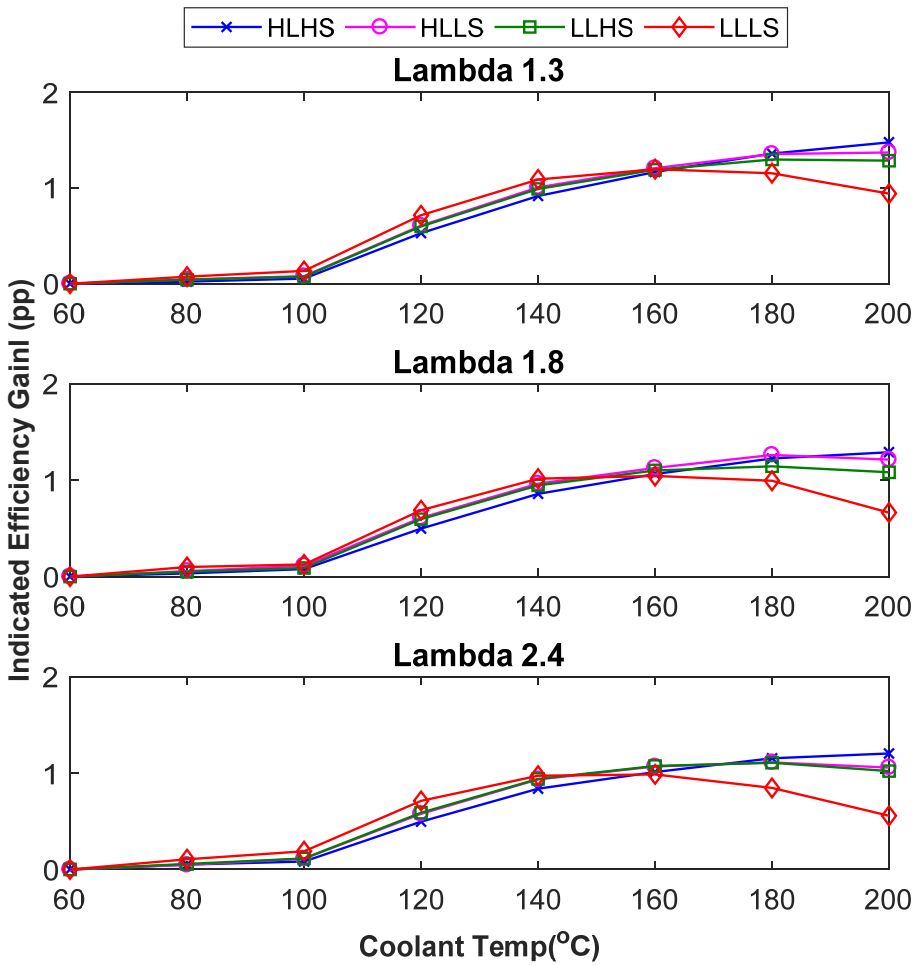

Figure 23: Gain in indicated efficiency in percentage points from base coolant temperature of 60°C

From the figure above it can be seen that at higher loads and higher speeds, the gain in indicated efficiency is higher and the optimum coolant temperature is higher. This is because at higher loads and speed (or higher power), the energy rejected to the coolant is higher and hence the balance point where the engine does not reject enough heat to the Rankine cycle occurs at higher coolant temperature.

3.2. Integrated Cooling System Simulation for HD Engine

The second study was aimed at evaluating the use of an integrated waste heat recovery cooling circuit and its potential for application in an HD engine. In an integrated waste heat recovery cooling circuit, the coolant also acts as the working fluid for the waste heat recovery cycle. The engine adds heat directly to the working fluid in such a system. The engine can in this case be used as a preheater or an evaporator for the working fluid, with the superheating being done using the exhaust gases. Such a system has the advantage of having the working fluid at a higher temperature than when using the engine to transfer the heat to the coolant which further transfers it to the working fluid. The study looks at how the engine and waste heat recovery system behave with the implementation of such a system.

For this study a simulation based approach was used for evaluating the use of evaporative cooling for low temperature waste heat recovery. A fully calibrated GT-Power model for a six-cylinder Scania D13 engine (described in Section 2.2.2), developed by Svensson et al. [47], was used for the purpose of the simulations. The heat transfer to the coolant and the exhaust gas temperatures were used in Rankine cycle simulations using a single working fluid as discussed in Section 2.3.1.

3.2.1. Simulation Setup

The data from the GT-Power model was taken for four different engine loads and four different speeds. The details for the GT-Power engine simulations are shown in Table 13.

Table 13: Parameters varied for the recovery system simulation

Loads (IMEP bar)	5, 13, 19, 25
Speeds (RPM)	800, 1300, 1600, 1900
Combustion Mode	PPC
Fuel	RON 89 Gasoline

The load and speed range were chosen to cover the normal operating range of the engine from low to high loads and speeds. The operating points run for the engine

were a combination of all 4 loads and 4 speeds, which means that 16 operatng points were run for the simulations. For each operating point, the SOI, the turbine geometry and the EGR rates were optimised for maximising efficiency.

There are multiple reasons why PPC was used as the combustion concept for this study instead of CDC. Firstly, PPC as a combustion concept has been shown to obtain high gross indicated efficiencies [9]. For the purpose of maximising powertrain efficiency, a high engine gross indicated efficiency is a good starting point. Another reason why PPC is well suited for waste heat recovery applications is the use of high EGR rates. This means that there is increased potential for recoverable power without taking heat from the exhaust gases that pass through the turbocharger. This further means that the components such as the turbocharger and the exhaust after treatment system (EATS) can operate as normal and does not need to be modified for lower gas temperatures, which would be the case if the waste heat is taken from the exhaust gases.

Two different configurations were tested for using the engine cooling circuit integrated with the waste heat recovery circuit: using the engine as a pre-heater and using the engine as an evaporator. The system layout circuits are shown in Figure 24.

Figure 24a shows the recovery circuit configuration when using the engine as an evaporator. Here the preheating and the superheating is done using the heat from the EGR gases. The vaporisation of the working fluid/coolant is done using the heat transferred in the coolant channels as well heat from the EGR heat exchanger. A bypass valve is also modeled in the circuit to bypass some of the working fluid across the superheater and the expander. The bypass valve is used to ensure a minimum amount of superheating. If the mass flow rate of the working fluid is high and the heat from the EGR gases is not sufficient to provide adequate superheated vapour, some of the working fluid is bypassed across the evaporator, superheater and the expander.

Figure 24b shows the system layout when using the engine as a preheater. Here, the assumption taken was that the energy required to heat up the working fluid to the liquid saturation point is provided by the engine heat. The energy then required to vaporise and superheat the working fluid is provided by the EGR gases. Similar to Figure 24a, a bypass valve is provided in the circuit to ensure that there is a minimum amount of superheating.

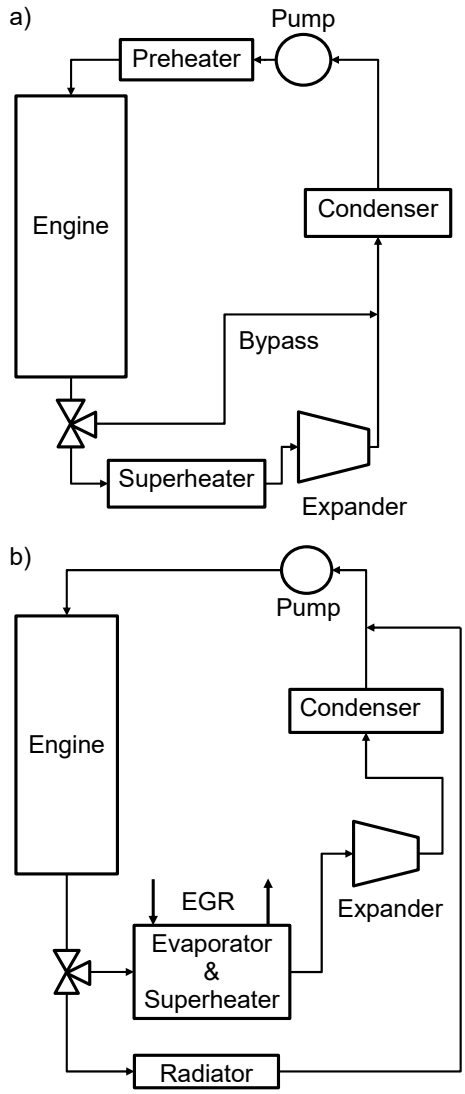

Figure 24: System layouts for simulation of Rankine cycle waste heat recovery when a) Using the engine as an evaporator b) Using the engine as a preheater

3.2.2. Results

Figure 25 shows the recoverable power from the waste heat recovery system comparing the use of the engine as a preheater, as an evaporator and only using the heat from the EGR gases. Higher loads and higher speeds also show more recoverable energy due to more waste heat available for the recovery system.

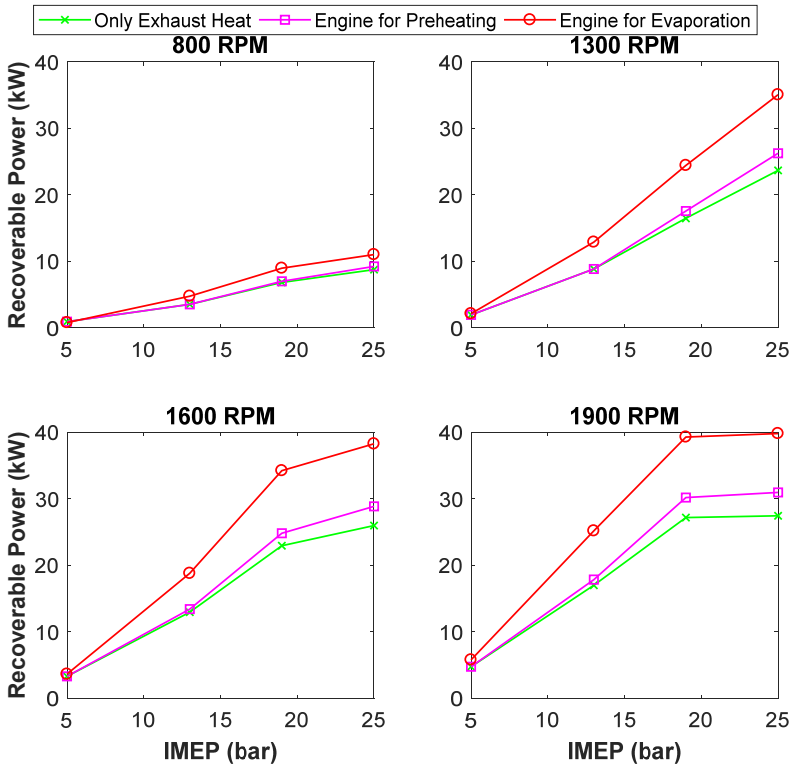

Figure 25: Recoverable power for different waste heat recovery systems

Similarly, the gain in system efficiency can be seen in Figure 26 when implementing these waste heat recovery systems. It is seen that when using the engine as an evaporator, the waste heat recovery system provides a significant increase in recoverable power. However, when using the engine for preheating the fluid, the change in system efficiency is minimal and only visible at high loads. This is explained in Figure 27.

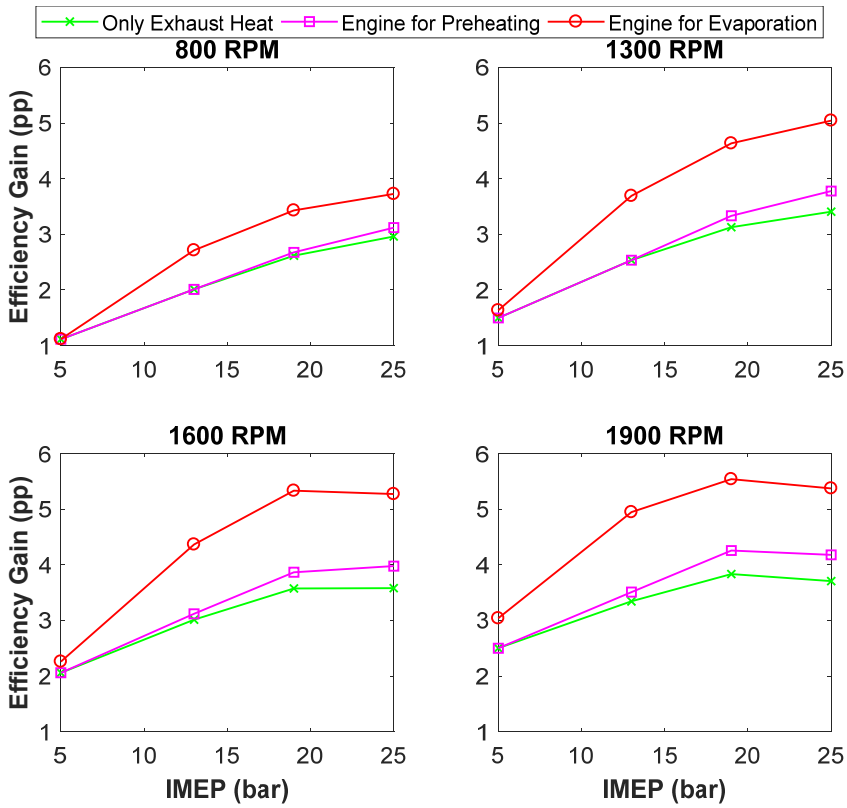

Figure 26: Efficiency gain in percentage points for the recovery systems

In Figure 27, the blue line shows the change in enthalpy with temperature for the EGR gases. The red line represents the relationship between enthalpy and temperature for the working fluid/coolant as it is heated up. On the working fluid line, line 1-2 represents the coolant, from the subcooled condition to saturated liquid condition. Line 2-3 represents the vaporisation phase and line 3-4 represents the superheating line.

In such diagrams, the limiting factor is the pinch point of the heat exchanger which is taken as 10 K for the simulation.

Figure 27a shows that for the lower load case, the pinch point is located at the saturated liquid point for the working fluid. Hence, using the engine for the preheating would still have the pinch point located at the same point. This means that there is no more additonal heat that can be extracted from the EGR gases.

However, Figure 27b shows that for the higher load case, the pinch point is located on line 1-2. This is because, at higher loads and speeds, the mass flow rate of the working fluid is increased, which reduces the slope of the working fluid lines in the

plot. This moves the pinch point lower to the condensation point for the water in the EGR gases.

Hence, if the heat for preheating the working fluid is taken from the engine, the mass flow rate of the working fluid can be increased till the pinch point is reached at the liquid saturation point.

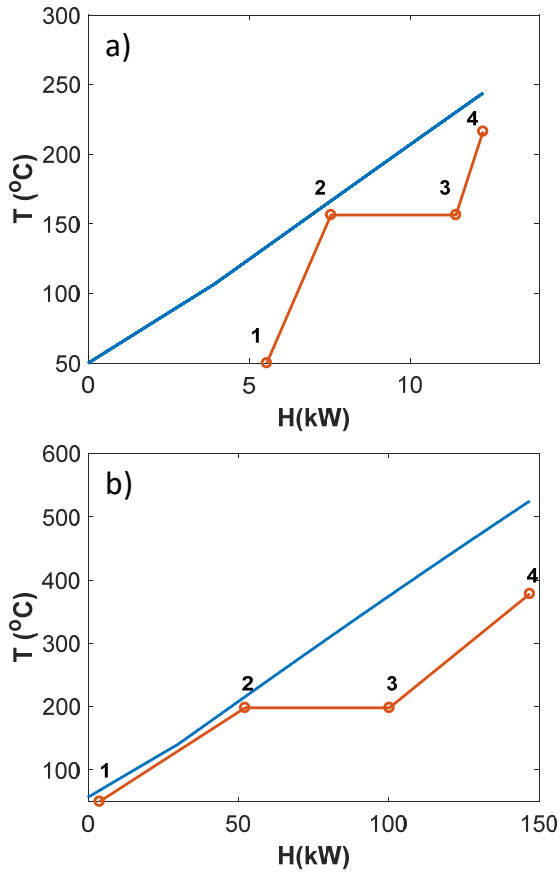

Figure 27: Pinch point curves for a) 5 bar IMEP, 800RPM and b) 25 bar IMEP, 1900 RPM

When using the engine as an evaporator, the pinch point curve is shown in Figure 28. Here, the pinch point occurs at Point 1 (subcooled liquid) as the engine provides the major part of the heat for vaporisation and the vaporisation line (line 2-3) is reduced. This allows for higher mass flow rates of the working fluid till the pinch point in the heat exchanger is reached, thus having a higher power output from the expander.

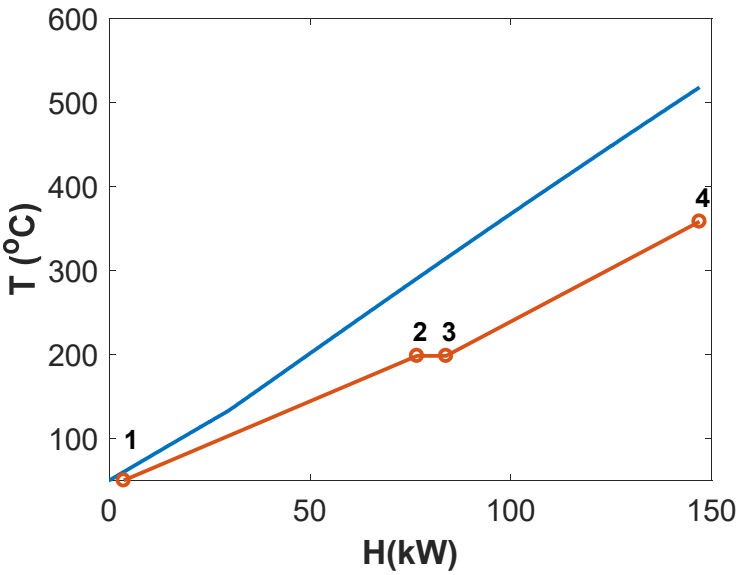

Figure 28: Pinch point curve when engine is used as an evaporator at 25 bar IMEP and 1900 RPM

It should be noted here that Figure 28 shows both the preheater and the superheater. From Point 1 to Point 2 shows the preheater, whereas from Point 2 to Point 4 shows the superheater.

3.2.3. Sensitivity Analysis

One of the main assumptions for this simulation study was taking the heat transfer from the coolant as constant, as per normal engine operation. The assumption essentially means that the higher heat transfer coefficients due to the vaporising flow of the coolant is sufficient to account for the higher coolant temperatures which means that the heat transferred to the coolant is remained unchanged. To study the implication of this assumption, a sensitivity analysis was done for all 16 operating points with respect to heat transfer from the engine.

First the GT Power simulation was modified to change the heat transfer to the working fluid/coolant by +/- 10% of its original value. This also affects the temperature of the EGR gases which was taken into account for the waste heat recovery simulations. These values are then used for determining the recoverable power and the variation in it with varying heat transfer. This is shown in Figure 29 where the error bars represent the change in values of recoverable power with changing heat transfer.

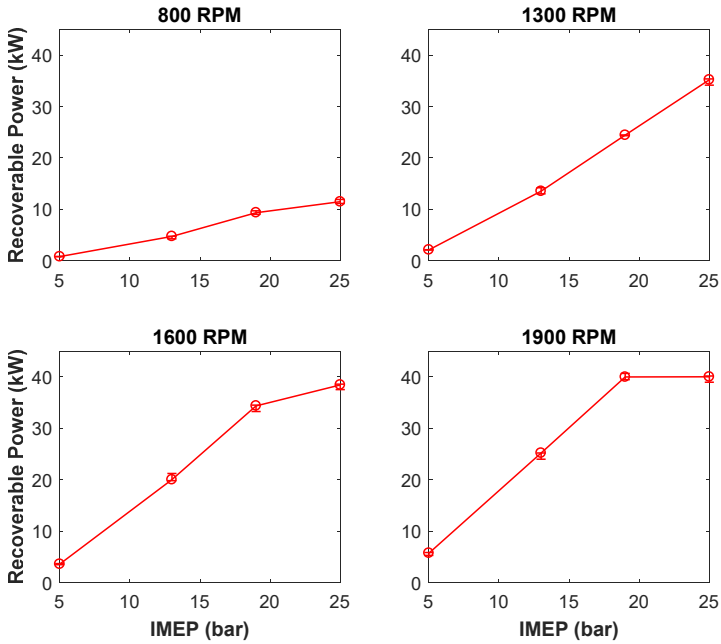

Figure 29: Sensitivity analysis for heat transferred to the coolant for the integrated evaporative cooling system. The error bars represent the change in recoverable power

As shown, the recoverable power does not vary significantly when changing heat transfer by +/- 10 %. This is because, as described before, the simulation optimises the system for obtaining the most power. For example, if the heat transfer to the coolant is reduced, then the temperature of the EGR gases is increased, this means that the system can increase the amount of superheat and increase the efficiency of the recovery cycle to compensate.

3.3. System Comparison – Integrated WHR and Dual-Loop WHR

The previous sections show the results of two different implementations of low temperature waste heat recovery and methods to increase the coolant exergy for an internal combustion engine.

Section 3.1 showed a dual-loop Rankine cycle setup with the coolant and exhaust gases having separate Rankine cycles for recovery of waste heat. The study looks into increasing the coolant temperature to reduce heat transfer to the coolant and also increase the exergy of the coolant and the exhaust gases to improve the waste heat recovery process.

Section 3.2 showed a system where evaporative cooling can be used to transfer the engine heat more effectively to the working fluid by using the coolant as the working fluid itself. It also shows that using evaporative cooling, a major benefit can be seen in recovering the heat more effectively from the exhaust gases and the engine cooling channels.

It is difficult to perform a fair comparison of these two systems as the simulation setups are different in engine configuration and combustion mode. However, one method to compare both systems would be to compare the overall cycle efficiencies. This is defined as the output power at the expander shaft divided by the input power from the coolant as well as the gases.

This method has a caveat, in that it only compares the efficiency of the two recovery systems, without taking into account changes in the engine itself. For example, some parameters might increase the efficiency of the recovery cycle but reduce the overall efficiency of the system. However, this can still be considered valid as the previous studies in elevated coolant temperatures show that the engine is not affected significantly with regards to gross indicated efficiency.

Figure 30 shows the recovery cycle efficiency for three different lambda values for a dual loop Rankine cycle waste heat recovery system with increasing coolant temperatures. The maximum cycle efficiency seen is 16% at the highest coolant temperature simulated, of 200 °C. The efficiency shown is higher at lower lambda values due to the higher exhaust gas temperatures.

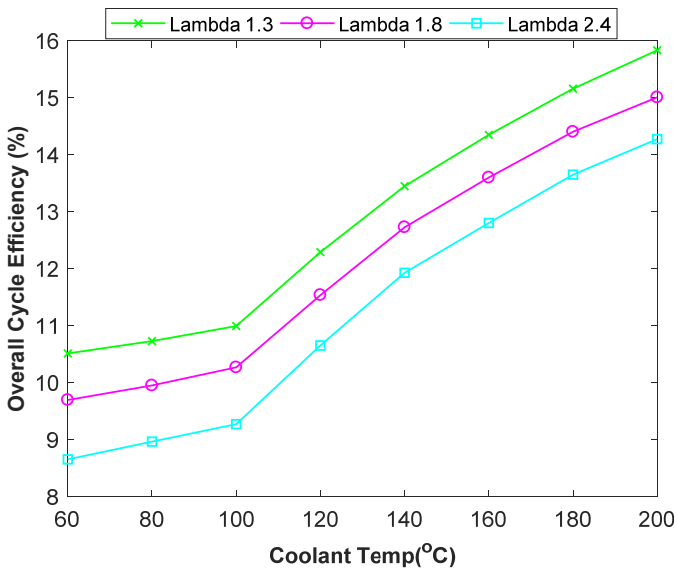

Figure 30: Overall cycle efficiency for coolant temperature sweep simulation for 18 bar, 1400 RPM

Similarly, the overall cycle efficiency for the integrated waste heat recovery loop is shown in Figure 31 for all simulated points at 1900 RPM. Here, the highest cycle efficiency obtained is 20% when using the engine as an evaporator.

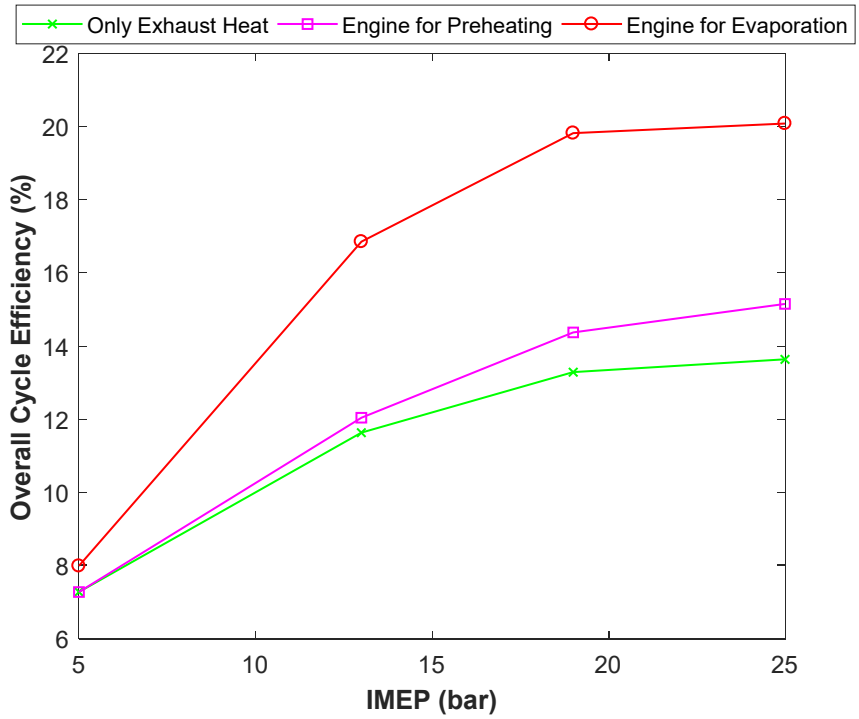

Figure 31:Overall cycle efficiency for the integrated waste heat recovery system at the highest speed point simulated

While at first glance an integrated coolant waste heat recovery system shows a better recovery efficiency for a thermal energy input, it also limits the waste heat recovery in some aspects. The vaporisation temperature of the working fluid/coolant and hence the pressure ratio is determined by the coolant temperature and the heat transfer required. In this way the recovery potential from the exhaust gases is also limited by the coolant temperature. It is possible that the exhaust gas or EGR gas is at higher temperatures, but cannot fully achieve the pressure ratio desired as it is limited by the coolant temperature required to achieve suitable heat transfer. In contrast, when using a dual-loop waste heat recovery system, the pressure ratio and operating parameters of both loops can be optimised according to the heat sources.

In addition to this, evaporative cooling itself has some mechanical challenges in implementation. To implement such a system would mean redesigning the coolant channels within the engine to account for the increased pressure in operation. Corrosive fluids like ethanol could also damage the engine so the range of working fluids that can be implemented would be limited. Prediction and control of boiling

flow regimes within the coolant channels is also not a predictable phenomenon, especially in harsh, vibrating conditions such as a running engine. Hence, to always ensure that a flow regime that enables complete wall wetting within the cooling channels is also a challenge.

3.4. Experimental Coolant Temperature Sweeps for LD Engine

The third study was aimed at evaluating the effect of elevated coolant temperatures on LD engines and the waste heat recovery system, using a Volvo D4 LD engine (specifications given in Section 2.1.2). For the engine part of the study, experiments were performed on the Volvo engine. The coolant temperature was swept from 80 °C to 160 °C for multiple operating points of the engine. Trends in the energy balance, heat transfer to the oil and coolant, engine efficiencies (brake, gross indicated and mechanical) and NOx emissions were studied. These results were then used for dual-loop Rankine cycle simulations (described in Section 2.3.2), performed by Jelmer Johannes Rijpkema at Chalmers University of Technology. The simulations were used to evaluate 48 working fluids for both high temperature and low temperature waste heat recovery. The results from the simulations showed the best working fluids for each application as well as the maximum recoverable power for each operating point.

3.4.1. Experimental Setup

The Volvo LD engine was run across two different engine loads and speeds, with the coolant temperature being increased from 80 °C to 160 °C in steps of 20 °C. However, at the lower load (IMEPg), it was seen that the coolant temperature could go up to only 120 °C after which the heat transferred to the coolant becomes negligible. This is caused by the lower amount of heat generated within the combustion chamber at lower loads. Two different loads were taken to see the change in response of recoverable power and optimum coolant temperature with load. Taking two different engine speeds also affects the heat transferred to the coolant by changing the coolant, fuel and air mass flow rates. Table 14 shows the operating points for the experimental temperature sweep for the engine.

Table 14: Operating points used for experimental campaign

	Point 1	Point 2	Point 3	Point 4
Load (Bar IMEPg)	10		15	
Engine Speed (RPM)	1200	1800	1200	1800
Indicated Power (kW)	20	30	30	45
Injection Pressure (Bar)	900			
CA50 (ATDC)	10		15	
Fuel	Diesel MK1			
Temperature Sweep (°C)	80 to 120		80 to 160	
Lambda	1.9		1.6	
Intake Temperature (°C)	50			
Back Pressure	~= Intake Pressure			
Oil Temperature (°C)	110			
Oil Type	SAE 10 W-60			
External EGR	0%			

A PID controlled heater was used to keep the intake temperature constant at 50 °C. This was to prevent an increase in intake air temperature at higher coolant temperatures due to hotter intake ports. The back pressure was maintained the same as the intake pressure to simulate a turbocharger. The oil temperature was kept at 110 °C with an SAE 10 W-60 oil being used. This is a higher viscosity oil than used in actual application, used as a preventive measure to keep the oil from losing viscosity and causing damage to engine components at higher temperatures.

Injection pressure was kept constant at 900 bar to keep the pressure rise rate under 10 bar/CAD for all operating points. For each operating point, the injection duration was kept constant, while varying the SOI to keep the combustion phasing (CA50) constant. However, it was seen that the combustion phasing is largely unaffected by the coolant temperature. Hence, the SOI for each sweep was effectively constant. The CA50 was changed for the different load points to keep the peak pressure rise

rate under 15 bar/CAD to prevent damage to the in-cylinder pressure sensor and stay within acceptable limits of NVH.

3.4.2. Uncertainty Analysis

For the experiments the accuracy of each sensor is detailed in Table 5 in the Methodology chapter. The errors computed here are for the major heat losses from the engine – to the coolant, oil and exhaust gases. The errors in brake power and frictional losses are not shown here as they are negligible compared to the other errors in the figure. The errors in the exhaust gas enthalpy are low due to high exhaust gas temperatures and the low relative error of the thermocouple in comparison.

For the measured results, the error analysis for the calculated parameters: heat transfer to the oil, heat transfer to the coolant and exhaust enthalpy is shown in Figure 32 over the coolant temperature sweep range. The errors in brake and friction are not shown as they are negligible compared to the other errors shown in the figure.

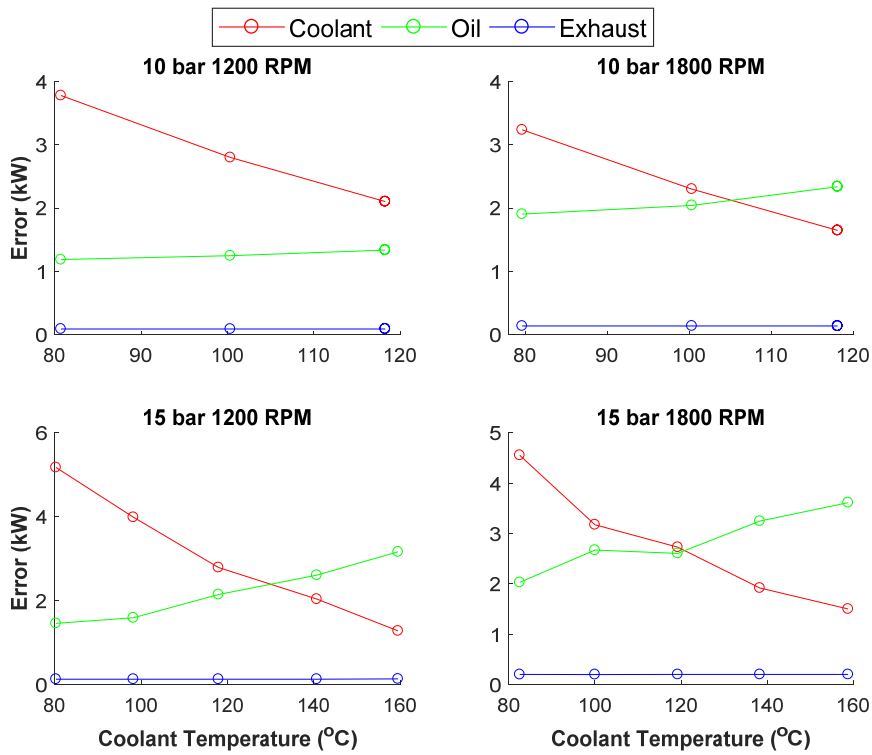

Figure 32: Experimental error for computed values

With increased coolant temperature, the absolute error in determination of heat transfer to the coolant is reduced. This is due to the reduction in the actual heat transfer to the coolant itself. Similarly at higher coolant temperatures, the heat transferred to the oil increases and the absolute error in computation also increases. While the error margin is high in relative terms, this is mainly because the flow rate of the engine coolant and oil is maintained to have a maximum temperature differential of 10 °C between inlet and outlet to the engine. This is to prevent large temperature gradients in the engine which would promote uneven metal temperatures and negatively affect the engine.

However, even with these error margins, trends can be observed in the computed values of heat transfer to the oil and coolant. For example, at the 15 bar, 1200 RPM operating point, the calculated errors in heat transfer to the coolant are 5.2 kW and 1.3 kW at 80 °C and 160 °C respectively. The absolute values of heat transfer going from a coolant temperature of 80 °C to 160 °C is from 19 kW to 1.3 kW. Hence, with these computed values a trend can be observed in the data with the given errors as the reduction is absolute values is much higher than the combined errors.

3.4.3. Experimental Results

Energy Balance

An energy balance done for the operating point of 15 bar IMEPg, 1200 RPM and 110 °C oil temperature is shown in Figure 33. Here, as was seen for the previous simulation studies on the Scania single cylinder D13 engine (Section 3.1), a reduction is seen in the heat transfer to the coolant, while the heat transfer to the oil is increasing. The ‘Remaining’ term in the energy balance is the energy remaining from the fuel energy injected per cycle that is not accounted for in the other terms. This includes all other kinds of losses, but mainly the heat loss from the engine to the ambient air in the test cell. It can be seen that the Remaining term is also increased at higher coolant temperatures, due to higher engine metal temperatures which increases the heat loss to the ambient air.

The exhaust brake and frictional losses seem unaffected but show significant trends and are discussed further down.

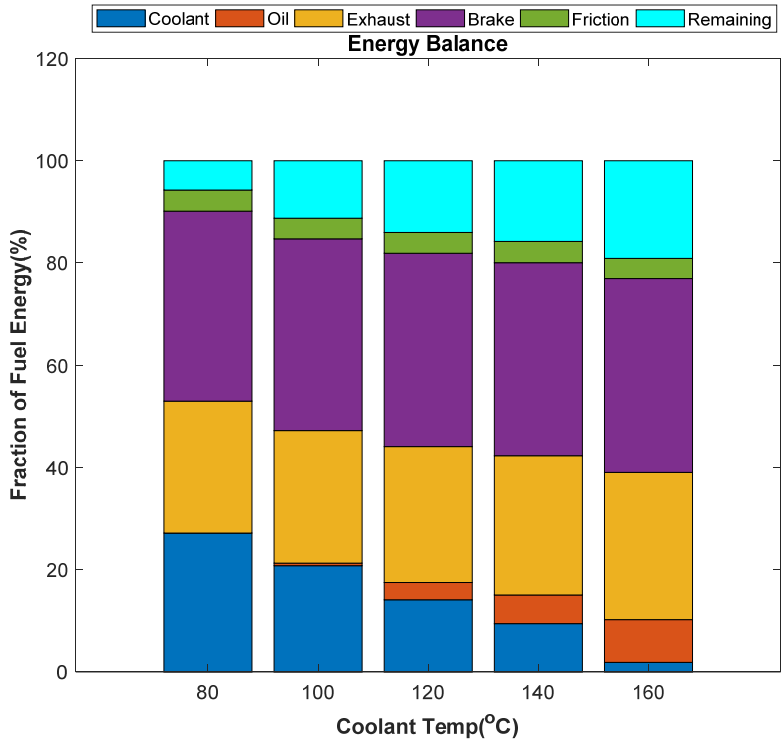

Figure 33: Energy balance for temperature sweep at 15 bar load, 1200 RPM, 110 °C oil temperature

For the energy balance, the frictional power is measured using the difference between the brake power measured by the torque sensor and the indicated power calculated from the in-cylinder pressure measurements. It is assumed here that the frictional power is transferred completely to the oil and acts to heat it up. Hence, for the energy balance, the frictional power is subtracted from the heat transfer to the oil to account for only the direct heat losses.

These trends in the energy balance with increasing coolant temperature were seen for all operating points tested.

Assuming the Remaining Energy term as primarily consisting of the energy lost to the ambient air, the direct heat losses for the engine can be considered as the sum of the heat loss to the oil, coolant and ambient air. Figure 34 shows the total heat loss to the ambient. It can be seen that the direct heat loss is also reduced for all operating points with increasing coolant temperatures.

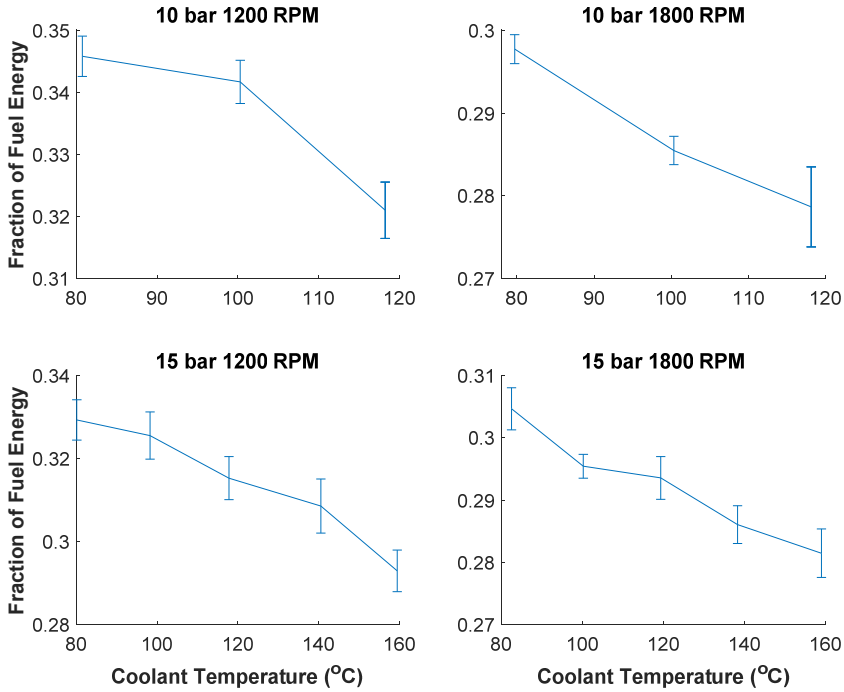

Figure 34: Net heat loss for 110 °C oil temperature points shown as a fraction of the fuel energy

Engine Efficiency

Figure 35 shows the change in brake efficiency with coolant temperature. The increase in brake efficiency is largely due to the increase in indicated efficiency due to the lowered heat loss (shown in Figure 36) and the mechanical efficiency due to lower oil viscosities (shown in Figure 37). It is also seen that at higher engine loads, the brake efficiency does not increase any further beyond a coolant temperature of 120 °C.

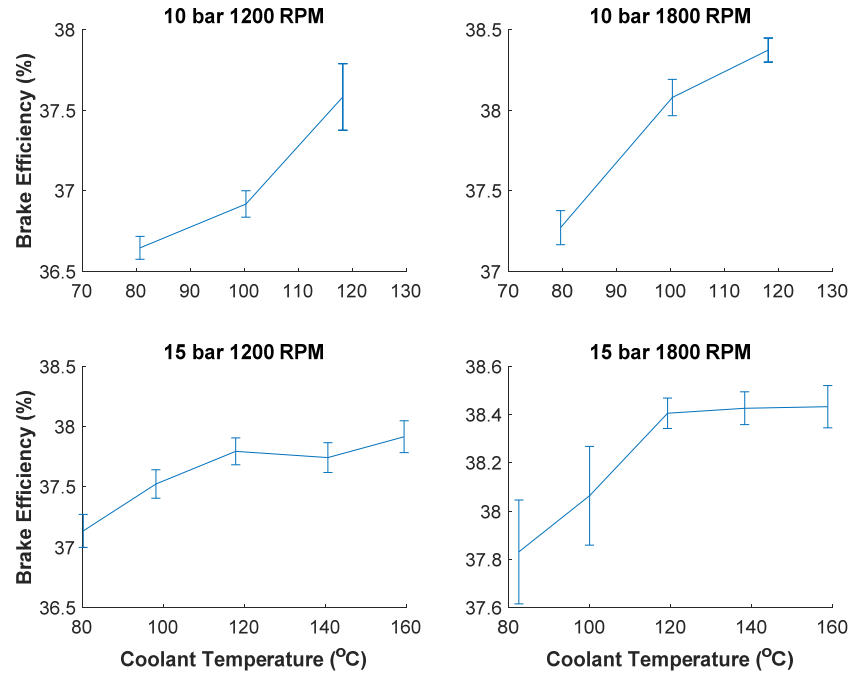

Figure 35: Engine brake efficiency with increasing coolant temperatures

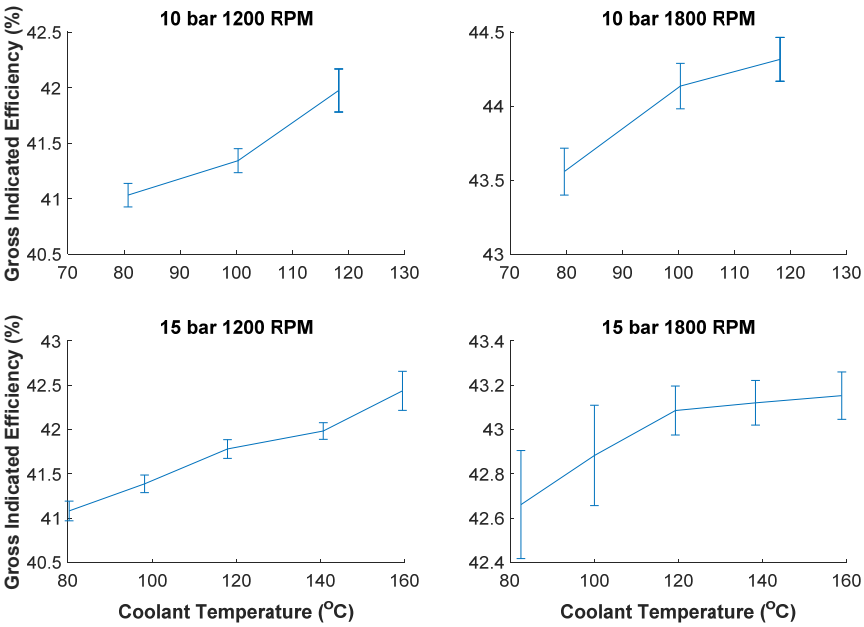

Figure 36: Gross Indicated efficiency with increasing coolant temperatures

From Figure 37, it can be observed that the gain in mechanical efficiency is higher for increasing engine speeds at higher coolant temperatures. Higher engine speeds mean higher frictional losses, which further makes it more sensitive to changes in oil viscosity. At the lower engine speed, the changes in mechanical efficiency are seen to be insignificant.

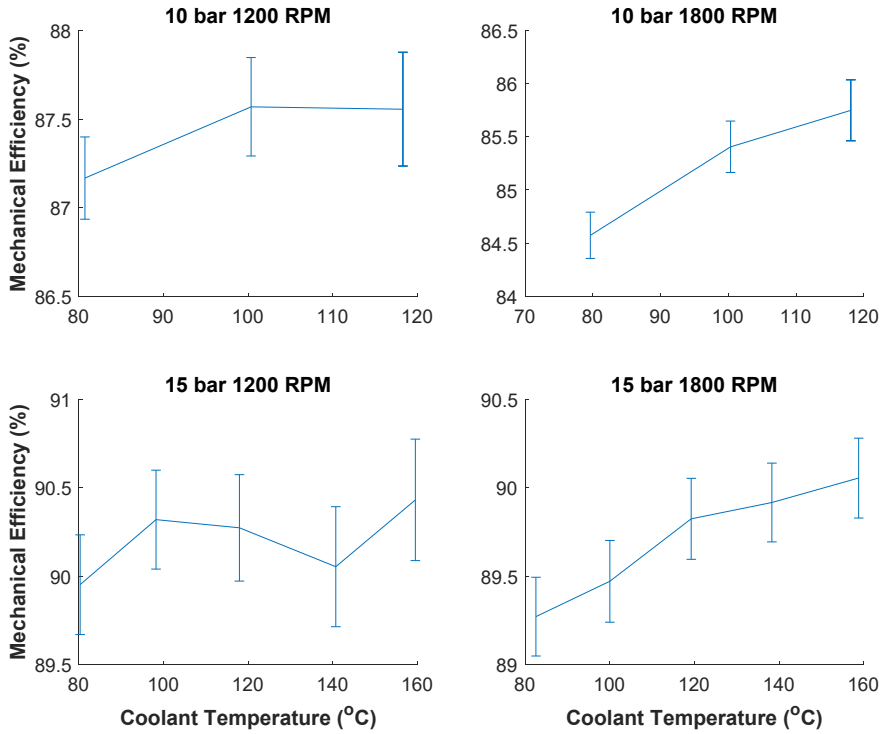

Figure 37: Mechanical efficiency for increasing coolant temperatures

Exhaust Gas Temperatures and Enthalpy

Increased exhaust gas temperatures are seen at higher coolant temperatures, as shown in Figure 38. At higher loads the increase in exhaust gas temperature is over 20 °C.

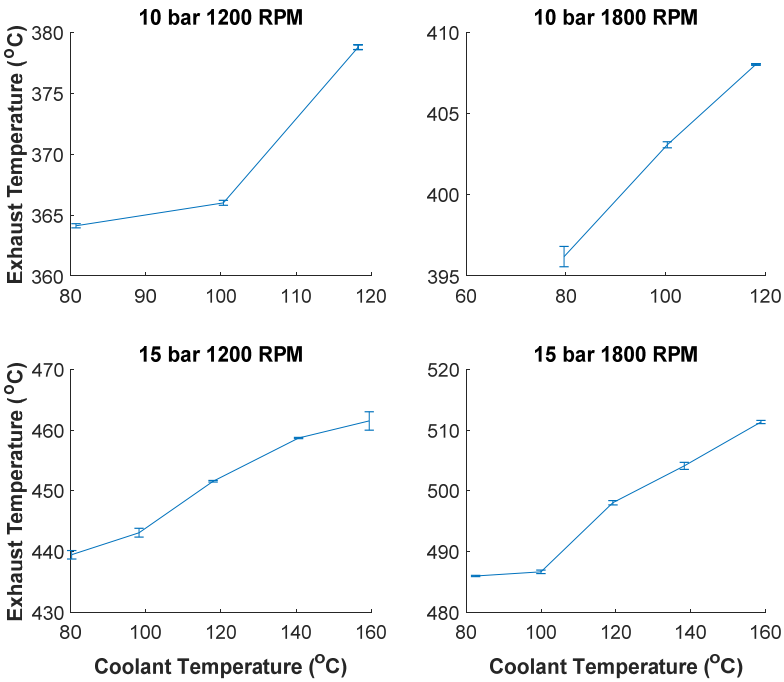

Figure 38: Exhaust gas temperatures (measured at ports) for changing engine temperatures

However, the exhaust gas enthalpy (shown in Figure 39) does not change significantly with the coolant temperature increase. While it does increase, at higher coolant temperatures the reduction in mass flow rate of air, due to higher cylinder temperatures, reduces the exhaust gas enthalpy. Hence, in some cases higher coolant temperatures show a plateau in exhaust gas enthalpy.

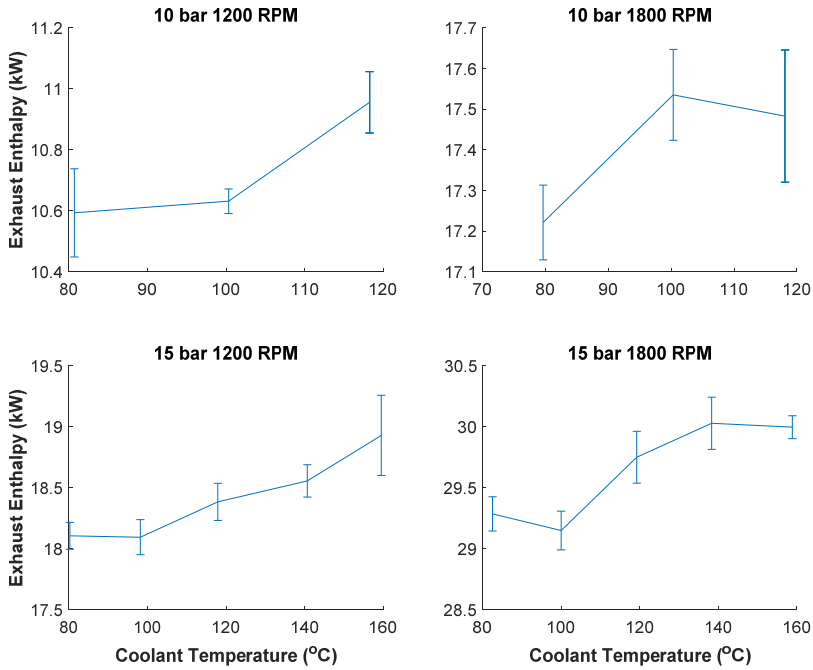

Figure 39: Change in exhaust enthalpy for increasing coolant temperatures

NOx Emissions

The NOx emissions for increasing coolant temperatures are shown in Figure 40. Higher coolant temperatures translate to higher in-cylinder temperatures which further means higher thermal NOx. At the 10 bar IMEP, 1800 RPM point the NOx emissions are reduced at higher temperatures. This is because of the reduced air flow at higher coolant temperatures. While the NOx emissions always increase in parts per million (ppm) with coolant temperature increase, because of the reduced airflow, the emissions in g/kWh are reduced as the total mass flow rate of NOx is reduced.

Another effect seen here is the higher NOx emissions at lower loads. This is because of the relatively advanced combustion phasing (CA50) for the 15 bar IMEPg load point. Earlier combustion also means higher in-cylinder temperatures and higher NOx emissions. The engine speed also affects NOx production in the combustion chamber, with higher engine speeds showing lower NOx production as higher engine speeds mean lower residence time for the combustion gases in the cylinder.

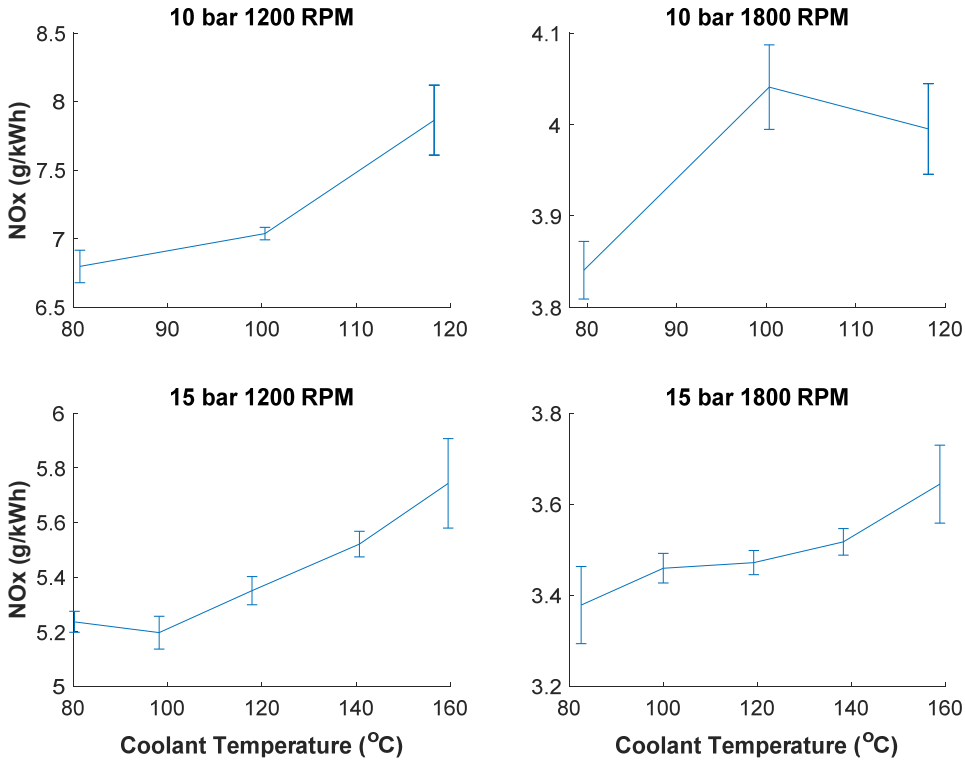

Figure 40: NOx emissions for increasing coolant temperatures

3.4.4. Simulation Results

The results from the experimental runs were used for the simulation in Modelica using 48 working fluids for the recovery cycles. Figure 41 shows a scatter plot of all the different working fluids plotted with the maximum recoverable power against the pressure ratio at which the maximum power is achieved. The plot is shown only for the 15 bar gross IMEPg and at 1800 RPM.

For the coolant, cyclopentane provides the highest recoverable power with up to 1 kW of power recovered for the highest load-speed point. This is seen for all operating points tested. The reason for this is that the best performing fluid depends largely on the temperature profile of the heat source, which for the coolant, is controlled for each engine operating point.

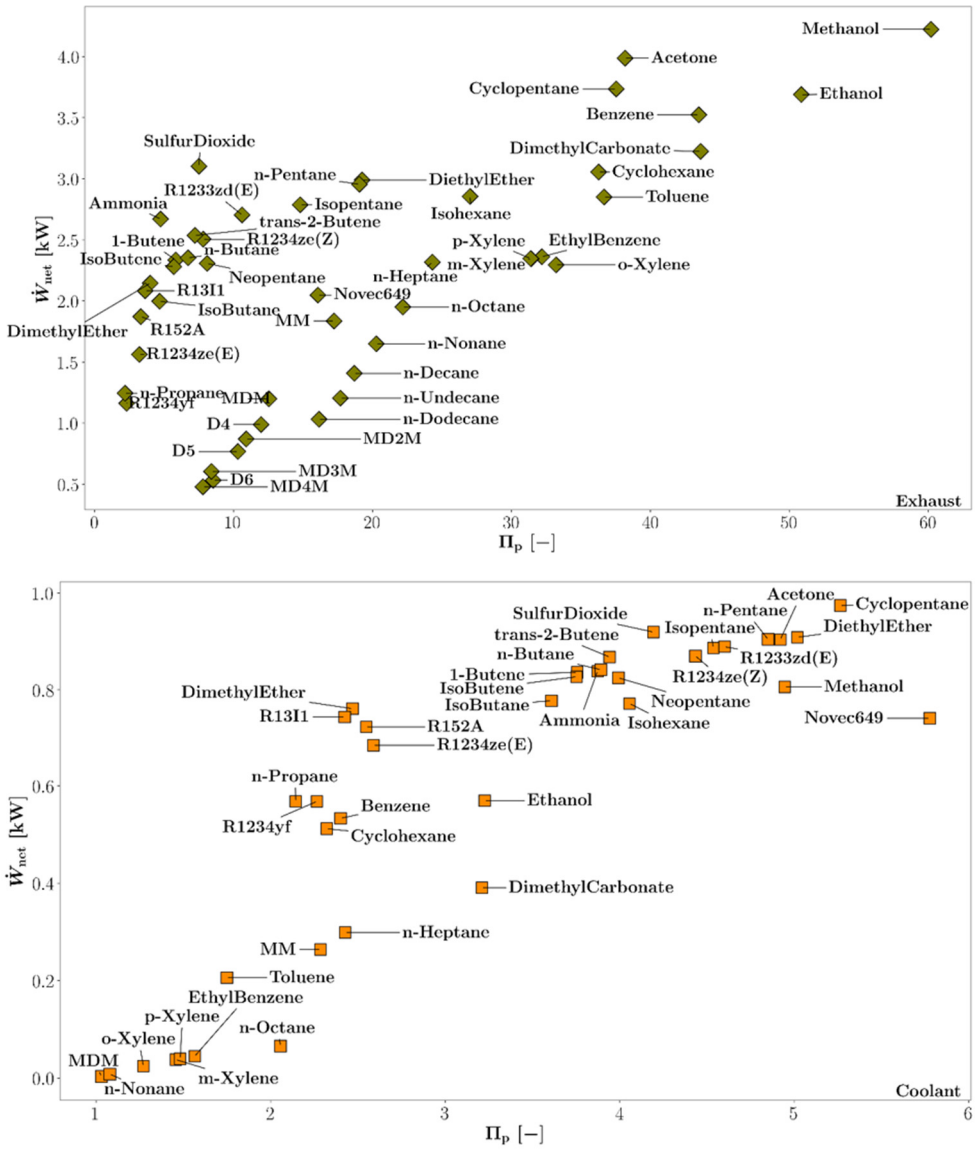

Figure 41: Maximum power output from the (top) exhaust and (bottom) coolant recovery loop for the different working fluids tested at 15 bar gross IMEP, 1800 RPM operating point

For the waste heat recovery from the exhaust gases, a maximum power output of 4.25 kW is seen from the results for the highest load-speed point. At lower loads (10 bar IMEPg), as the exhaust gas temperature and the flow rate changes, the temperature profile of the heat source changes as well. Hence, at lower loads, acetone is the best working fluid. However, with higher loads and speeds, methanol becomes exceedingly better than the other working fluids.

Figure 42 shows the recoverable power from the best performing fluids for each operating point. For the coolant, as shown in previous studies, there is an optimum coolant temperature to maximise recoverable power. For the exhaust gases, the recoverable power generally increases with increasing coolant temperatures. However, there are points where this trend is not followed and this is because of the reduction in exhaust mass flow rates and hence a reduction in exhaust gas enthalpy. The change in recoverable power from the exhaust gases is also not as large as from the coolant. This is because of the relatively low change in exhaust gas temperatures and exhaust gas enthalpy.

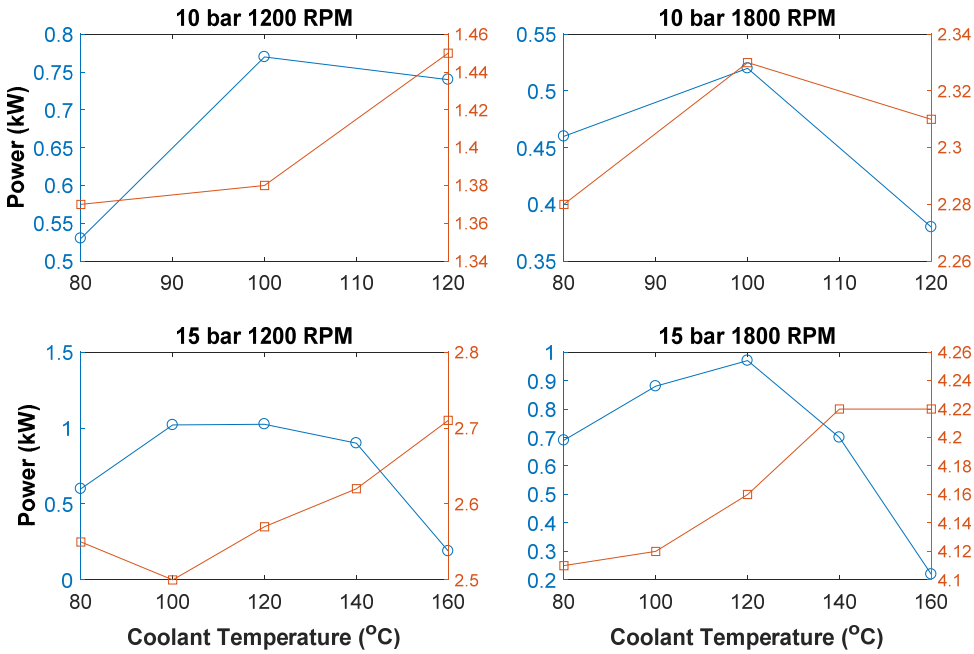

Figure 42: Recoverable Power from the expander for the best performing working fluids for each operating point. The blue line shows the power recovered from the coolant and the orange line represents power recovered from the exhaust

The combined change in system efficiency as a result of recovering power from both the sources is shown in Figure 43. The system efficiency is calculated as per Equation 9.

$$\eta = \frac{Brake\ Power + Recovered\ Power}{Fuel\ Power} . 100 \qquad (9)$$

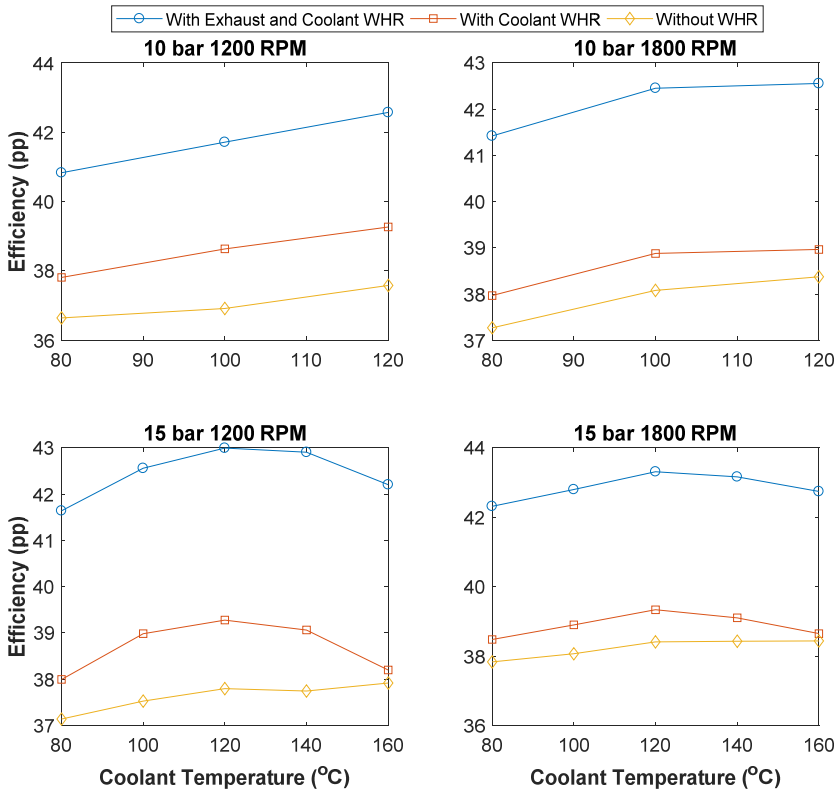

Figure 43: Overall system efficiency with and without the use of a waste heat recovery system

In Figure 44 it can be seen that the implementation of a waste heat recovery system has a significant effect on the system efficiency. The maximum gain in efficiency is 5.2 percentage points, with the contribution from the coolant waste heat recovery amounting to approximately 1.7 percentage points.

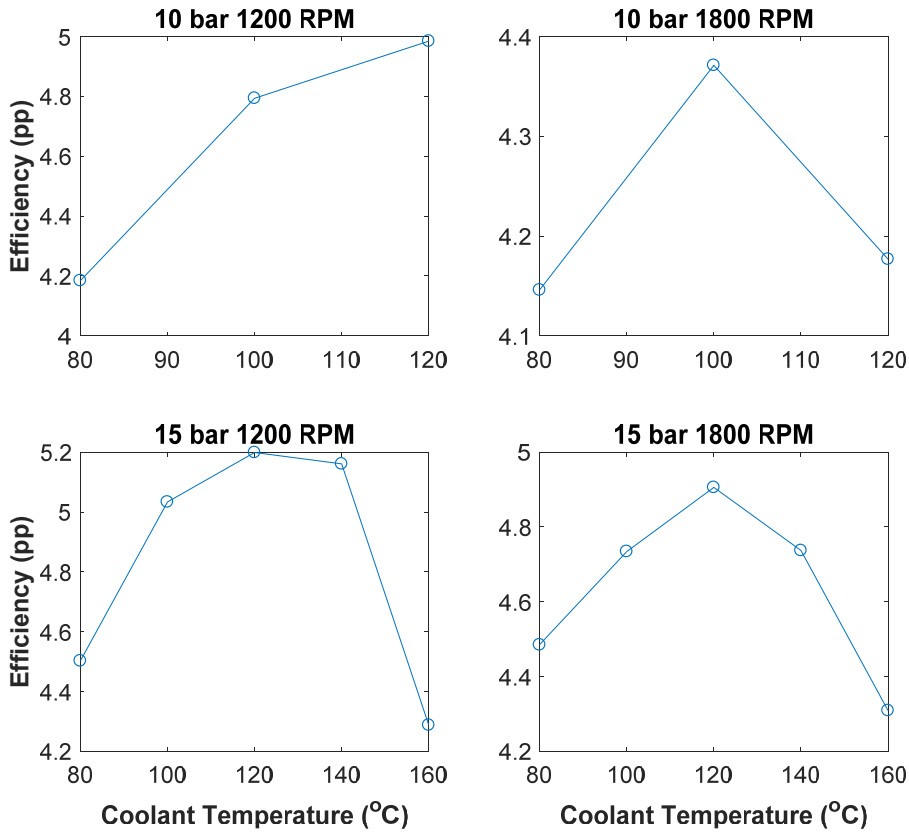

Figure 44: Efficiency improvements in percentage points from the implementation of a waste heat recovery system

3.5. Low Temperature WHR Optimisation and Evaluation over a Transient Cycle

The final study of the thesis aimed at evaluating the potential reduction in fuel consumption for the six cylinder Scania D13 heavy duty engine (described in Section 2.1.3) over the World Harmonized Transient Cycle (WHTC). The effect of coolant temperature on the fuel consumption was also studied.

For the experimental part of the study, the engine was varied in load, speed and coolant temperature. The data from the experiments was first used to generate models for the net indicated efficiency, the heat transfer to the coolant and the exhaust gas enthalpy for the engine using a multi-linear regression analysis. The experimental data was also used for Rankine cycle simulations (detailed in Section

2.3.2) using 10 working fluids for both the exhaust gases and the coolant. The analysis then proceeded in Matlab, to calculate the potential reduction in fuel consumption when implementing a dual loop Rankine cycle WHR system with elevated coolant temperatures.

3.5.1. Experimental Setup

For the study, the Scania D13 six cylinder engine was run for multiple load, speed and coolant temperature points to generate a model for the engine. The range of values selected for the experimental runs is shown in Table 15.

Table 15: Range for experimental parameters for the Scania D13 mapping experiments

	Minimum	**Maximum**
Load (IMEPn bar)	5	16
Speed (RPM)	800	1600
Coolant Temperature (°C)	80	140

The coolant used for the engine was pure ethylene glycol. For the coolant temperature, the initial map was designed to be varied up to a coolant temperature limit of 160 °C. However, it was seen that the coolant overflowed from the expansion tank due to excessive boiling at a temperature of 145 °C. Hence, the maximum coolant temperature limit was taken as 140 °C and the experiments were redesigned.

On a load-speed map, the operating points can be seen in Figure 45. In the figure, the highest load point was 16 bar in net IMEP. This is due to the non-stock turbocharger used for the engine which results in the lambda for the engine going below a value of 1 at higher engine loads.

The engine mapping was initially done using an inscribed central composite design between the loads of 8 bar to 16 bar net IMEP and the engine speeds of 800 RPM to 1600 RPM. However, it was seen that the model for heat transfer to the coolant lost accuracy over the lower load range. Additional points were then run for the engine over the load range of 5 bar to 8 bar net IMEP to better capture the low load range behaviour.

In total, 41 operating points were measured in the operating range described in Table 15.

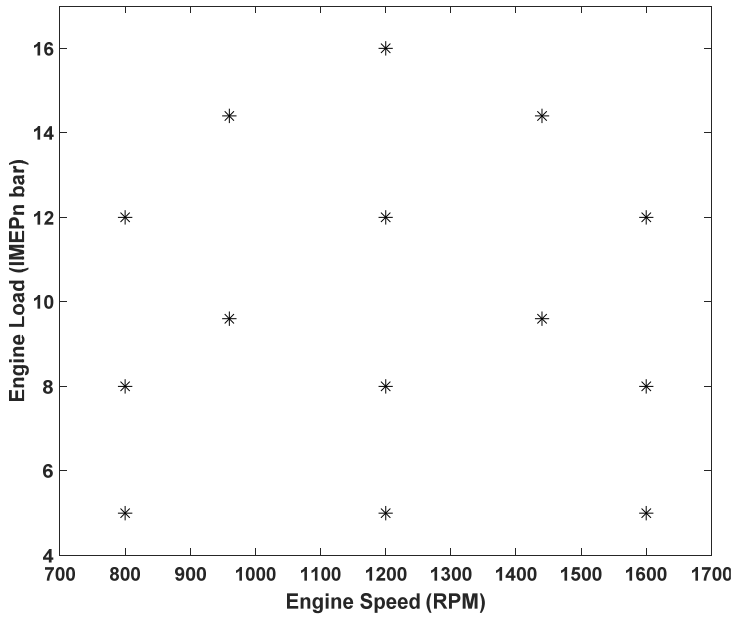

Figure 45: Load-speed points for the Scania D13 multicylinder engine setup mapping

The fuel injection pressure for all points was fixed at 1000 bar. The combustion phasing for all engine operating points is taken as linearly varying with load. The combustion phasing (CA50), depended on engine load as can be seen in Figure 46.

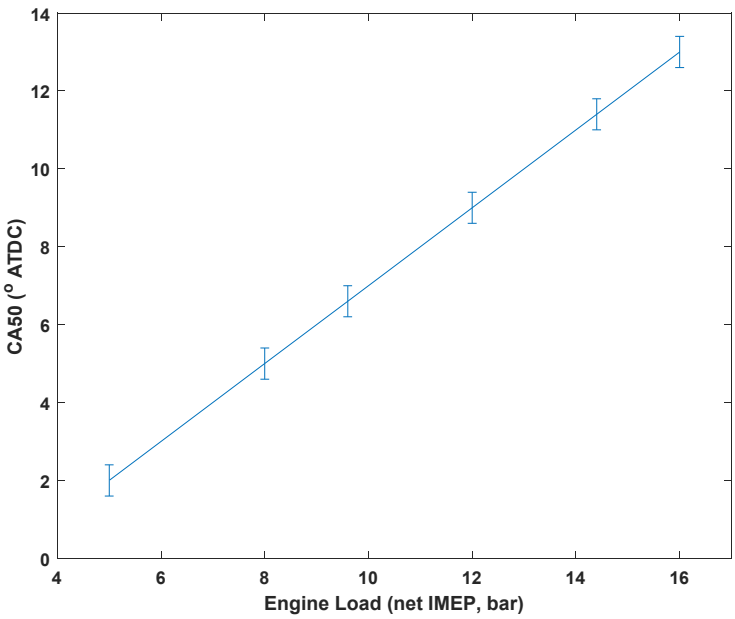

Figure 46: Combustion phasing (CA50) versus engine load for the mapping runs

While the combustion phasing strategy is not based on actual application of the Scania D13 engine, it was not considered as a critical aspect of the study. This is because the study is comparative for only looking at the effect of increased coolant temperatures independent of the combustion control of the engine. A linearly varying combustion phasing strategy was used to have predictable behaviour for the regression analysis.

The error bars in Figure 46 show the maximum variation in combustion phasing control for each engine load. The combustion phasing was controlled for only one cylinder of the engine as there is cylinder-to-cylinder variation. Accordingly, the model generated for the net indicated efficiency is only based on data from the controlled cylinder.

The oil used for engine lubrication was taken as an SAE 10W-60 oil to prevent engine damage and a loss in lubrication at higher coolant and oil temperatures.

3.5.2. Uncertainty Analysis

The uncertainty on the heat transferred parameters was computed as detailed in Section 2.4. The uncertainty in heat transfer to the coolant is shown in Figure 47 for all operating points.

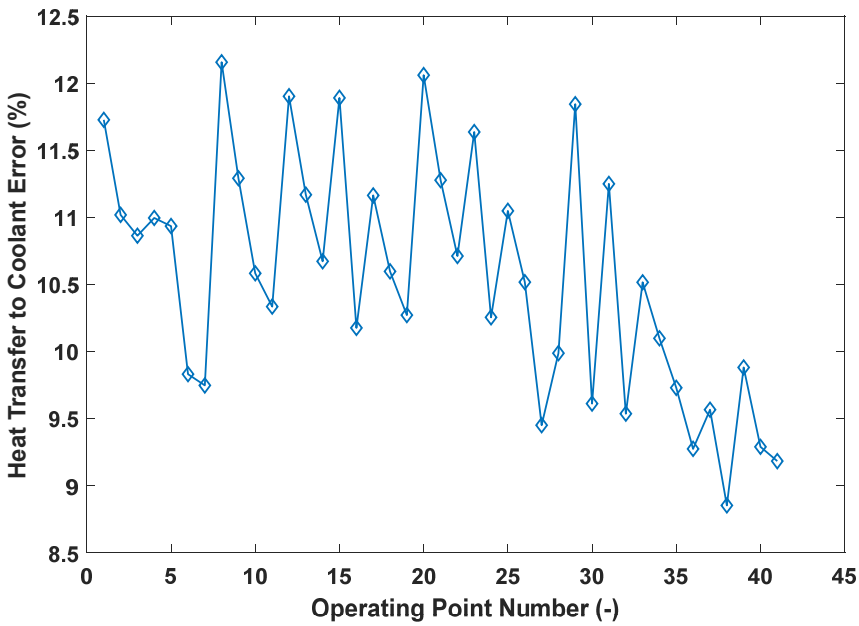

Figure 47: Error in calculation of heat transfer to the coolant for the engine speed of 1200 RPM

The maximum uncertainty seen from the heat transfer term over the entire load, speed and coolant temperature range was 12.16% of the total value. Most of this uncertainty is from the measurement of the temperature difference between the coolant inlet and outlet temperatures. While this is a large relative error margin in the heat transfer calculation, this was seen to be sufficient in predicting trends in the data due to the large changes in heat transfer itself.

The uncertainties in the computation of exhaust gas enthalpy and net indicated efficiency were seen to be less than 5% and were considered acceptable for the measurements.

3.5.3. Experimental Results

The data from the engine experiments was used to calculate the models in Matlab. A quadratic multi-linear regression model was taken to describe the different engine parameters as a function of engine load, speed and coolant temperature. The interaction effects between the different terms were also included for the model. It should be noted that the models generated from this are based on a curve fitting approach and do not try and represent any physics behind the phenomena.

The statistics for the regression models for different engine parameters are shown in Table 16 and the models themselves are shown in Table 17.

Table 16: Regression statistics for six cylinder Scania D13 model

	Adjusted R^2	**RMSE**
Exhaust Enthalpy	0.9963	1.3 kW
Coolant Heat Transfer	0.8682	1.6 kW
Net Indicated Efficiency	0.7214	1.2%

Table 17: Coefficients and corresponding p-values for the regression models for exhaust gas enthalpy, heat transfer to the coolant and net indicated efficiency. In the table, L= Load, S = Speed, T = Coolant Temperature

	Exhaust Enthalpy		**Coolant H.T.**		**Net Indicated Eff.**	
	Coeff	**p**	**Coeff**	**p**	**Coeff**	**p**
Intercept	20.3	1.1E-03	-46.4	3.8E-03	25.6	3.2E-06
L	-3.7	1.1E-06	-1.5	7.4E-02	-1.6	4.1E-05
S	-3.1E-02	6.1E-04	4.2E-02	1.3E-04	4.6E-02	4.0E-07
T	5.5E-02	1.3E-03	7.1E-01	7.5E-03	(-)	(-)
LxS	5.4E-03	1.4E-18	(-)	(-)	9.3E-04	1.7E-03
SxT	(-)	(-)	(-)	(-)	(-)	(-)
LxT	(-)	(-)	1.5E-02	5.6E-02	(-)	(-)
L^2	0.2	4.1E-09	(-)	(-)	(-)	(-)
S^2	1.3E-05	4.2E-04	-1.6E-05	3.6E-04	-2.2E-05	1.3E-08
T^2	(-)	(-)	-2.8E-03	2.4E-02	(-)	(-)

The trends in exhaust gas enthalpy with changing coolant temperature is shown in Figure 48 at an engine load of 12 bar net IMEP. The exhaust gas enthalpy increases with higher coolant temperatures, largely because of higher exhaust gas temperatures. On the other hand, the exhaust enthalpy is negatively affected by the reduction in gas density at higher coolant temperatures, which reduces the mass flow rate of the exhaust gases. However, the effect of the reduced mass flow rate on exhaust gas enthalpy is lower than the effect of the increased exhaust gas temperatures. The exhaust gas enthalpy can also be seen to increase with engine speed. With increasing engine speeds, the mass flow rate of the exhaust gases is increased, however the exhaust gas temperature is reduced as the lambda value is increased for a fixed engine load. The overall effect of this however, is an increase in exhaust gas enthalpy as the effect of the increased mass flow of gases is higher.

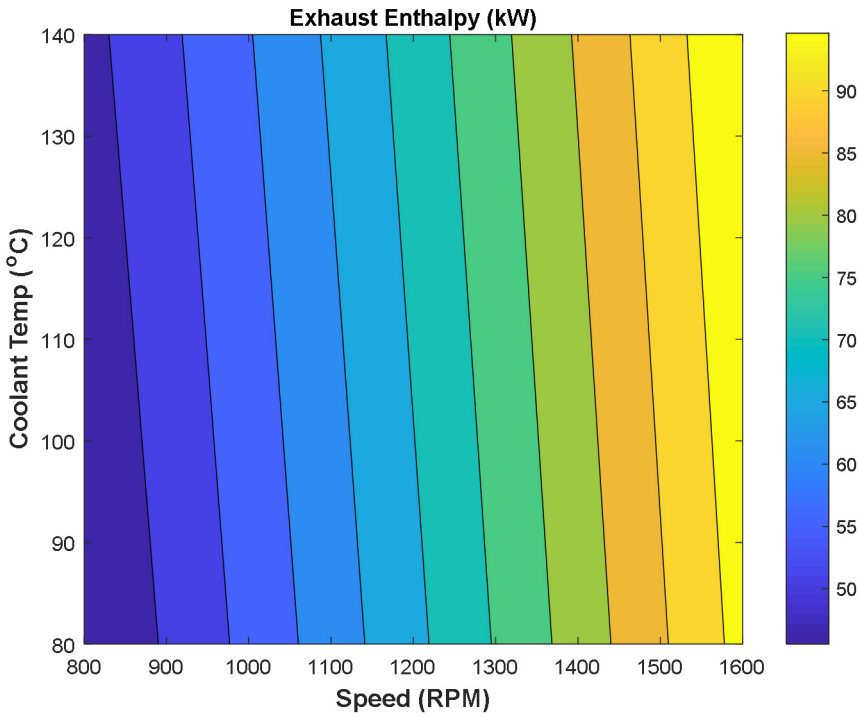

Figure 48: Exhaust enthalpy plot as a function of speed and coolant temperature at the engine load of 12 bar net IMEP

The net indicated efficiency as a function of coolant temperature is shown in Figure 49 at the engine load of 12 bar net IMEP. The net indicated efficiency can be seen to not be affected by coolant temperature as per the model. This does not mean that the coolant temperature does not affect the net indicated efficiency, but that the model takes these effects as statistically insignificant compared to the uncertainty on the measurements. This can be further seen in Table 17, where none of the coolant temperature terms show a significance of $p<0.05$.

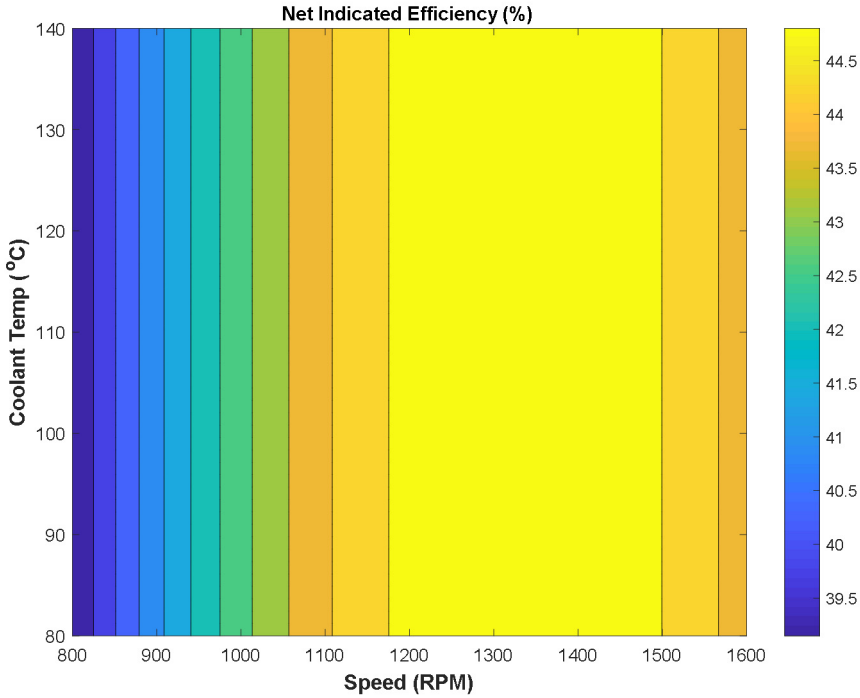

Figure 49: Net indicated efficiency as a function of engine speed and coolant temperature for an engine load of 12 bar net IMEP

The heat transfer to the coolant is shown in Figure 50. Here, a large increase in heat transfer can be seen with increased coolant temperatures. This is contrary to results from previous studies in Section 3.1 and Section 3.4. This is due to several reasons. Primarily, the oil in this setup is itself cooled by the coolant, using an internal oil heat exchanger. In this case, the heat rejected to the oil is thus further rejected to the coolant. This is further compounded by the effect of the internal oil thermostat which opens progressively at higher temperatures to reject increased heat from the oil to the coolant.

Additionally, the increase in heat transfer is possibly due to localised boiling within the cooling channels which increases the heat transfer coefficient of the coolant flow. At higher coolant temperatures, the boiling phenomena is exaggerated leading to higher heat transfer coefficients and higher heat transfer losses.

As the heat transfer to the coolant is seen to increase with increasing coolant temperature within the temperature range studied, for the recovery of low temperature waste heat it is always beneficial to operate at the highest coolant temperature possible for this setup.

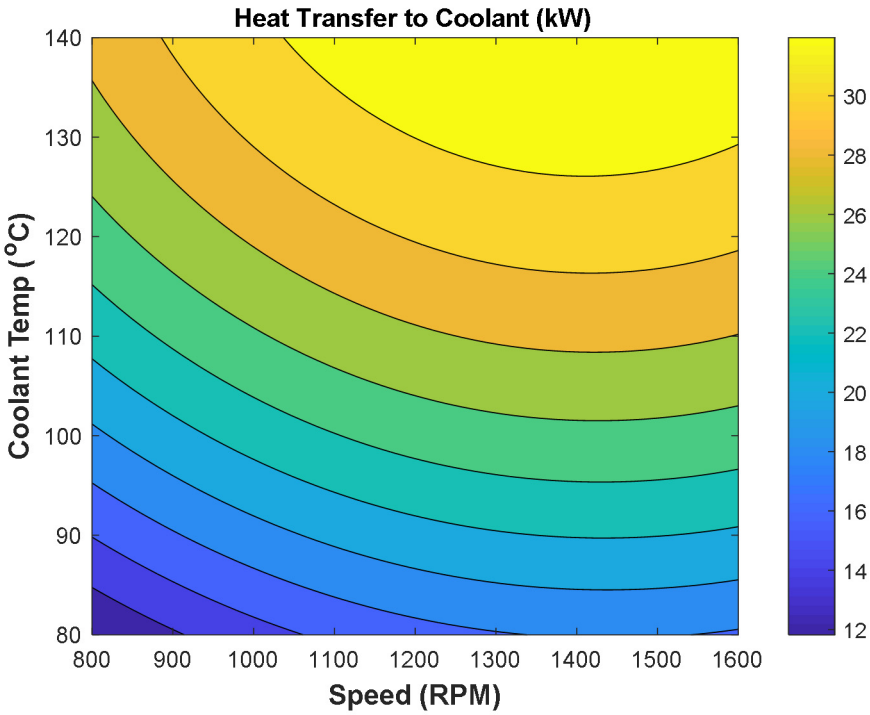

Figure 50: Heat Transfer to the coolant as a function of engine speed and coolant temperature at an engine load of 12 bar net IMEP

3.5.4. Simulation Results

The data from the experimental engine runs was then used for simulations of a dual loop Rankine cycle system with 10 working fluids. For the 41 operating points taken, the recoverable power from the coolant is shown in Figure 51.

For the coolant, the best performing working fluid can be seen to be cyclopentane, showing the highest recoverable power for most operating points.

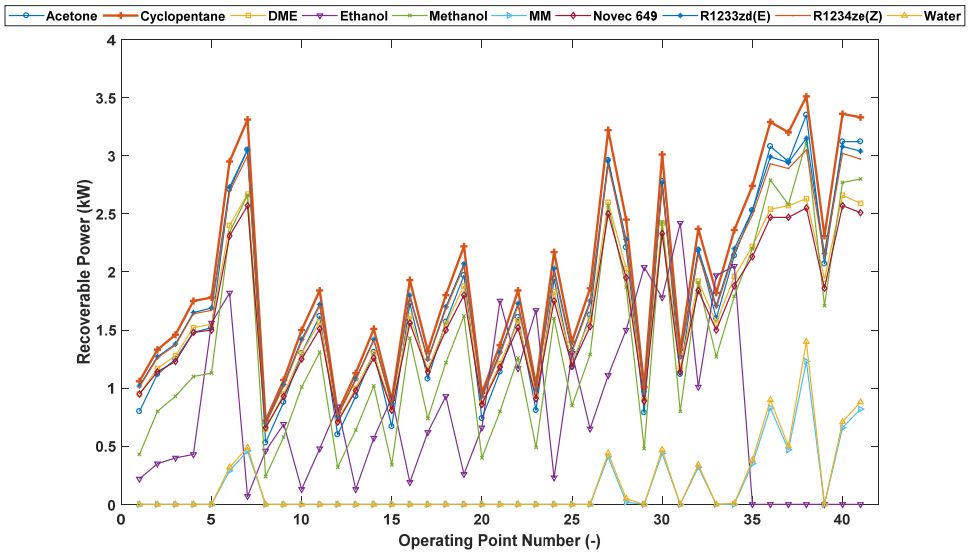

Figure 51: Recoverable power from the coolant for the operating points tested on the Scania D13 six cylinder engine

The recoverable power from the exhaust gases for the 10 working fluids is shown in Figure 52.

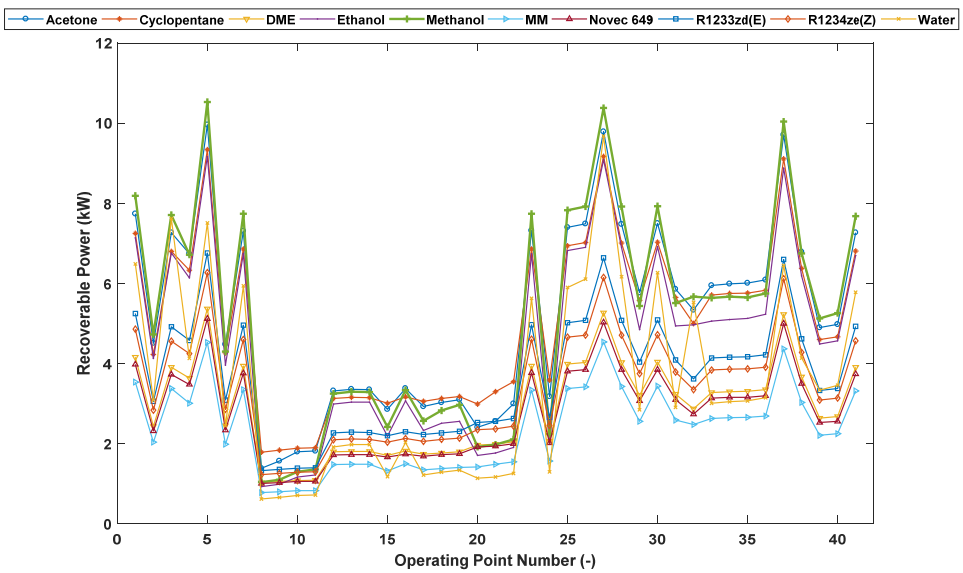

Figure 52: Recoverable power from the exhaust for the operating points tested on the Scania D13 six cylinder engine

For the exhaust gases, methanol shows the highest recoverable power for most operating points. On operating points with lower exhaust gas temperatures, cyclopentane and acetone can be seen to perform better.

These trends in the selection of best performing working fluids is similar to the ones seen for the light duty Volvo engine in Section 3.4.4. This is the case for both, waste heat recovery from the coolant as well as from the exhaust gases. An analysis of this is shown in Section 3.6.

3.5.5. WHTC Analysis

From the results shown above, the working fluids for the Rankine cycles were taken as cyclopentane and methanol for the coolant and exhaust gases respectively. The analysis for the reduction in fuel consumption is hence, done using only these two working fluids.

The WHTC test is a standardised transient engine dynamometer test for heavy duty engines. The cycle (shown in Figure 53) is defined over a period of 1800 s with the normalised load and speed of the engine specified.

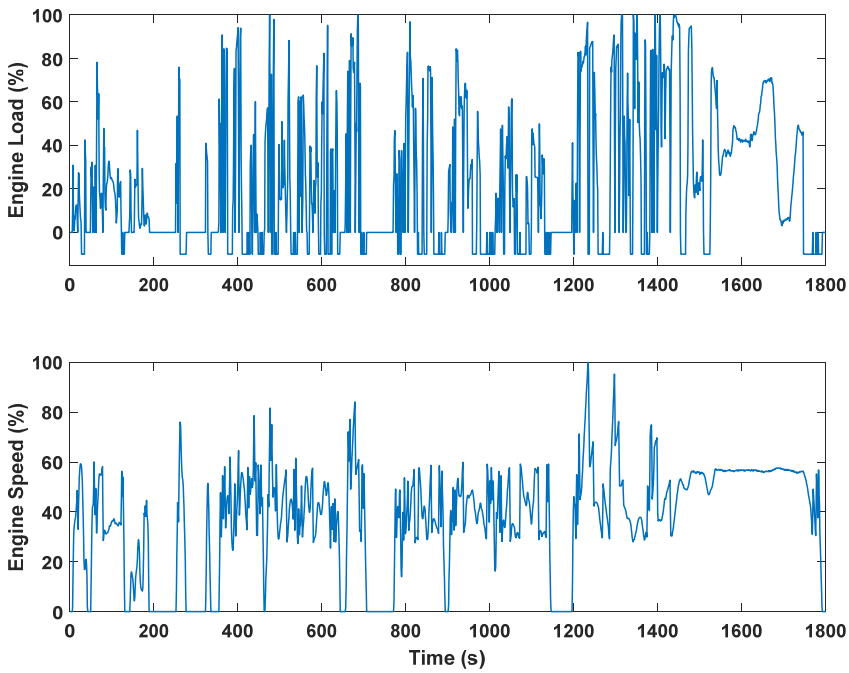

Figure 53: WHTC test for heavy duty engines specified in terms of normalised engine load and speed

In the cycle above, there are multiple points with negative torque. These negative values represent engine motoring points. For these points, the recoverable power from the coolant and the exhaust is taken as 0 kW and hence is not considered in the fuel consumption calculation. While heat from the engine's friction is still partly rejected to the coolant during motoring and hence, there should still be some recoverable power being obtained from the engine, it would be a major assumption to extrapolate the coolant recoverable power to motored conditions as that is well outside the model calibration range.

For the analysis, the definitions for engine load and speed were taken as per Table 18.

Table 18: Engine load and speed definitions taken for WHTC test analysis

	0%	**100%**
Engine Load (bar IMEPn)	2	16
Engine Speed (RPM)	500	2000

It should be stated here, that the engine definitions are expanded beyond the mapping of the engine test points (on the lower end of the load range and both ends of the speed range). This means that there is a possible loss in accuracy at the extreme points of the engine operating range. However, as most of the WHTC test points are placed in intermediate points, the results are expected to be valid.

The analysis on the WHTC was done by using the models generated for the fuel flow and the recoverable power from the coolant and exhaust gases. The recoverable power models were used to compute the reduction in load for the engine to meet the same torque requirements as an engine without a waste heat recovery system running on the test cycle. The fuel flow model was then used to compute the fuel consumption at the reduced engine load.

The data from the Rankine cycle simulations is then used to generate a quadratic multi-linear regression model using the engine load, speed and coolant temperature as inputs. The regression statistics for the models are shown in Table 19 and the models described are shown in Table 20.

Table 19: Regression statistics for the recoverable power and fuel flow models

	Adjusted R^2	**RMSE**
Exhaust Recoverable Power	0.9945	0.1988 kW
Coolant Recoverable Power	0.9628	0.162 kW
Fuel Flow	0.9907	0.2253 g/s

Table 20: Coefficients and corresponding p-values for the regression models for the recoverable power from the exhaust gases and the coolant, and the fuel flow. In the table, L= Load, S = Speed, T = Coolant Temperature

	Exhaust		Coolant		Fuel Flow	
	Coeff	**p**	**Coeff**	**p**	**Coeff**	**p**
Intercept	-4.1	4.0E-05	-4.3	1.4E-05	1.6	1.0E-01
L	0.3	1.0E-03	-0.2	4.3E-02	2.1E-02	8.4E-01
S	1.3E-03	3.2E-01	3.2E-03	2.0E-03	-2.8E-03	4.4E-02
T	1.1E-02	5.4E-05	4.0E-02	1.4E-06	(-)	(-)
LxS	6.3E-04	2.6E-15	(-)	(-)	4.0E-04	2.0E-09
SxT	(-)	(-)	(-)	(-)	(-)	(-)
LxT	(-)	(-)	1.6E-03	3.2E-02	(-)	(-)
L2	-1.4E-02	2.3E-03	(-)	(-)	1.2E-02	1.2E-02
S2	-1.1E-06	3.0E-02	-1.2E-06	4.2E-03	1.5E-06	7.1E-03
T2	(-)	(-)	(-)	(-)	(-)	(-)

Figure 54 shows the power recovered from the coolant and the exhaust gases for the WHTC test for a constant coolant temperature of 120 °C.

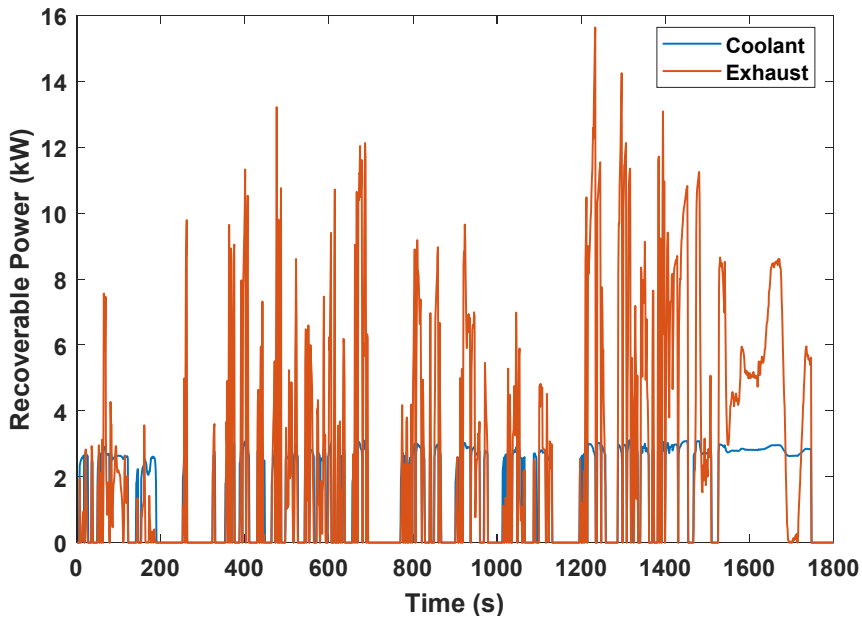

Figure 54: Recoverable power from the coolant and exhaust at a constant coolant temperature of 120 °C

Figure 55 shows the fuel consumption with a varying constant coolant temperature.

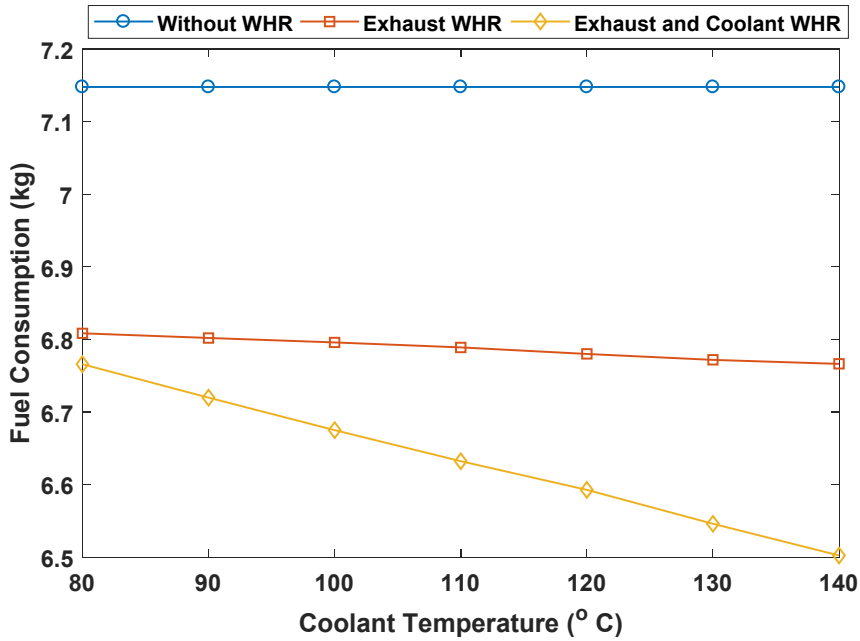

Figure 55: Fuel consumption over the WHTC for varying coolant temperature

From Figure 55, it can be seen that increasing the coolant temperature has no effect on the fuel consumption without the use of a waste heat recovery device. This is due to the non-dependence of the engine efficiency on the coolant temperature as shown in Figure 49.

When using only the exhaust gases for WHR, the fuel consumption is reduced with increased coolant temperature, as the exhaust gas temperature and enthalpy increases. The reduction in fuel consumption is 4.7% to 5.3% for a coolant temperature of 80 °C to 140 °C.

For the coolant, the fuel consumption is reduced dramatically at increased coolant temperatures. The reduction in fuel consumption is 5.3% to 9% on increasing the coolant temperature from 80 °C to 140 °C.

These figures, however, only represent the potential reduction in fuel consumption across the cycle. This is because with true transient behaviour, the components of the cooling system have thermal inertia, which could negatively affect the recovery of waste heat. For a true transient analysis, these figures are expected to be lower [51].

3.6. Working Fluid Selection

From the studies shown above, there are some questions that need to be addressed regarding the selection of the working fluid itself. While the studies above evaluate the performance of a large number of working fluids, they do not go into detail as to why some working fluids perform better than others. Why does cyclopentane consistently perform better than the other working fluids in the temperature range shown? Why do some fluids like ethanol perform so well for recovering energy from the exhaust gases and not from the coolant? What are the characteristics that are needed from a working fluid to maximise recoverable power? The answer to these questions is a combination of multiple factors which are described in detail below.

3.6.1. Low Temperature Heat Sources

One of the reasons for cyclopentane showing a high recoverable power from the simulations is the constraints applied for the simulations themselves. For the ORC simulations with multiple working fluids (described in Section 2.3.2), the minimum condensation temperature and pressure were taken as 50 °C and 1.013 bar respectively. This matches very well with cyclopentane which has a condensation temperature of 49 °C at 1.013 bar (or atmospheric pressure). This means that cyclopentane can operate approximately at the lowest pressure and temperature allowed by the constraints imposed on the simulations. This increases the pressure ratio at which the cycle (expander) can operate when using the heat source for the ORC.

For fluids with a condensation temperature lower than 50 °C at 1.013 bar, the lower pressure in the cycle must be increased till the minimum condensation temperature constraint is met, which also means lowering the pressure ratio of the cycle and expander. Having a higher condensation temperature than 50 °C at 1.013 bar is also an issue as it means that the pressure ratio is limited by the heat source. For example, water has a boiling point of 100 °C. This means that at a coolant temperature of 160 °C, the maximum achievable pressure ratio is approximately 6.5 (assuming the coolant temperature is also the maximum temperature of the ORC).This is significantly lower than the maximum achievable pressure ratio of cyclopentane at 12.5.

However, it should be pointed out that the effect due to matching the constraints with the working fluid condensation conditions is not that strong and is highly dependent on other fluid properties. For example, ethanol has a higher condensation

temperature (78 °C) at 1.013 bar, but has approximately the same maximum achievable pressure ratio as cyclopentane at 160 °C coolant temperature.

Another reason that cyclopentane performs well is that it is a dry working fluid. A dry working fluid is a fluid for which the slope of the vapour saturation line (highlighted in red) shown in Figure 56 is positive. This means that superheating is not required (apart from a minimal superheat for safety reasons) as there is no risk of the expander operating in the two phase zone, which is potentially harmful for the expander. This further means that if the heat source for the ORC is higher in temperature, the cycle pressure ratio can be increased in comparison to using the higher temperatures to increase the superheating of the working fluid. This can be seen clearly when using ethanol as the working fluid for the coolant waste heat cycle.

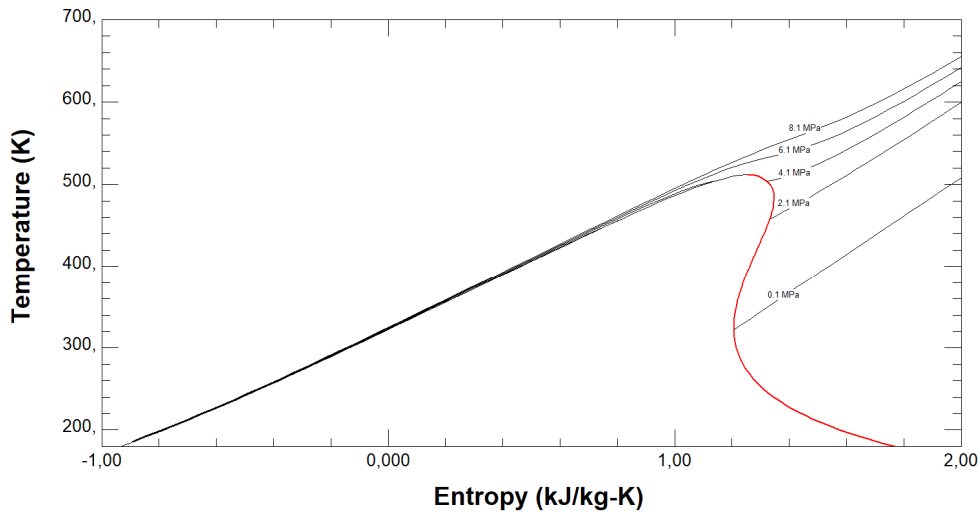

Figure 56: T-S diagram for cyclopentane showing isobaric line. the red line is highlighted to show the positive slope of the saturated vapour line (Source: REFPROP)

Studying the T-S Diagram of ethanol (shown in Figure 57), it can be seen that the slope of the saturated vapour line (highlighted in red) is negative at the lower temperatures. This means that to prevent two phase conditions in the expander, ethanol requires a high degree of superheat which would reduce the effective pressure ratio it could obtain. This is reflected in Figure 41 as ethanol can be seen to be operating at a much lower pressure ratio than cyclopentane despite having approximately the same saturation pressure at 160 °C (the maximum coolant temperature).

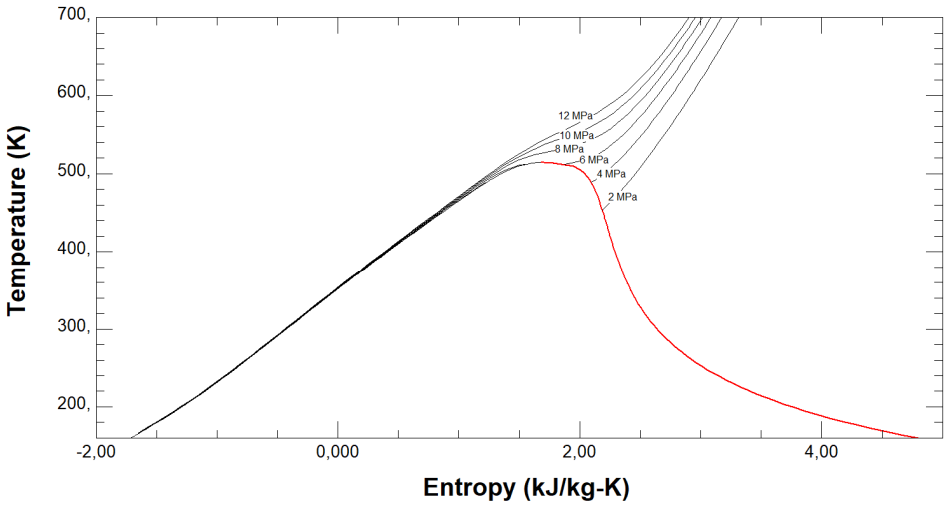

Figure 57: T-S diagram for ethanol showing isobaric line. the red line is highlighted to show the negative slope of the saturated vapour line (Source: REFPROP)

3.6.2. High Temperature Heat Sources

When studying the waste heat recovery from the exhaust gases, cyclopentane was seen to perform well (within the top 5 performing working fluids). It performs comparably to methanol and acetone but at a much lower pressure ratio. However, it is restricted by its critical pressure and temperature. It cannot go above a pressure ratio of approximately 36 and is limited in recovering power at higher temperatures.

For the exhaust gases, methanol and acetone perform best with the maximum amount of power recovered. This is largely because of the high critical pressure and temperatures for both these working fluids. This allows the working fluid to reach pressure ratios as high as 60. While acetone is an isentropic working fluid, methanol is a wet working fluid. This would naturally make acetone as the better working fluid, allowing for lower superheat requirements than methanol. However, that is seen not to be the case, especially at higher exhaust gas temperatures.

The reason for this is the lower critical pressure of acetone in comparison to methanol. As the temperature of the exhaust gases is much higher than the critical temperatures of both working fluids, acetone can only use the additional temperature through increasing the superheat as it is limited in its pressure ratio. Methanol on the other hand, is required to have increased superheat, due to it being a wet fluid. However, as it has a much higher critical pressure, it can achieve much higher pressure ratios for the exhaust gases, resulting in more power delivered from the expander.

This also explains why acetone performs better at operating points with lower exhaust gas temperatures. As the achievable pressure ratio is limited by the exhaust gas temperature itself, acetone can have a lower superheat and increase the pressure ratio. However, in such points methanol still needs to maintain some superheating to prevent two phase conditions in the expander.

Up until this point, the recoverable power is largely discussed as to be dependent on the pressure ratio. However, there are variations within the scatter plot in Figure 41 that cannot be explained by simply looking at the pressure ratio. While there is a strong correlation between the pressure ratio and the recoverable power, some fluids are seen to perform better even at lower pressure ratios as compared to other fluids. An example of this can be seen with ammonia and n-dodecane in Figure 41.

Ammonia can be seen to generate 2.5 kW or higher from the exhaust gas heat in comparison to n-dodecane, which generates approximately 1 kW, while operating at a lower pressure ratio. This difference in pressure ratio is because of the low condensation temperature (-33 °C) of ammonia at 1.013 bar which means that the lower operating pressure for ammonia is higher, thus reducing the pressure ratio. Additionally, ammonia is also a wet working fluid in comparison to n-dodecane which is very dry. Considering all these factors, ammonia should not be able to perform better than n-dodecane in terms of energy recovery.

This can be explained by looking at the H-S diagrams for both working fluids. Figure 58 shows the H-S diagram for ammonia with the isobars drawn. For the operating point shown in Figure 41 (15 bar gross IMEP, 1800 RPM), the reduction in pressure through the expander is from 9.6 MPa to 2 MPa. On the H-S diagram, this represents a large change in enthalpy. This further means a large amount of energy is delivered to the expander for that change in pressure.

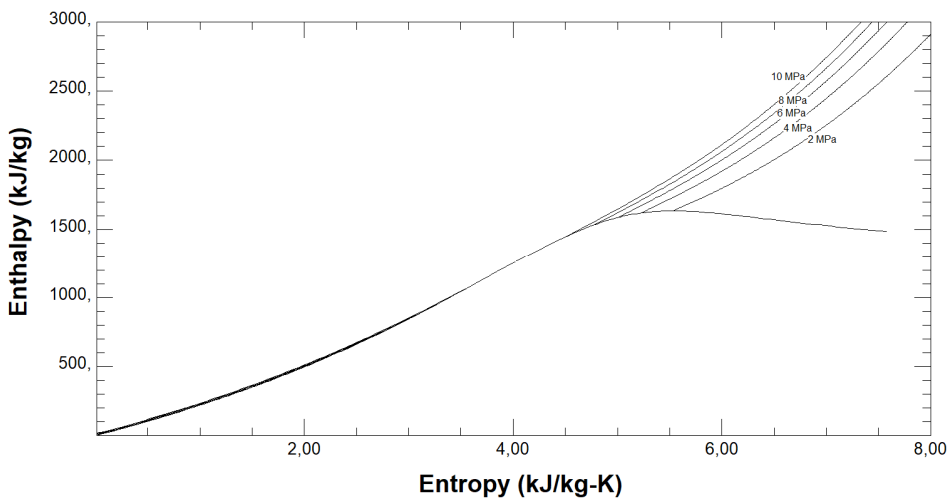

Figure 58: H-S diagram for ammonia showing isobaric lines (Source: REFPROP)

In contrast to this, the H-S diagram of n-dodecane can be seen in Figure 59. Here, the isobaric lines are very closely positioned. This means that the enthalpy change for a specified pressure drop is lower and hence, the expander delivers a lower amount of power.

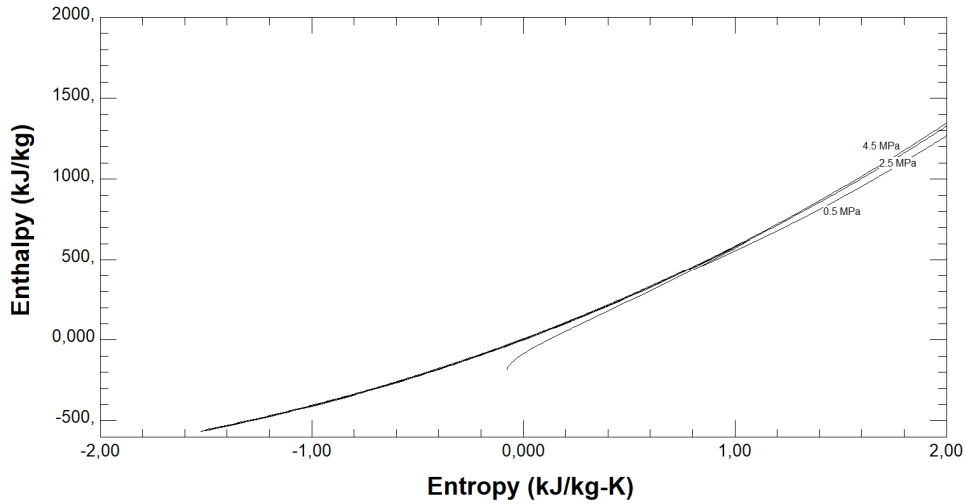

Figure 59: H-S diagram for n-dodecane showing isobaric lines (Source: REFPROP)

Hence, while n-dodecane has a larger pressure ratio across the expander compared to ammonia, the enthalpy drop across the expander when using ammonia is higher, thus delivering higher power.

There are many other factors that need to be considered when looking at the practical aspects of selecting working fluids for ORC applications. This includes the thermophysical properties such as vaporisation heat and density which affects the flow rates of the working fluid and hence the size of the system implemented. The environmental characteristics are also important such as the Ozone Depletion Potential and the Global Warming Potential. However, the discussion for these aspects is outside the scope of this thesis and has been discussed in previous literature in detail [51].

3.6.3. Working Fluid Selection Guidelines

From the sections above, there are certain guidelines that can be deduced when looking at working fluids for an ORC application. The following recommendations can be made for when selecting a working fluid for an ORC system.

- The working fluid should ideally be a dry working fluid. This is to minimise the requirement for superheat in the system so that higher pressure ratios can be attained in the ORC.
- The working fluid should ideally have a high critical pressure and temperature, preferably higher than the heat source temperature itself. This is again, to increase the pressure ratio of the ORC without using increased superheating.
- The working fluid should preferably have isobaric lines on its H-S diagram spread out as much as possible. This is to maximise the change in enthalpy across the expander, which would further increase recoverable power.
- The working fluid condensation temperature at the minimum cycle condensation pressure constraint should be similar to the minimum condensation temperature constraint for the cycle.

Of these four recommendations stated above, the first three are the most important and contribute significantly to the performance of the cycle. While the last point above also affects the performance of the ORC, it is not a key criterion in judging working fluid performance.

4. Conclusions and Future Work

This chapter briefly summarises the main contributions of the different studies presented in this thesis. It also highlights some of the work that can be done to have a more complete understanding of low temperature waste heat recovery in internal combustion engines.

4.1. Conclusions

The work described in this thesis primarily aimed at increasing the powertrain efficiency and the efficiency of waste heat recovery from internal combustion engines. This thesis has looked at different methods to not just optimise the waste heat recovery system, but the *combined* system of the engine and waste heat recovery system. The main conclusions and contributions from this thesis work are shown below:

- An increase in coolant temperature is an effective method to increase the viability of low temperature waste heat recovery in internal combustion engines. In simulations, when using ethanol as a working fluid, up to 1.5 percentage points (pp) improvement in the system indicated efficiency was seen solely as the effect from increased coolant temperatures.
- An integrated waste heat recovery cooling system with phase change cooling is also an effective method to increase the exergy of the coolant/ working fluid in the engine. In simulation studies, it showed an increase of up to 1.7 pp in indicated efficiency over using only exhaust gas heat for the waste heat recovery process. However, the implementation of such a system also poses mechanical challenges and requires a redesign of major engine components.
- Due to the challenges stated in the previous point, the thesis prescribes the use of elevated coolant temperatures, over an integrated waste heat recovery cooling circuit, to increase the viability of low temperature waste heat recovery. This is taken as a subjective assessment due to the increased complexity of the powertrain and thermal management system.

- For separated cooling systems (systems using separate cooling loops for the oil and coolant), there exists an optimum coolant temperature to maximize recoverable power. This optimum temperature exists because a higher coolant temperature translates to a higher recovery cycle efficiency. However, it also means reduced heat transfer to the coolant and hence lower energy input for the recovery cycle.
- At engine operating points with higher heat transfer to the coolant (such as higher engine loads and speeds), the optimum coolant temperature for separated cooling systems is at a higher temperature.
- An increase in coolant temperatures also increases the exhaust gas temperature and exergy. However, the mass flow rate of exhaust gases might decrease due to increased gas temperatures and lower density for the same volume flow rate of gas.
- Cyclopentane was seen to consistently perform as the best working fluid for low temperature WHR, for both HD and LD engines. This was seen to be due to a combination of the properties of cyclopentane and the constraints imposed for the Rankine cycle simulations.
- For the high temperature heat sources, methanol and acetone show the best performance. For operating points with higher exhaust gas temperatures, methanol showed increasingly improved performance over acetone. This was seen to be largely because of the higher critical pressure and temperature of methanol.
- Using Rankine cycle simulations, a dual-loop waste heat recovery system shows a significant improvement in system brake efficiency with the use of optimised coolant temperatures and suitable working fluids. For the Volvo LD engine, this was seen to be up to 5.2 percentage points, with 1.7 pp gain being from the effect of the increased coolant temperature.
- NOx emissions were seen to increase by up to 0.9 g/kWh with increasing coolant temperatures because of increased gas temperatures within the combustion chamber and higher combustion temperatures.
- For combined cooling systems (where the oil is cooled by the coolant), higher coolant temperatures were seen to increase the recoverable power from both the coolant and the exhaust gases in the temperature range studied.
- In the evaluation of a WHTC test for the Scania D13 engine, elevated coolant temperatures showed up to a potential 9.3% reduction in fuel consumption.

These findings were obtained from a series of studies summarised as follows. In the first study of the thesis, the coolant temperature was swept up to 200 °C for a Scania HD engine using simulations in GT-Power. Here, some clear trends in the data were seen. Primarily, the reduction of heat transfer to the coolant and the increase in heat transfer to the oil. The combined heat transfer from the combustion chamber to the oil and coolant was seen to decrease with increasing coolant temperatures. With regards to the energy balance, most of the reduction in heat transfer was shifted to the exhaust gases, with there being minimal changes in the indicated efficiency of the engine with increasing cooling media temperature. Combustion characteristics were also largely unaffected, showing insignificant trends. This is to be expected for a mixing-controlled combustion process.

With increased coolant temperatures, an increase in recoverable power was also seen from the Rankine cycle simulations. Isolating the effect of only increasing the coolant temperature, an increase in system efficiency of 1.5 percentage points was seen. This was due to an increase in recoverable power from both the exhaust gases (due to higher exhaust gas temperatures) and also from the coolant (due to higher recovery efficiency). At this point, there had been very little optimisation done on the waste heat recovery system, with the use of a single working fluid to see the potential of increasing the coolant temperature.

The second study in the thesis explored the potential of using phase change cooling as part of the Rankine cycle recovery system. The study showed that phase change cooling could show increased potential for recoverable power in comparison to using only exhaust gases for waste heat recovery. A comparison between the two studies was also done to compare an integrated cooling waste heat recovery circuit to a dual-loop waste heat recovery circuit.

While the integrated cooling waste heat recovery system showed a higher performance in terms of converting waste heat input to recovered power, it also showed disadvantages. In performance terms, the integrated system became more restricted due to the cooling system being in-line with the heat exchanger for the exhaust gases. This means that if the exhaust gases are at a higher temperature but the cooling requirement for the engine requires the coolant/working fluid to be at a certain temperature, that would restrict the saturation pressure of the Rankine cycle and hence the pressure ratio. There would also be a need to redesign the engine block with cooling channels which can withstand much higher pressures and also mechanical design changes for many connecting components.

Hence, in light of these limitations, it was seen that the practicality of increasing the coolant temperature was a more viable path towards increasing the coolant exergy than using phase change cooling along with waste heat recovery.

The next study then focused on experimental results from a Volvo D4 LD engine, using elevated coolant temperatures. The experimental data was used for Rankine cycle simulations for the comparison of a large number of potential working fluids.

With the use of a dual-loop waste heat recovery system, it was seen that the system brake efficiency could be improved by up to 5.2 percentage point (pp). For the Volvo engine, the brake efficiency increased by up to 1 percentage point with an increase in coolant temperature. However, this seems dependent on the engine itself as in later studies for the Scania HD engine the brake efficiency does not show the same positive dependence on coolant temperature. The NOx shows an increase with increasing coolant temperature as well with up to 0.9 g/kWh increase going from a coolant temperature of 80 °C to 160 °C.

The working fluids that were seen to perform the best out of the 48 working fluids tested were cyclopentane for the coolant, and methanol and acetone for the exhaust gases. Cyclopentane performed consistently as the best working fluid for the coolant for all operating points tested. Methanol and acetone were seen to change places depending on the amount of waste heat from the engine. Operating points with higher amounts of waste heat favour methanol as the working fluid, while lower engine loads, which generate lower amounts of waste heat, favoured acetone.

Finally, a study was done for evaluating the potential reduction in fuel consumption over the WHTC test for the Scania D13 engine. A model for the recoverable power for the engine was made using regression analysis. The model was then used for the analysis of fuel consumption over the cycle using a steady state approach. It was seen that for the cooling setup tested, higher coolant temperatures showed an increase in recoverable power. Over the WHTC, a potential reduction in fuel consumption of 9% was seen with the implementation of a low temperature waste heat recovery system using elevated coolant temperatures.

The studies summarised above present a more complete picture of low temperature waste heat recovery than those shown in the literature study. While there are some questions that are not addressed in this thesis, such as the best performing architecture of the waste heat recovery system itself, these have been sufficiently covered in the works cited in the literature review. It was seen from multiple studies where different system architectures were simulated that the highest amount of recoverable power is obtained from using separated recovery cycles for the high temperature sources and the low temperature sources for the engine.

The thesis discusses the different methods of increasing the energy quality in the coolant and compares in quantitative and qualitative terms, the advantages and disadvantages of these methods. The thesis also looks at a vast selection of working fluids to narrow down the best performing ones for the different heat sources considered.

Keeping the above contributions in mind, there are ways in which the understanding of low temperature waste heat recovery can be further advanced with regards to internal combustion engines, as explained next.

4.2. Future Work

Based on the studies already done in the thesis, the following are recommendations to further expand on the knowledge base of low temperature waste heat recovery and further optimise the engine.

Firstly, the Rankine cycle simulations can be updated to have a more accurate representation of the recovered power from the Rankine cycle. This includes better models for the expander, better representation for the heat losses in the system and a model that is calibrated for transient operation.

To further validate the results of these studies, an actual experimental setup should be designed for the optimised setup i.e. using the best performing working fluid, the optimised expander setup and the controllers needed to have the system working as per the simulated optimum working conditions.

The study for working fluid selection can also be expanded to binary mixtures to compare the performance of some mixtures to traditional single component working fluids.

Finally, even though there are some challenges with integrating phase change cooling and waste heat recovery systems, it is still worth investigating further, experimentally, how much of a gain can be achieved from using such a system over traditional Rankine cycle methods for waste heat recovery.

References

[1] O. Edenhofer, R. Pichs-Madruga, Y. Sokona, J. Minx and et al., “Climate Change 2014: Mitigation of Climate Change,” Cambridge University Press, New York, 2014.

[2] McKinsey and Company, “Electric vehicles in Europe: Gearing up for a new phase?,” Amsterdam, 2014.

[3] World Energy Council, “Global Transport Scenarios 2050,” World Energy Council, London, 2011.

[4] European Comission, “The roadmap for transforming the EU into a competitive, low-carbon economy by 2050,” European Commission, 2011.

[5] M. Nesbit, M. Fergusson, A. Colsa, J. Ohlendorf and et al., “Comparative study on the differences between the EU and US legslation on emissions in the automotive sector,” European Parliament, Brussels, 2016.

[6] N. Mirgal, “Indian automotive industry towards Bharat Stage-VI emission norms: A technical review,” *International Journal of Engineering Research And Advanced Technology,* vol. 3, no. 11, pp. 9-14, 2017.

[7] N. Abani, N. Nagar, R. Zermeno, M. Chiang and et al., “Developing a 55% BTE Commercial Heavy-Duty Opposed-Piston Engine without a Waste Heat Recovery System,” *SAE Technical Paper 2017-01-0638,* 2017.

[8] J. O'Connor, M. Borz, D. Ruth, J. Han and et al., “Optimization of an Advanced Combustion Strategy Towards 55% BTE for the Volvo SuperTruck Program,” *SAE Int. J. Engines,* vol. 10, no. 3, 2017.

[9] V. Manente, B. Johansson and P. Tunestal, “Partially Premixed Combustion at High Load using Gasoline and Ethanol, a Comparison with Diesel,” *SAE Technical Paper 2009-01-0944,* 2009.

[10] D. D. Battista and R. Cipollone, “Improving Engine Oil Warm Up through Waste Heat Recovery,” *Energies,* vol. 11, 2018.

[11] R. Cipollone, D. D. Battista and M. Mauriello, “Effects of oil warm up acceleration on the fuel consumption of reciprocating internal combustion engines,” *Energy Procedia,* vol. 82, pp. 1-8, 2015.

[12] A. Greszler, “A Diesel Turbo-Compound Technology,” in *In Proceedings of DEER Confrerence*, Dearborn, Michigan, 2008.

[13] J. Bass, N. Elsner and F. Leavitt, “Performance of the 1 kw thermoelectric generator for diesel engines,” in *In Proceedings of 13th International Conference on Thermoelectrics*, Kansas City, 1995.

[14] K. Smith and M. Thornton, “Feasibility of Thermoelectrics for Waste Heat Recovery in Conventional Vehicles,” National Renewable energy Laboratory, 2009.

[15] S. Backhaus and G. Swift, “A thermoacoustic-Stirling heat engine: Detailed study,” *J. Acoust. Soc. Am,* vol. 107, pp. 3148-3166, 2000.

[16] D. G. Thombare and S. K. Verma, “Technological development in the Stirling cycle engines,” *Renewable and Sustainable Energy Reviews,* vol. 12, pp. 1-38, 2008.

[17] M. Guven, H. Bedir and G. Anlas, “Optimization and application of Stirling engine for waste heat recovery from a heavy-duty truck engine,” *Energy Conversion and Management,* vol. 180, pp. 411-424, 2019.

[18] A. Legros, L. Guillaume, M. Diny, H. Zaidi and V. Lemort, “Comparison and Impact of Waste Heat Recovery Technologies on Passenger Car Fuel Consumption in a Normalized Driving Cycle,” *Energies,* vol. 7, pp. 5273-5290, 2014.

[19] J. Rijpkema, K. Munch and S. Andersson, “Thermodynamic potential of Rankine and flash cycles for waste heat recovery in a heavy duty Diesel engine,” *Energy Procedia,* vol. 129, pp. 746-753, 2017.

[20] V. Grelet, P. Dufour, M. Nadri, T. Reiche and V. Lemort, “Modeling and control of Rankine based waste heat recovery systems for heavy duty trucks,” *IFAC-PapersOnLine,* vol. 48, no. 8, 568-573.

[21] S. Trabucchi, C. Servi, F. Casella and P. Colonna, “Design, Modelling, and Control of a Waste Heat Recovery Unit for Heavy-Duty Truck Engines,” *Energy Procedia,* vol. 129, pp. 802-809, 2017.

[22] A. M. Attar, “The Effects of Coolant Temperature on Spark Ignition Engine Performance,” Western Michigan University, Kalamazoo, 2009.

[23] M. Mamun and M. Ehsan, “Effect of Coolant Temperature on Performance of a SI Engine,” in *4th International Conference on Mechanical Engineering*, Dhaka, 2001.

[24] A. Slatar, “Influence of coolant temperature and flow on engine efficiency,” Department of Aeronautical and Vehicle Engineering, KTH Royal Institute of Technology, Stockholm, 2015.

[25] J. Adler and T. Bandhauer, “Performance of a Diesel Engine at High Coolant Temperatures,” *Journal of Energy Resources Technology,* vol. 139, 2017.

[26] W. A. Abdelghaffar, M. M. Osman, M. N. Saeed and A. I. Abdelfatteh, “Effects of Coolant Temperature on the Performance and Emissions of a Diesel Engine,” in *ASME 2002 Internal Combustion Engine Division Spring Technical Conference*, Rockford, 2002.

[27] T. Endo, S. Kawajiri, Y. Kojima, K. Takahashi and e. al., “Study on Maximizing Exergy in Automotive Engines,” *SAE Technical Paper 2007-01-0257,* 2007.

[28] J. Fu, J. Liu, Z. Xu, B. Deng and Q. Liu, “An approach for IC engine coolant energy recovery based on low-temperature organic Rankine cycle,” *Journal of Central South University,* vol. 22, no. 2, pp. 727-734, 2015.

[29] V. Dolz, R. Novella, A. Garcia and J. Sanchez, “HD Diesel engine equipped with a bottoming Rankine cycle as a waste heat recovery system. Part 1: Study and analysis of the waste heat energy,” *Applied Thermal Engineering,* vol. 36, pp. 269-278, 2012.

[30] J. Serrano, V. Dolz, R. Novella and A. Garcia, “HD Diesel engine equipped with a bottoming Rankine cycle as a waste heat recovery system. Part 2: Evaluation of alternative solutions,” *Applied Thermal Engineering,* vol. 36, pp. 279-287, 2012.

[31] P. Leduc, P. Smague, A. Leroux and G. Henry, “Low temperature heat recovery in engine coolant for stationary and road transport applications,” *Energy Procedia,* vol. 129, pp. 834-842, 2017.

[32] J. Song, Y. Song and C. Gu, “Thermodynamic analysis and performance optimization of an Organic Rankine Cycle (ORC) waste heat recovery system for marine diesel engines,” *Energy,* vol. 82, pp. 976-985, 2015.

[33] M. Yang and R. Yeh, “Thermo-economic optimization of an organic Rankine cycle system for large marine diesel engine waste heat recovery,” *Energy,* vol. 82, pp. 256-268, 2015.

[34] J. Song and C. Gu, “Performance analysis of a dual-loop organic Rankine cycle (ORC) system with wet steam expansion for engine waste heat recovery,” *Applied Energy,* vol. 156, pp. 280-289, 2015.

[35] J. Song and C. Gu, “Parametric analysis of a dual loop Organic Rankine Cycle (ORC) system for engine waste heat recovery,” *Energy Conversion and Management,* vol. 105, pp. 995-1005, 2015.

[36] G. Shu, G. Yu, H. Tian, H. Wei, X. Liang and Z. Huang, “Multi-approach evaluations of a cascade-Organic Rankine Cycle (C-ORC) system driven by diesel engine waste heat: Part A – Thermodynamic evaluations,” *Energy Conversion and Management,* vol. 108, pp. 575-595, 2016.

[37] A. N. Anderson, A. Tacchella and J. A. Fawcett, “Dual-circuit ebullition cooling for automotive engines,” *SAE Technical Papers Series (640452),* 1964.

[38] H. C. Harrison, “Evaporative cooling,” *SAE Technical Papers Series (260015),* 1926.

[39] J. G. Hawley, D. G. Tilley, K. Robinson and N. Campbell, “A review of precision engine cooling,” *SAE Technical Papers Series (1999-01-0578),* 1999.

[40] K. Robinson, S. Joyce, M. Haigh, N. Campbell and J. Hawley, “Predictions for nucleate boiling – results from a thermal bench marking exercise under low flow conditions,” *SAE Technical Papers Series (2002-01-1028),* 2002.

[41] M. Kind, “Flow Boiling - An Introduction,” in *VDI Heat Atlas*, Dusseldorf, Springer, 2010, pp. 793-795.

[42] O. Dingel, D. Luederitz and T. Arnold, “Investigation of an ORC System with Integrated Phase Change Engine Cooling,” in *Proceedings of the 5th International Seminar on ORC Power Systems*, Athens, 2019.

[43] P. Tunestal, “TDC Offset Estimation from Motored CylinderPressure Data based on Heat Release Shaping,” *Oil and Gas Science and Technology – Rev. IFP Energies nouvelles,* vol. 66, pp. 705-716, 2011.

[44] T. Morel and R. Keribar, “A Model for Predicting Spatially and Time Resolved Convective Heat Transfer in Bowl-in-Piston Combustion Chambers,” *SAE Technical Paper 850204,* 1985.

[45] R. H. Winterton, “Where did the Dittus and Boelter equation come from?,” *Int. J. Heat Mass Transfer,* vol. 41, no. 4-5, pp. 809-810, 1998.

[46] K. Robinson, J. G. Hawley, G. P. Hammond and N. J. Owen, “Convective coolant heat transfer in internal combustion engines,” *Proceedings of the Institution of Mechanical Engineers, Part D: Journal of Automobile Engineering,* 2003.

[47] E. Svensson, L. Yin, P. Tunestal and M. Tuner, “Combined Low and High Pressure EGR for Higher Brake Efficiency with Partially Premixed Combustion,” *SAE Technical Paper 2017-01-2267,* 2017.

[48] L. R. Pascual, Study of Organic Rankine Cycles for Waste Heat Recovery in Transportation Vehicles, Valencia: Universitat Politecnica de Valencia, 2017.

[49] J. Rijpkema, S. Andersson and K. Munch, “Thermodynamic Cycle and Working Fluid Selection for Waste Heat Recovery in a Heavy Duty Diesel Engine,” *SAE Technical Paper 2018-01-1371,* 2018.

[50] V. Singh, P. Tunestal and M. Tuner, “A Study on the Effect of Elevated Coolant Temperatures on HD Engines,” *SAE Technical Paper 2017-01-2223,* 2017.

[51] D. C. Bandean, S. Smolen and J. T. Cieslinski, “Working fluid selection for Organic Rankine Cycle applied to heat recovery systems,” in *World Renewable Energy Congress*, Sweden, 2011.

Scientific Publications

Contributions

Paper I

The paper was written by the first author, Vikram Singh. Per Tunestål and Martin Tuner acted as the supervisors for the experimental and simulation work done. The work itself was done by the first author.

Paper II

The paper was written by the lead author, Vikram Singh. Sebastian Verhelst and Martin Tuner acted as the supervisors for the work done. Erik Svensson provided the model for the Scania D13 engine which was used in the paper. The work detailed in the paper itself was done by the lead author.

Paper III

The paper was written by the lead author, Vikram Singh. The experimental work was done by the lead author with Sebastian Verhelst acting as a supervisor for the work done. The Rankine cycle simulations were done by Jelmer Johannes Rijpkema with Karin Munch and Sven B. Andersson acting as supervisors.

Paper IV

The paper was written by the lead author, Vikram Singh. The experimental work was done by the lead author with assistance from Xiufei Li and with Sebastian Verhelst acting as the supervisor for the work done. The Rankine cycle simulations were performed by Jelmer Johannes Rijpkema with Karin Munch and Sven B. Andersson acting as supervisors.